ROBUST AND RELIABILITY-BASED MULTIDISCIPLINARY OPTIMIZATION OF INJECTION MOLDING SYSTEM

by

NAZMUL HASAN

A thesis

Submitted to the

Department of Industrial and Production Engineering,

Bangladesh University of Engineering and Technology,

in partial fulfillment of the requirements

for the degree of

MASTER OF SCIENCE

in

Industrial and Production Engineering

Department of Industrial and Production Engineering (IPE)

Bangladesh University of Engineering and Technology (BUET)

2020

CERTIFICATE OF APPROVAL

The thesis titled "Robust and Reliability-based Multidisciplinary Optimization of Injection Molding System" submitted by Nazmul Hasan, student ID. 0417082004, Session: April, 2017 has been accepted as satisfactory in partial fulfillment of the requirements for the degree of Master of Science in Industrial and Production Engineering on February 19, 2020.

BOARD OF EXAMINERS

Dr. AKM Kais Bin Zaman Professor Department of IPE, BUET, Dhaka	Chairman (Supervisor)
Dr. Nikhil Ranjan Dhar Professor and Head Department of IPE, BUET, Dhaka	Member (Ex-Officio)
Dr. A.K.M. Masud Professor Department of IPE, BUET, Dhaka	Member
Dr. Ferdous Sarwar Associate Professor Department of IPE, BUET, Dhaka	Member
Dr. Mohammed Forhad Uddin Professor Department of Mathematics, BUET, Dhaka	Member (External)

CANDIDATE'S DECLARATION

It is hereby declared that this thesis or any part of it has not been submitted elsewhere for the award of any degree or diploma.

Nazmul

Nazmul Hasan

Student ID: 0417082004

To the Most Merciful

To my family

Acknowledgment

By the grace of the most benevolent and Almighty God, the thesis titled “Robust and Reliability-Based Multidisciplinary Optimization of Injection Molding System” has been completed followed by report submission. The author of this report thinks that it is his moral duty to convey his earnest gratitude to a number of extra-ordinary people without whom this study would have not been possible.

Firstly, the author of this thesis report would like to express his sincere respect and heartfelt gratitude to his thesis supervisor Dr. AKM Kais Bin Zaman, Professor, Department of Industrial and Production Engineering (IPE), Bangladesh University of Engineering and Technology (BUET), for his whole-hearted supervision. His clear guidance, timely instructions, invaluable advice, prudent suggestions, and sheer encouragements throughout the progress of the thesis and report writing have made this thesis possible.

Next, the author would like to convey his sincere gratitude to Dr. Nikhil Ranjan Dhar, Professor and Head, Department of IPE, BUET; Dr. A.K.M. Masud, Professor, Department of IPE, BUET; Dr. Ferdous Sarwar, Associate Professor, Department of IPE, BUET; and Dr. Mohammed Forhad Uddin, Professor, Department of Mathematics, BUET, for their constructive remarks and kind evaluations of this study.

The author would also like to acknowledge the kind assistance of Md. Faruk Hossen, Engineer, Machine Shop, Pilot Plant & Process Development Centre (PP&PDC), Bangladesh Council of Scientific and Industrial Research (BCSIR), in determining bounds for the design variables for this study.

The authors would like to express appreciation to all of his well-wishers who inspired him to continue this work. He is grateful to his family members for their support and encouragement. Last but not least, the author wants to convey his appreciations to all of those who have supported him in any respect during the study.

Abstract

This thesis focuses on multidisciplinary design optimization (MDO) of a multi-cavity injection mold insert taking into account the multidisciplinary nature of the injection molding system. The proposed modifications in the conventional multi-cavity insert will allow flexibility in the production of a specified plastic part family. The use of the proposed flexible multi-cavity injection mold insert can contribute to the reduction of overall mold manufacturing costs. An injection molding machine using flexible multi-cavity inserts need to mold different part family members, whose specifications vary within a permissible limit. Hence, there exists uncertainty in the input variables. Two approaches: robustness-based design optimization (RDO) and reliability-based design optimization (RBDO) are used to handle the uncertainty in the input variables. The optimal design for the proposed multi-cavity insert considers the minimization of cycle time and pressure drop simultaneously. Therefore, a multi-objective optimization method is used in the problem formulation. Thus, this thesis solves the design problem using two formulations: the first one integrates MDO, RDO, and multi-objective optimization; the second one integrates MDO, RBDO, and multi-objective optimization. A numerical illustration of the design problem is presented specifying a part family with respect to a particular model of injection molding machine and a particular polymer material. Finally, Pareto optimal solutions are obtained including alternative combinations of cycle time and pressure drop. The flexible multi-cavity insert can be manufactured using the optimal values of the design variables corresponding to the selected combination of cycle time and pressure drop. The proposed mold insert will be an economical solution for the production of small plastic parts having dimensional similarity, e.g., components of toys, cosmetic boxes, household containers, electric switches, etc.

Table of Contents

List of Tables

List of Figures

List of Abbreviations

MDO	:	Multidisciplinary Design Optimization
RDO	:	Robustness-based Design Optimization
RBDO	:	Reliability-based Design Optimization
MDF	:	Multidisciplinary Feasible
AAO	:	All-at-once
IDF	:	Individual Disciplinary Feasible
CO	:	Collaborative Optimization
BLISS	:	Bi-level Integrated System Synthesis
FORM	:	First Order Reliability Method
SORM	:	Second Order Reliability Method
RIA	:	Reliability Index Approach
PMA	:	Performance Measure Approach
PDF	:	Probability Density Function
CDF	:	Cumulative Distribution Function
MPP	:	Most Probable Point

Nomenclature

A_j	=	System compatibility equation corresponding jth discipline
A_{part}	=	Projected area of the part to be molded on the parting plane, m^2
A_{proj}	=	Total projected area of the cavity (along-with runner system), m^2
$\boldsymbol{cv}$	=	Vector of all disciplinary coupling variables
$\boldsymbol{cv}_s$	=	Vector of surrogate coupling variable corresponding to $\boldsymbol{cv}$
d_p	=	Depth of the part, m
$\boldsymbol{d}$	=	Vector of deterministic design variables ($\boldsymbol{x}_d$) as well as the mean values of the random design variables ($\boldsymbol{x}_r$), i.e., $\boldsymbol{d} = [\boldsymbol{x}_d\ \boldsymbol{\mu}_{x_r}]$
d_{gate}	=	Diameter of gate, m
$d_{release}$	=	Mold opening distance, m
d_{runner}	=	Diameter of runner, m
d_{sprue}	=	Initial diameter of sprue, m
$E(g_j)$	=	Expected value or mean of the jth inequality constraint
f	=	Objective function
$F_{clamp\ max}$	=	Maximum clamping force, N
$F_{\boldsymbol{cv}_j}$	=	Functional relationship representing jth coupling variable
$f_i^{max}(\boldsymbol{x}^*)$	=	Maximum functional value of ith objective function
$f_i^{min}(\boldsymbol{x}^*)$	=	Minimum functional value of ith objective function
$f_{\boldsymbol{r}}(\boldsymbol{r})$	=	Joint probability density function (PDF) of random vector $\boldsymbol{r}$
g	=	Inequality constraint
h	=	Equality constraint
k	=	Viscosity evaluated at a shear rate of one reciprocal second, Pa·s^n
l_{gate}	=	Length of gate, m
l_{part}	=	Length of the part, m
l_{runner}	=	Length of runner, m
l_{sprue}	=	Length of sprue, m
$\boldsymbol{lb}$	=	Vector of lower bounds of design variables
$\boldsymbol{LB}$	=	Vector of lower bounds of inequality constraints

Nomenclature (Continued)

Max_D	=	Maximum dimension corresponding to the largest cross-section, perpendicular to the direction of melt flow, m
min_D	=	Minimum dimension corresponding to the smallest cross-section, perpendicular to the direction of melt flow, m
n	=	Power law index
n_c	=	Number of part cavities
$n_{downstream}$	=	Number of ramification streams
ncv	=	Number of the coupling variables
$nddv$	=	Numbers of the deterministic design variables
$nrdv$	=	Numbers of the random design variables
$\boldsymbol{p}$	=	Vector of random design parameters
P_{f_j}	=	Failure probability for jth inequality constraint
$P_{f_j}^{allowable}$	=	Allowable (maximum) failure probability for jth inequality constraint
P_{inj}	=	Required injection power, W
Q	=	Volumetric flow rate of the melt, m^3/s
Q_{max}	=	Maximum volumetric flow rate of the melt, m^3/s
$\boldsymbol{r}$	=	Vector of all the random variables, i.e., $\boldsymbol{r} = [\boldsymbol{x}_r\ \boldsymbol{p}]$
T_{eject}	=	Recommended part ejection temperature, °C
t_{inj}	=	Injection time, s
T_{melt}	=	Recommended polymer melt temperature, °C
T_{mold}	=	Recommended mold temperature, °C
$\boldsymbol{u}$	=	Standard normal space vector corresponding to the vector of random variables, $\boldsymbol{r}$
$\Vert\boldsymbol{u}\Vert$	=	Euclidean norm of vector $\boldsymbol{u}$
$\boldsymbol{u}^*.$	=	Most probable point (MPP) of failure
$\boldsymbol{ub}$	=	Vector of upper bounds of design variables
$\boldsymbol{UB}$	=	Vector of upper bounds of inequality constraints
$\bar{v}_F$	=	Velocity of the flow front, m/s
v_p	=	Volume of the injection molded part, m^3

Nomenclature (Continued)

w	=	Weighting coefficient
$\boldsymbol{x}$	=	Vector of design variables
$\boldsymbol{x}_d$	=	Vector of deterministic design variables
$\boldsymbol{x}_r$	=	Vector of random design variables
$\boldsymbol{x}_s$	=	Vector of shared input variables
α	=	Thermal diffusivity of the polymer material, m^2/s
α_{sprue}	=	Draft angle of sprue, degree
β	=	Reliability index
β^T	=	Target reliability index
$\dot{\gamma}_{max}$	=	Maximum shear rate for the plastic, s^{-1}
η_{aeff}	=	Apparent effective viscosity, Pa·s
$\boldsymbol{\mu}_{x_r}$	=	Vector of mean values of the random design variables
μ_f	=	Mean value of the objective function
$\boldsymbol{\mu}_p$	=	Vector of mean values of random design parameters
$\sigma(\boldsymbol{x}_r)$	=	Vector of standard deviations of the random design variables
$\sigma^2_{cv_j}$	=	Variance of jth coupling variable
$\sigma^2_{d_i}$	=	Variance of ith random design variable
σ_{g_j}	=	Standard deviation of the jth inequality constraint
$\sigma^2_{p_i}$	=	Variance of ith random design parameter
σ_f	=	Standard deviation of the objective function
φ	=	Ratio between width and thickness of the mold cavity
Φ	=	Standard Gaussian cumulative distribution function (CDF)

CHAPTER 1

INTRODUCTION

1.1 Background of the study

Injection molding machine is a plastic parts manufacturing machine, where the injection mold plays the role of giving final shape to the molten polymer that flows into the mold cavity. Figure 1.1 depicts the components of a typical injection mold. The injection mold components can be grouped into two assembled halves— stationary mold half and movable mold half. The stationary half includes items 1 to 4 and the movable half includes items 5 to 10. Stationary and movable clamping plates assist in mounting the corresponding mold assembled half in the injection molding machine. Sprue bushing (item 3) creates an internal channel, referred to as sprue, for the flow of molten polymer. Cavity retainer plates (items 2 and 6) contain corresponding cavity inserts. Ejector plate (item 8) and ejector retainer plate (7) assist in ejecting the molded part without damage to either part or cavity. Cavity inserts (items 4 and 5) combinedly contribute to the creation of the cavity for molding the part (item 11).

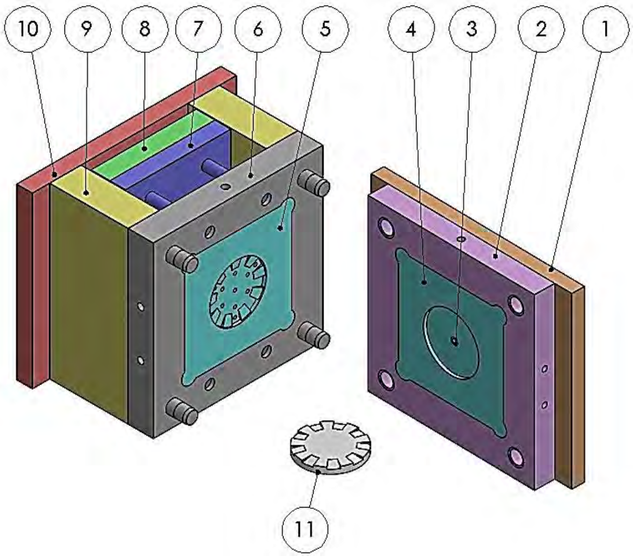

Item	Designation
1	Stationary clamping plate
2	Cavity retainer plate A
3	Sprue bushing
4	Cavity insert A
5	Cavity insert B
6	Cavity retainer plate B
7	Ejector retainer plate
8	Ejector plate
9	Support pillar
10	Movable clamping plate
11	Part to be molded

Figure 1.1: Common components of an injection mold (typical European design (Menges et al., 2013)) along with fitted cavity inserts for molding a specific part

If a different part is to be molded instead of item 11, cavity inserts (items 4 and 5) are to be replaced with appropriate cavity inserts containing the cavity features of the new part. Hence, the production of different parts requires manufacturing different cavity inserts. A substantial investment of time and money is needed for manufacturing a cavity insert. This requirement is obvious in the case of a single cavity insert (Figure 1.2), where only one part can be produced at a time. In such cavity inserts, the molten plastic reaches the cavity through sprue only; no runner or gate is usually involved (Menges et al., 2013). Change in the mold cavity may require a change in sprue bushing dimensions as well.

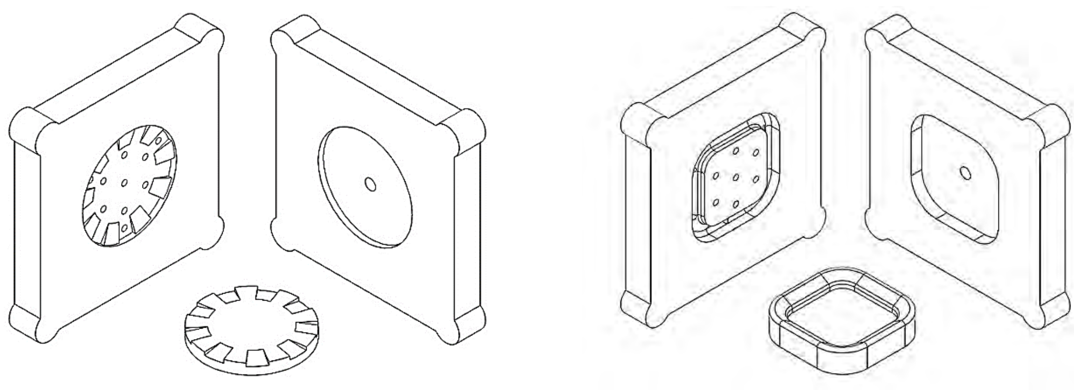

(a) Cavity inserts for sample part I (b) Cavity inserts for sample part II

Figure 1.2: Sets of single cavity inserts for molding two different sample parts

Multi-cavity inserts, as shown in Figure 1.3(a), are used to produce more than one part at a time and such inserts require runner and gate along with sprue for molten plastic to reach the cavities. For a change in a part to be molded using the multi-cavity insert, the cavity features along with runner, gate, and sprue need to be redesigned. A new set of multi-cavity inserts is required to be manufactured to include the redesigned features. However, the robust design of the runner, gate, and sprue can contribute to the creation of a *flexible* multi-cavity insert as shown in Figure 1.3(b), replacing conventional multi-cavity inserts in Figure 1.3(a).

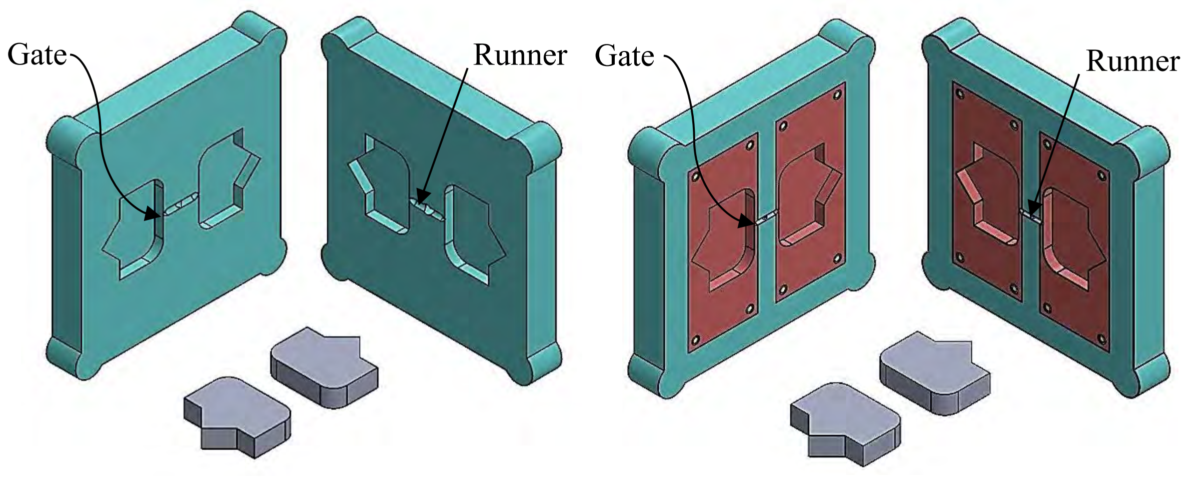

(a) Conventional multi-cavity inserts (b) Proposed *flexible* multi-cavity inserts

Figure 1.3: Contrast between conventional and proposed multi-cavity inserts for molding two identical parts (channels for ejector pins are omitted for clarity of the cavities)

A detailed structure of the proposed flexible multi-cavity insert is presented in Figure 1.4, which includes two runners and two master cavities to accommodate the sub-inserts. The sub-inserts contain cavity features of the part to be molded and a gate connecting the runner and the cavity. The gate is included in the sub-insert to avoid flash in the molded parts since small clearance is expected in the assembly of the master cavity and sub-insert. The sub-insert is to be fitted in the master cavity with the help of mechanical fasteners (e.g., hex bolt).

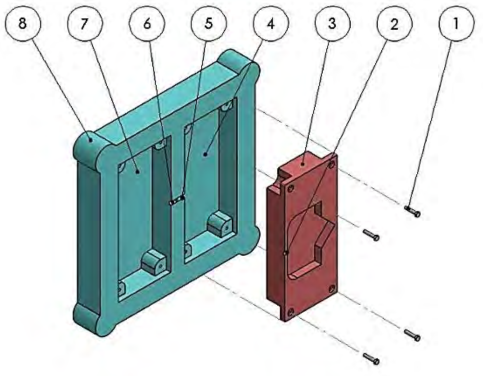

Item	Designation
1	Hex bolt
2	Gate
3	Sub-insert (right)
4	Master cavity (right)
5	Runner (right)
6	Runner (left)
7	Master cavity (left)
8	Multi-cavity insert base

Figure 1.4: Components of flexible multi-cavity insert (sub-insert of the left half, associated hex bolts, and channels for ejector pins are omitted for clarity of the cavities)

The term 'flexible' implies that if a new part is to be molded, only the sub-inserts need to be replaced, rather than the whole insert. As a result, the cost incurred in mold making for the production of a new part can be reduced to a great extent. However, the flexible multi-cavity insert is limited to the production of members of a specific part family who share a resemblance in part-volume, size, and shape. A sample part family is illustrated in Figure 1.5. A significant change in part features and specifications cannot be adopted with the flexible multi-cavity insert. Parts with complex and intricate geometric features may require a dedicated cavity insert. The flexible multi-cavity insert will be well-suited for the toy industry, where a large number of parts need to be produced and these parts can be logically grouped into part families based on similarities of their geometric features.

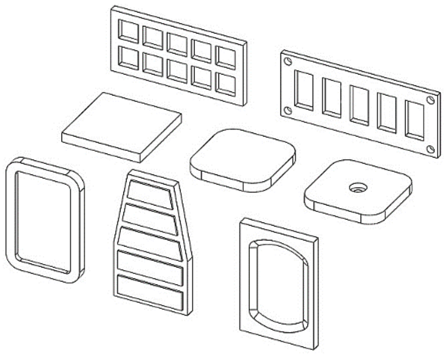

Figure 1.5: Sample part family members

The proposed insert, as shown in Figure 1.3(b), is designed for the production of two molded parts at a time. The proposed design of the flexible multi-cavity insert considers variation in part volume, projected area, length, depth among the part family members. An additional advantage offered by the flexible multi-cavity insert is that, besides two identical parts, two different part family members can be molded at a time by fitting suitable sub-inserts as shown in Figure 1.6 below.

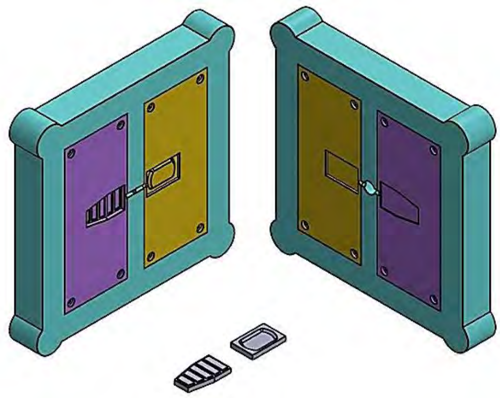

Figure 1.6: Flexible multi-cavity inserts for molding two different parts simultaneously (channels for ejector pins are omitted for clarity of the cavities)

Machining the mold materials to obtain high precision injection mold components involves time and cost consuming procedures. Materials for making injection mold include different types of steel (e.g., carbon steel, alloy steel, tool steel, cold-work steels, hot-work steels, mold steels, stainless steel, etc.) and non-ferrous metal alloys (e.g., copper alloys, zinc alloys, aluminum alloys, bismuth-tin alloys, etc.) (Menges et al., 2013). The cost of the mold making plays a decisive role in the cost of injection molded parts. The introduction of the flexible multi-cavity insert can contribute to significant cost reduction through the use of sub-inserts. However, the main challenge lies in the determination of appropriate dimensions for the elements (sprue, runner and gate) of the flexible multi-cavity insert.

Optimization of dimensional values of cavity insert elements needs to take the whole system of injection molding machine into consideration due to the multidisciplinary nature of the machine (Ferreira et al., 2010). The injection molding machine is a complex engineering system consisting of four sub-systems— structural, feeding/injection, heat transfer, and ejection. The interaction between the subsystems demands the use of multidisciplinary design optimization (MDO) of the system to ensure the best possible performance. The MDO problem needs to include multi-objective optimization of 'cycle time' and 'pressure drop' in the molding process. Cycle time needs to be minimized to ensure high productivity. However, the quality of the produced parts should not be jeopardized in the process of gaining high productivity. A large magnitude of pressure drop can hinder the quality of the plastic parts. Loss of pressure hinders molten polymer to travel through the nozzle into the mold cavity and the polymer may dry up before filling the mold cavity. Thus, to shorten lead time and to obtain good quality parts both cycle time and pressure drop need to be minimized simultaneously, which makes the mold design a multi-objective MDO problem. Moreover, an injection molding machine using flexible multi-cavity inserts need to work with different part family members, whose specifications vary within a permissible limit. Hence, the uncertainty in the input variables needs to be considered. Robustness-based design and reliability-based design are two approaches that deal with the design under uncertainty (Zaman et al., 2011). Therefore, the robust and reliability-based design of a flexible multi-cavity insert for an injection mold yields the scope of this thesis considering multi-objective multidisciplinary optimization.

1.2 Objectives of the study

The specific objectives of this research are as follows:

- To design a flexible multi-cavity insert for an injection mold through developing robustness-based multi-objective MDO formulations of the injection molding system using two approaches– multidisciplinary feasible (MDF) method and all-at-once (AAO) method.
- To design a flexible multi-cavity insert for an injection mold through developing reliability-based multi-objective MDO formulation of the injection molding system using two approaches– multidisciplinary feasible (MDF) method and all-at-once (AAO) method.

1.3 Contributions of the study

This thesis solves the design problem of a flexible multi-cavity injection mold insert by developing a multidisciplinary design optimization (MDO) formulation of the injection molding system considering uncertainty in the input variables. The outcome of this thesis provides Pareto optimal solutions for multi-cavity inserts that will allow flexibility in molding a plastic part family through a modular design. Therefore, overall mold manufacturing costs for the production of the part family can be reduced. The numerical illustration included in the thesis can readily help a designer solve the design problem of flexible multi-cavity insert for molding a specified part family with a particular model of injection molding machine and a particular polymer material. The proposed mold insert can be an economical solution for the production of small plastic parts having dimensional similarity, e.g., components of toys, cosmetic boxes, household containers, electric switches, etc.

1.4 Organization of the thesis

The rest of this thesis report is organized in the following manner:

Chapter 2 reviews the literature relevant to this study. Chapter 3 explains the multidisciplinary nature of the injection molding system and defines the design optimization problem of the flexible multi-cavity insert in terms of objective functions, constraints, design variables, coupling variables, design constants, and parameters. Chapter 4 contains a discussion on deterministic optimization, robustness-based design optimization (RDO), reliability-based design optimization (RBDO), and multi-objective optimization techniques. Chapter 5 presents both deterministic and probabilistic formulation of multidisciplinary design optimization (MDO). Chapter 6 includes integrated formulations of robustness-based multi-objective MDO and reliability-based multi-objective MDO developed for the injection molding system. This chapter also presents a numerical illustration of the design problem defined in Chapter 3, considering a particular model of injection molding machine and a particular polymer material. Chapter 7 presents and discusses the results obtained by solving the numerical illustration of the design problem using the formulations presented in Chapter 6. Finally, Chapter 8 contains conclusive statements about this study and discusses the potential directions for future research.

CHAPTER 2

LITERATURE REVIEW

Injection molding machine is a versatile addition in the field of manufacturing plastic parts. The first injection molding machine was patented in the late nineteenth century (Evans, 2006). The use of the injection molding machine expanded with the growth of the plastic industry during World War II to achieve the mass-production of parts with reduced cost. The first screw injection machine was invented in 1946 that contributed to precise control over the injection speed, and the good quality of the molded parts (Merrill, 1955). The reciprocating-screw injection molding machine is the most commonly used molding system in the present plastic industry. Hence, this thesis considers a standard model (SUN-110, Steady Stream Business Co., Ltd.) of a plastic injection molding machine with a reciprocating screw.

A volume of research works regarding injection molding is reported in the literature. The steps in an injection molding cycle involving polymer flow are studied extensively in Spencer and Gilmore (1951). The authors identified the effect of polymer melt viscosity, injection power, the mold-wall temperature on the mold filling time. Rheological and thermal properties of polymer materials in injection molding are investigated in Baliman et al. (1959). The authors studied the way in which the polymer materials flow inside the mold cavity in response to the applied injection temperature and pressure. They revealed that provision for heat transfer, and geometry of the runner system and mold cavity influence the flow velocity of the melt. A theoretical model for the quantitative representation of the injection molding of thermoplastics, considering the flow behavior of polymer in the cavity, is presented in Kamal and Kenig (1972a). The model is developed on the basis of the equations of motion, continuity, and energy for the injection molding system during the filling, packing and cooling stages of the molding cycle considering appropriate boundary conditions. Non-Newtonian behavior of the molten polymer, the effect of temperature on viscosity and density of the melt, the latent heat of solidification, and the differences in thermal properties between the solid and the melt are addressed in the model formulation. The model outputs include – data on the progression of the melt front, the flow rate, and the velocity profiles at different times and positions inside the mold cavity; temperature and pressure profiles throughout the packing and cooling stages of the molding cycle. The theoretical model of Kamal and Kenig (1972a) is validated through the experimental studies with polyethylene in Kamal and Kenig (1972b). The experimental results support the predictions of the proposed theoretical model for all stages of the injection molding cycle. Fluid mechanical analysis of isothermal and non-isothermal mold filling is reported in White (1975). The authors investigated the hydrodynamics of a molten polymer flowing inside a rectangular mold cavity. In Broyer et al. (1975), a simulator is proposed on the basis of a theoretical cavity filling model for the complete injection molding process using the flow analysis network (FAN) method. The simulator can help calculate the injection molding cycle time, identify weld lines locations, molecular orientation, and approximate conditions for short-shot injection. All these preliminary studies paved the way to further research work in the area of injection molding.

In the injection molding process, the mold plays the role of giving the final shape to the molten polymer that flows into its cavity. The mold is an intricate tool that consists of a large number of assembled components, e.g., typical European design (Menges et al., 2013) of an injection mold includes twenty-one different components. Significant components of a typical mold include –cavity inserts, cavity retainer plates, clamping plates, sprue bushing, ejector retainer plate, ejector plate, support pillar as shown earlier in Figure 1.1. Molds can be categorized into single cavity mold and multi-cavity mold on the basis of the number of machined cavities in the insert (Menges et al., 2013). The single cavity mold produces one part per cycle and the multi-cavity mold produces two or more parts per cycle. Several studies regarding multi-cavity mold are reported in the literature involving different aspects, e.g., heat transfer system (Tang et al., 1997), cavity pressure control (Kazmer and Barkan, 1997), runner system (Lee and Lin, 2006), cavity filling (Kang and Lyu, 2008), etc. These research studies investigated the conventional design of the multi-cavity mold. This thesis proposes a modified design for the multi-cavity mold inserts to achieve flexibility in molding different parts with the use of sub-inserts. Note that the selection of mold materials, mold-making techniques, coolant and the design of ejection, venting, and heat transfer systems are out of the scope of this thesis.

The injection molding process involves the coupled interaction of multiple components of the mold during the filling, packing and cooling stages of the molding cycle. The design of an injection mold requires considerable expertise in multiple areas, e.g., mold materials, mold manufacturing processes, mold design features, design of runner, ejection, heat transfer and venting systems, etc.; all of which are highly coupled to each other. Extensive discussion on different aspects of mold design is reported in many standard textbooks (e.g., Rubin and Rubin, 1972; Rosato and Rosato, 2012; Menges et al., 2013) that aggregate the findings of different major research work in the area of injection molding. Furthermore, investigations have been carried out in different directions for the optimization of the injection mold design. Most of the research work concentrated on the optimization of the heat transfer system (Tang et al., 1997; Lam et al., 2004; Dimla et al., 2005; Park and Dang, 2010; Choi et al., 2012; Li et al., 2018) and gate location (Pandelidis and Zou, 1990; Shen et al., 2004; Li et al., 2007; Zhai and Xie, 2010) since these are the critical factors in the design of the mold. Optimization of process parameters (Kumar et al., 2002; Oktem et al., 2007; Shen et al., 2007; Yin et al., 2011; Dang, 2014; Moayyedian et al., 2018) is also reported in the literature to help produce defect-free and good quality parts. The reported research studies in the area of injection molding generally involve one or a few aspects of the total design and perform single disciplinary optimization for the corresponding design problem.

The multidisciplinary nature of the injection molding system was first addressed in Ferreira et al. (2010). The authors presented a Multidisciplinary Design Optimization (MDO) based framework to deal with the design of an injection mold by integrating the sub-systems of the injection mold. A few other research studies (e.g., Van Dijk et al., 2011; Ferreira et al., 2014) also consider the multidisciplinary nature of the injection mold design. However, these research studies (Ferreira et al., 2010; Van Dijk et al., 2011; Ferreira et al., 2014) do not include the use of coupling variables in the MDO formulation of the mold design problem. Coupling variables are used in the MDO literature to represent interdisciplinary interactions. Moreover, uncertainty in the input variables is not considered in the optimization of the mold design. This thesis intends to formulate the MDO problem of the flexible multi-cavity mold insert with the use of coupling variables in the system compatibility equations.

MDO is a tool for the optimization of a complex system containing two or more disciplines that are coupled (Chiralaksanakul and Mahadevan, 2007). Two disciplines are said to be coupled if the analysis of one discipline depends on the output from the other one and vice versa; this is called system compatibility requirement in MDO literature. The output of MDO gives such values of design variables that optimize the overall system-level output ensuring compatibility among the coupled disciplines. The feasibility of a multidisciplinary system depends on a set of compatible coupling variables that satisfy all the system compatibility equations simultaneously (Cramer et al., 1994). Several methodologies are found in MDO literature that deals with the system compatibility equations using different approaches. Common MDO methods include – multidisciplinary feasible (MDF) method, the all-at-once (AAO) method, and the individual disciplinary feasible (IDF) method, etc. All these methods are applicable to deterministic MDO problems. A detailed survey on the MDF, AAO, and IDF methods can be found in Cramer et al. (1994), Hulme and Bloebaum (2000) and Chiralaksanakul and Mahadevan (2007). There exists another group of solution approach that deals with deterministic MDO problem by decomposing the problem to attain disciplinary autonomy. The decomposition-based methods include collaborative optimization (CO) (Braun and Kroo, 1997), and bi-level integrated system synthesis (BLISS) (Sobieszczanski-Sobieski et al., 2000; Sobieszczanski-Sobieski and Kodiyalam, 2001). The decomposition-based methods allow the design parameters to be fully controlled by the design engineers of the individual discipline. The benefits of MDO methods are vast yet limited to only a few fields, like aerospace (e.g., Sobieszczanski-Sobieski and Haftka, 1997; Perez et al., 2004), automobile (e.g., LIU and Cui, 2004; Hao et al., 2013), etc. A few research studies are also reported in the field of manufacturing that include application of MDO (e.g., Zhao et al., 2008; Liu et al., 2013).

For non-deterministic engineering problems, deterministic formulation of MDO problems (i.e., assuming all design variables and system variables are precisely known) can yield infeasible or inappropriate solutions (Sim, 2004). The optimality and feasibility of the design can be jeopardized as the influence of natural variability and data uncertainty is not considered in a deterministic formulation. Design of the flexible multi-cavity insert needs to handle molding of part family members whose dimensions are allowed to vary within a specified range. Therefore, the MDO of the injection molding system for designing the flexible multi-cavity insert includes uncertainty that is essential to be considered. Robustness-based design (e.g., Parkinson et al., 1993; Ben-Tal and Nemirovski, 2002; Doltsinis and Kang, 2004) and reliability-based design (e.g., Chiralaksanakul and Mahadevan, 2005; Ramu et al., 2006; Agarwal et al., 2007; Du and Huang, 2007) are two approaches that deal with design under uncertainty. Thus, this thesis requires the integration of MDO formulation with RDO or RBDO formulation.

Robustness-based design optimization (RDO) considers the uncertainty in the design variables and system parameters into its formulation and provides such a solution that the design outputs remain less sensitive to the variation of input variables. Four elements of RDO are outlined in Zaman et al. (2011), as follows: (1) objective robustness; (2) feasibility robustness; (3) estimating mean and measure of variation (variance) of the performance function; and (4) multi-objective optimization. A detailed discussion of RDO methodologies for single disciplinary systems can be found in Park et al. (2006). For the optimization of multidisciplinary systems under uncertainty, the application of robustness-based design is reported in a volume of literature (e.g., Chen and Lewis, 1999; Du and Chen, 2002; Zaman and Mahadevan, 2013). Multidisciplinary RDO integrates the formulation of multidisciplinary design optimization (MDO) with that of robustness-based design. A detailed review of methods for multidisciplinary RDO is reported in Allen et al. (2006).

Reliability-based design optimization (RBDO) is a tool that optimizes the objective function(s) ensuring that the reliabilities of the limit state functions are above an acceptable threshold limit, taking into account the uncertainty in the design variables and system parameters. The limit state functions are the expressions to represent the criteria of failure of a system, e.g., the inequality constraints in an optimization problem. There is now an extensive volume of literature on RBDO methods and applications for both single and multidisciplinary systems (e.g., Youn et al., 2003; Youn et al., 2004; Aoues and Chateauneuf, 2010; Yao et al., 2011). Reliability estimation involves the analysis of uncertainty in the input variables to calculate the failure probability or reliability index that is used in the probabilistic formulation of the constraint. Several methods have been developed to estimate the failure probability that can be categorized into three major classes (Lopez et al., 2011), such as: (1) Simulation methods (e.g., Niederreiter and Spanier, 2000; Rubinstein and Kroese, 2016), (2) Numerical integration (e.g., Lee and Kwak, 2006), and (3) Analytical methods (e.g., Mahadevan and Haldar, 2000). First Order Reliability Method (FORM) and Second Order Reliability Method (SORM) are common analytical approaches for estimating the failure probability. RBDO methods can be classified into three groups based on how reliability analysis is handled in the optimization process, such as: (i) nested double loop methods (e.g., Rackwitz and Flessler, 1978; Lopez and Beck, 2012), (ii) single loop methods (e.g., Madsen and Hansen, 1992; Chen et al., 1997; Liang et al., 2004), and (iii) decoupled methods (e.g., Royset et al., 2001; Du and Chen, 2004). RBDO based on FORM is a nested double loop approach that requires an optimization loop as well as a reliability loop, i.e., two optimizations, are coupled. FORM methods can be classified into two approaches–Reliability Index Approach (RIA) (Madsen et al., 1986; Melchers, 1999; Haldar and Mahadevan, 2000) and Performance Measure Approach (PMA) (Tu et al., 1999). The difference between RIA and PMA lies in the approach in which the most probable point (MPP) of failure is calculated to estimate the reliability index.

Multidisciplinary RBDO integrates the formulation of MDO with that of reliability-based design. The computational effort of RBDO methodologies is high due to the inherent reliability analysis. The integration of MDO and RBDO further adds to the computational effort. A detailed discussion on the RBDO of a multidisciplinary system under aleatory and epistemic uncertainty is reported in Zaman and Mahadevan (2017). Aleatory uncertainty arises due to natural variation and epistemic uncertainty arises due to lack of knowledge of the system under consideration, or unavailability of data, etc. Note that this thesis considers design under aleatory uncertainty only.

The design of the flexible multi-cavity insert considers the minimization of both cycle time and pressure drop during the injection molding process. Therefore, a multi-objective optimization technique is to be incorporated into the problem formulation. Common methods of multi-objective optimization include the weighted-sum method, ε-constraint method, global criterion method, lexicographic method, and genetic algorithm. An extensive survey on multi-objective optimization methods is reported in Arora (2004) and Marler and Arora (2004).

Two approaches are used in this thesis to solve the design problem of the flexible multi-cavity insert. The first approach integrates formulations of MDO, RDO, and multi-objective optimization and the second approach integrates formulations of MDO, RBDO, and multi-objective optimization.

CHAPTER 3

INJECTION MOLDING SYSTEM

Injection molding is the most commonly used commercial plastic processing technique for mass production of discrete thin-walled plastic parts in cycles. Each cycle completes through a complex sequential process. The process starts with melting the plastic granules fed from a hopper into the injection unit. The injection unit consists of a barrel surrounded by heater bands that melt the plastic granules. The barrel houses a co-axial screw that can rotate and reciprocate inside the barrel. The granules are transported forward by the screw and gradually melt by the combined actions of the heater bands and the rotating screw. The molten polymer accumulates at the front of the barrel and the screw advances forward to inject the melt into a clamped mold cavity. The melt then cools by the action of the heat transfer system and solidifies inside the mold assuming the shape of the cavity. When the part is rigid enough to be demolded, the mold halves open and the part is ejected by the action of the ejection system of the mold. Afterward, the mold closes and the process repeats. The whole process is accomplished by the injection molding system that can be divided into four functional subsystems or disciplines (Ferreira et al., 2010), as follows:

1. Structural subsystem
2. Injection subsystem
3. Heat-transfer subsystem
4. Ejection subsystem

The injection molding system itself is a part of the whole injection molding machine that handles the task of molding the molten plastic material into its final shape. In the following sections, the four subsystems of the injection molding system are discussed briefly.

3.1 Structural subsystem

The structural subsystem is the basic building block of the injection mold that houses the heat-transfer subsystem and the ejection subsystem. Components of the structural subsystem include the cavity inserts, clamping plates, cavity retainer plates, support plates, support pillars and other accessories (e.g., leader pin, locating rings, guide pins, guide bushings, compression spring, etc.). The structural subsystem also accommodates sprue bushing, machined channels for runner and gate, and vents (to allow displaced air to escape from the mold cavity). Proper alignment of the injection mold components and guiding of the assembled mold are guaranteed by the structural subsystem (Ferreira et al., 2010).

3.2 Injection subsystem

The injection subsystem feeds the molten plastic material to the mold cavity at the melting temperature. The injection unit consists of a barrel surrounded by heater bands that melt the plastic granules. The barrel houses a co-axial screw actuated by a hydraulic cylinder that can rotate and reciprocate inside the barrel. The combined actions of the rotating screw and the heater bands form a melt that is injected into the clamped mold cavity. The melt reaches the mold cavity through the runner system (i.e., sprue, runner and gate). The runner system can be classified into three types depending on temperature control (Menges et al., 2013). These are – (i) standard runner system, (ii) hot-runner system, and (iii) cold-runner system. The standard runners are directly machined into the mold plates or inserts. Therefore, the runner system remains at the temperature of the mold. Hot-runners are designed in the form of a block and the temperature of this block lies in the melting range of the thermoplastic melts. Cold runners are used in molds for reactive materials such as thermosets and rubber. The cold runner must be kept at 80–120°C in order that the material may not react prematurely in the runner. The melt is required to be injected with appropriate injection pressure that can counter the resistance to flow inside the mold cavity. The role of the injection subsystem is more significant in filling multi-cavity molds since the filling process must be completed for all the cavities. The injection time needs to be set carefully such that sufficient melt is allowed to be injected to fill the runner system as well as the cavities.

3.3 Heat-transfer subsystem

The melt starts to solidify within the mold cavity after the injection is complete. The heat-transfer subsystem takes away heat from the melt to accelerate the solidification process until a stable state has been reached, which permits the ejection of the finished part. The amount of heat to be carried off depends on the temperature of the melt, the ejection temperature, and the specific heat of the plastic material. The heat-transfer subsystem consists of cooling channels through which a coolant is pumped to remove the heat from the molded part. The quality of a molded part depends on maintaining a constant temperature profile throughout the whole production time. The efficiency of production is very much affected by the heat-transfer subsystem (Menges et al., 2013).

3.4 Ejection subsystem

The ejection subsystem pushes the molded part out of the cavity by ejectors when the molded part is solidified enough to retain its final shape without any external support. The ejection subsystem is normally housed in the movable mold half. Mold opening causes the ejection subsystem to be moved forward to eject the molded part. Ejection equipment is usually actuated mechanically by the opening stroke of the machine. However, ejection equipment can also be actuated pneumatically or hydraulically in special cases (Menges et al., 2013). It is required that the ejection subsystem ejects the molded part without damage to either part or cavity.

The design of a flexible multi-cavity insert requires consideration of all the four functional subsystems – structural, injection, heat transfer, and ejection that form the complex injection molding system. Optimization of dimensional values of flexible multi-cavity insert elements (sprue, runner and gate) needs to consider the multidisciplinary nature of the injection molding machine (Ferreira et al., 2010). Interaction between the subsystems or disciplines demands that the design of a flexible multi-cavity insert be modeled as a multidisciplinary design optimization (MDO) problem. The interaction between the subsystems of the injection molding system is depicted in Figure 3.1, as follows:

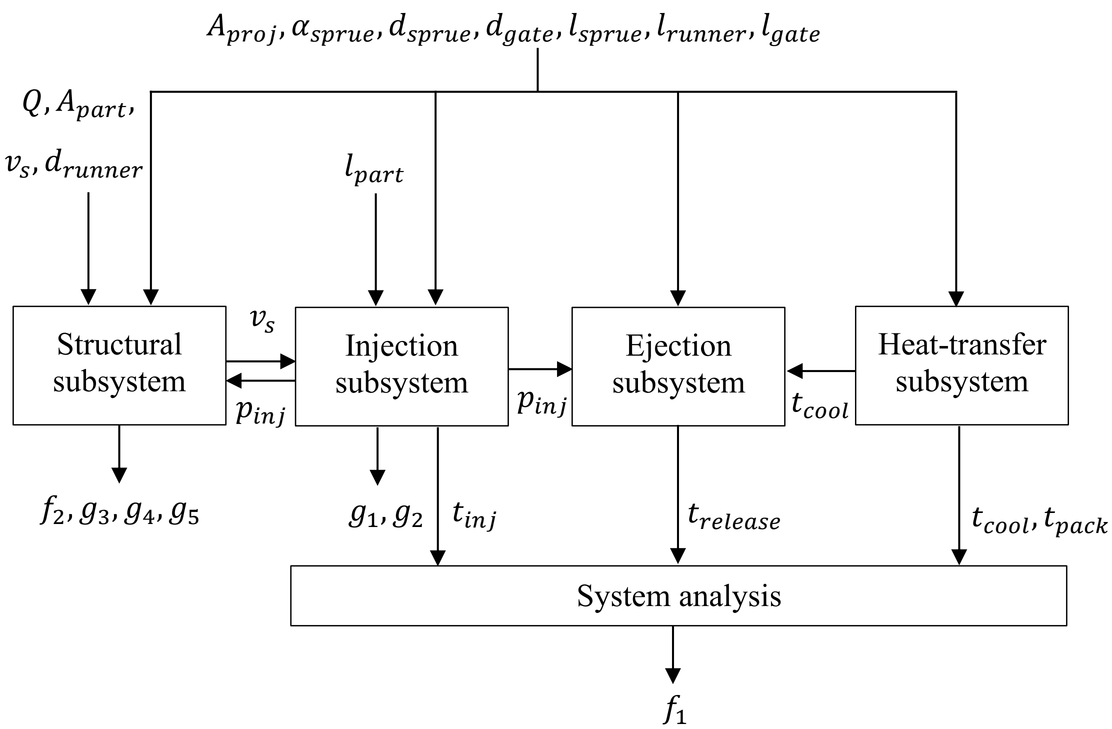

Figure 3.1: Four subsystems representation of the injection molding machine.

Interaction between two disciplines is mathematically represented by coupling variables that are derived as output from one discipline but required as input to other disciplines. The coupling variables identified in the injection molding system are discussed in the following section.

3.5 Coupling variables in the injection molding system

Two disciplines or subsystems are said to be coupled if the analysis of one discipline depends on the output from the other one and vice versa (Chiralaksanakul and Mahadevan, 2007). Therefore, from Figure 3.1, the injection subsystem and structural subsystem can be said to be coupled with the coupling variables– injection pressure (p_{inj}) and shot volume (v_s). These coupling variables can be defined as follows:

Injection pressure (p_{inj}): Injection pressure refers to the pressure exerted on the melt in front of the screw tip during the injection stage.

Shot volume (v_s): Shot volume for a cavity is the amount of molten polymer required to fill the mold cavity, in each cycle.

Injection pressure and shot volume are the outputs of the injection subsystem and the structural subsystem, respectively. An appropriate amount of injection pressure is to be exerted to inject the shot volume within the allotted injection time. Thus, the calculation of required injection pressure can be related to the magnitude of shot volume as shown in Eq. (1) (Nannapaneni and Mahadevan, 2014).

$$p_{inj} = \frac{P_{inj} \times t_{inj}}{2 \times v_s} \tag{1}$$

Here, p_{inj} is the injection pressure; P_{inj} is the injection power, t_{inj} is the injection time, and v_s is the shot volume.

On the other hand, the determination of shot volume that can be injected by the injection molding system, within existing clamping capacity depends on the magnitude of injection pressure, as shown in Eq. (2) (Madan et al., 2013).

$$v_s = \frac{F_{clamp} \times v_p}{p_{inj} \times A_{part}} \tag{2}$$

Here, F_{clamp} is the clamping force, v_p is the volume of the molded part, and A_{part} is the projected area of the molded part on the parting plane.

The variables – injection pressure (p_{inj}) and shot volume (v_s) are thus coupled through Eqs. (1) and (2) and these two equations represent the system compatibility requirements. This coupling results in the multidisciplinary nature of the injection molding system. Chapter 5 discusses methodologies to deal with the optimization of multidisciplinary systems.

The multidisciplinary design optimization (MDO) problem of the injection molding system includes optimization of both cycle time and pressure drop in the molding process, as discussed in Section 1.1. The magnitude of cycle time and pressure drop largely depends on the dimensions of the runner system, e.g., smaller dimensions of the runner system correspond to smaller cycle time but higher pressure drop. Note that, in this thesis, the standard runner system with the circular cross-sectional area is considered, as shown in Figure 3.2.

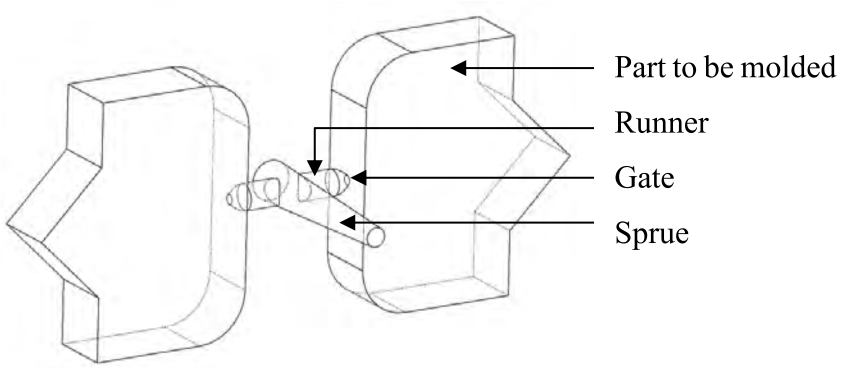

Figure 3.2: Runner system with circular cross-section

3.6 Objective functions in MDO of the injection molding system

The two objective functions – cycle time and pressure drop are discussed in the following subsections.

<u>3.6.1 Cycle time</u>

In the injection molding machine, plastic parts are produced discontinuously in cycles. The cycle time is referred to as the total time required for – closing the mold, injecting the melt into the mold cavity, packing and cooling of the melt inside the cavity, opening the mold and ejecting the finished part from the mold. Thus, cycle time can be theoretically computed as a summation of five major time components (Ferreira et al., 2010), as follows:

1. Plasticizing time: It involves the heating and melting of the plastic in the plasticator.
2. Injection time: It involves injecting the shot volume of melt into the closed mold.
3. Packing time: After filling the mold, packing time is allowed to prevent backflow. It also compensates for the decrease in the volume of melt during solidification.

4. Cooling time: It permits the molded part to be sufficiently rigid for ejection.
5. Release time: It allows the removal of the part by opening and closing the mold to start the next cycle.

In practice, in the computation of cycle time, plasticizing time is ignored since it occurs simultaneously with the cooling and packing stages of the previous part. The injection time can be calculated using Eq. (3) (Nannapaneni and Mahadevan, 2014), as follows:

$$t_{inj} = \frac{2 \times v_s}{P_{inj} \times p_{inj}} \tag{3}$$

The packing time is determined based on the gate dimensions since if the gate is too small it will cause premature solidification of the melt and hinder additional material to enter into the mold cavity (Ferreira et al., 2010). The packing time can be calculated using Eq. (4), as follows:

$$t_{pack} = \frac{d_{gate}^2}{23.1\ \alpha} \times ln\left(0.692 \times \frac{T_{melt} - T_{mold}}{T_{eject} - T_{mold}}\right) \tag{4}$$

Here, t_{pack} is the packing time, d_{gate} is the gate diameter, α is the thermal diffusivity of the molten polymer material, T_{melt} is the recommended polymer melt temperature, T_{mold} is the recommended mold temperature, and T_{eject} is the recommended part ejection temperature. Note that the melt is assumed to be injected in the cavity at a constant temperature of T_{melt}, and the temperature of the mold cavity walls is assumed to be maintained at the constant value T_{mold} by circulating coolant through the cooling channels.
The cooling time can be calculated using Eq. (5) (Ferreira et al., 2010), as follows:

$$t_{cool} = \frac{\left(d_{sprue} + \tan\left(\frac{\pi\ \alpha_{sprue}}{180}\right) \times l_{sprue}\right)^2}{23.1\ \alpha} \times ln\left(0.692 \times \frac{T_{melt} - T_{mold}}{T_{eject} - T_{mold}}\right) \tag{5}$$

Here, t_{cool} is the cooling time, d_{sprue} is the sprue initial diameter, and l_{sprue} is the sprue length.
Release time can be calculated using Eq. (6) (Ferreira et al., 2010), as follows:

$$t_{release} = 2 \times \frac{1000\ d_{release}}{184 + 13 \log\left(\frac{p_{inj} \times A_{proj}}{9.8 \times 10^3 F_{ref}}\right)} \tag{6}$$

Here, $t_{release}$ is the release time, $d_{release}$ is the mold opening distance, A_{proj} is the total projected area of the cavity (along-with runner system), and F_{ref} is the reference force of value

1 ton. In the calculation of release time, it is assumed that an equal amount of time is needed for mold closing and mold opening.

Now, the cycle time can be computed as follows:

$$t_{cycle} = t_{inj} + t_{pack} + t_{cool} + t_{release}$$

$$t_{cycle} = \frac{2 \times v_s}{P_{inj} \times p_{inj}} + \frac{d_{gate}^2}{23.1\,\alpha} \times ln\left(0.692 \times \frac{T_{melt} - T_{mold}}{T_{eject} - T_{mold}}\right)$$
$$+ \frac{\left(d_{sprue} + \tan\left(\frac{\pi\,\alpha_{sprue}}{180}\right) \times l_{sprue}\right)^2}{23.1\,\alpha} \times ln\left(0.692 \times \frac{T_{melt} - T_{mold}}{T_{eject} - T_{mold}}\right) \quad (7)$$
$$+ 2 \times \frac{1000\,d_{release}}{184 + 13\log\left(\frac{p_{inj} \times A_{proj}}{9.8 \times 10^3 F_{ref}}\right)}$$

Here, t_{cycle} is the cycle time. Cycle time is the key metric of injection molding productivity. Eq. (7) is used as the first objective function in the optimization process.

3.6.2 Pressure drop

When the melt is injected from the injection unit into the cavity as the mold flows through the sprue, runner and gate, the pressure of the melt drops. The pressure drop can be calculated using Eq. (8) (Ferreira et al., 2010), as follows:

$$\Delta p = \frac{4\,k\,l_{sprue}}{\bar{d}_{sprue}}\left(\frac{\left(3 + \frac{1}{n}\right)Q}{\pi\left(\frac{\bar{d}_{sprue}}{2}\right)^3}\right)^n + \frac{4\,k\,l_{runner}}{d_{runner}}\left(\frac{\left(3 + \frac{1}{n}\right)Q}{\pi\left(\frac{d_{runner}}{2}\right)^3}\right)^n + \frac{4\,k\,l_{gate}}{d_{gate}}\left(\frac{\left(3 + \frac{1}{n}\right)Q}{\pi\left(\frac{d_{gate}}{2}\right)^3}\right)^n \quad (8)$$

Here, Δp is the pressure drop, k is the viscosity evaluated at a shear rate of one reciprocal second, $\bar{d}_{sprue}$ is the sprue mean diameter, Q is the volumetric flow rate of the melt, n is the power law index, l_{runner} is the runner length, d_{runner} is the runner diameter, and l_{gate} is the gate length.

Since the injection mold design considers a conical-shaped sprue, the mean diameter of the sprue is considered in the calculation of the pressure drop in Eq. (8). The sprue mean diameter can be calculated using Eq. (9) (Ferreira et al., 2010), as follows:

$$\bar{d}_{sprue} = d_{sprue} + \tan\left(\frac{\pi\,\alpha_{sprue}}{180}\right) \times l_{sprue} \quad (9)$$

Pressure drop is a critical factor in maintaining quality products. High magnitude of pressure drop can cause incomplete filling of the mold cavity, which results in defective molded parts. Therefore, the design of the flexible multi-cavity injection mold includes minimization of the pressure drop as the second objective to ensure good quality of the molded parts.

Inclusion of two objective functions – cycle time (Eq. (7)) and pressure drop (Eq. (8)) in the MDO of injection molding system requires the incorporation of multi-objective optimization methodologies within the MDO formulation of the problem. Several multi-objective optimization methodologies are discussed in Chapter 4.

3.7 Constraints in MDO of the injection molding system

In the multi-objective MDO of injection molding system, the constraints as shown in Eqs. (10)-(16) are considered, which are identified using existing literature (e.g., Ferreira et al., 2010; Weissman et al., 2010; Madan et al., 2013). The first constraint as shown in Eq. (10) represents the pressure demand to counter the resistance to flow in the plate (flow length/wall thickness ratio derived from Hagen–Pouseuille's law) (Ferreira et al., 2010).

$$\frac{32\left(l_{sprue}+l_{runner}+l_{gate}+l_{part}\right)\varphi\,\bar{v}_F\eta_{aeff}}{\left(\frac{2\,Max_D\,min_D}{Max_D+min_D}\right)}\leq p_{inj} \tag{10}$$

Here, φ is the ratio between the width and thickness of the mold cavity; $\bar{v}_F$ is the velocity of the flow front; η_{aeff} is apparent effective viscosity; Max_D and min_D is maximum and minimum dimension corresponding to the largest cross-section, perpendicular to the direction of melt flow, respectively.

The second constraint as shown in Eq. (11) implies that the melt pressure acting in the projected area of the mold cavities must not exceed the maximum clamp force (required to hold the mold closed during operation) (Ferreira et al., 2010; Weissman et al., 2010; Madan et al., 2013).

$$p_{inj}\times A_{proj}\leq F_{clamp\,max} \tag{11}$$

Here, $F_{clamp\,max}$ is the maximum clamping force that the machine can withstand.

The third constraint as shown in Eq. (12) implies that the shear rate for flow in gates must not surpass the maximum allowable shear (Ferreira et al., 2010).

$$2\times\left(\frac{\left(3+\frac{1}{n}\right)Q}{\pi\,\dot{\gamma}_{max}}\right)^{\frac{1}{3}}\leq d_{gate} \tag{12}$$

Here, $\dot{\gamma}_{max}$ is the maximum shear rate for the plastic.

The fourth constraint in Eq. (13) implies that the sprue must have enough capacity to fulfill all the downstream runners (Ferreira et al., 2010).

$$d_{runner}\sqrt{n_{downstream}} \leq d_{sprue} \tag{13}$$

Here, $n_{downstream}$ is the number of ramification streams.

The fifth constraint in Eq. (14) implies that the shot volume must be enough to fill the runner system, and the part cavities taking into account the shrinkage of the polymer during solidification (Madan et al., 2013).

$$v_p\,(1+\varepsilon)\,n_c + v_{rs} \leq v_s \tag{14}$$

Here, ε is the percentage shrinkage rate of the polymer from injection temperature to room temperature; n_c is the number of part cavities; v_{rs} is the volume of the runner system. In the design consideration of this thesis, the volume of the runner system can be calculated as follows:

$$v_{rs} = \frac{\pi d_{sprue}^2 l_{sprue}}{4} + 2 \times \left(\frac{\pi d_{gate}^2 l_{gate}}{4} + \frac{\pi d_{runner}^2 l_{runner}}{4}\right) \tag{15}$$

The sixth constraint in Eq. (16) implies that the cooling time must greater than 3 seconds (Madan et al., 2013). Eq. (16) uses the expression for the cooling time stated in Eq. (5).

$$3 \leq \left(\frac{\left(d_{sprue} + \tan\left(\frac{\pi\,\alpha_{sprue}}{180}\right) \times l_{sprue}\right)^2}{23.1\,\alpha} \times ln\left(0.692 \times \frac{T_{melt} - T_{mold}}{T_{eject} - T_{mold}}\right)\right) \tag{16}$$

Note that all the constraints stated in Eqs. (10) to (16) need to be satisfied simultaneously by the optimal design of the flexible multi-cavity injection mold that aims to minimize cycle time and pressure drop.

3.8 Selection of design variables, constants, and parameters

The symbols involved in the objective functions (Eqs. (7)-(8)), constraints (Eqs. (10)-(14), (16)) and system compatibility equations (Eqs. (1)-(2)) are categorized into design or system variables, constants, and parameters. Distinguishing attributes of variables, constants, and parameters are discussed with example in Chapter 4. Selected design variables, parameters, and constants are listed in Tables 3.1, 3.2 and 3.3, respectively.

Table 3.1: List of design variables

Serial No.	Term	Nomenclature
1.	Q	Volumetric flow rate of the melt, m^3/s
2.	α_{sprue}	Draft angle of sprue, degree
3.	d_{sprue}	Initial diameter of sprue, m
4.	d_{runner}	Diameter of runner, m
5.	d_{gate}	Diameter of gate, m
6.	l_{sprue}	Length of sprue, m
7.	l_{runner}	Length of runner, m
8.	l_{gate}	Length of gate, m
9.	t_{inj}	Injection time, s

Note that the flexible multi-cavity insert is not a function of the design variables Q and t_{inj}. However, these are the control variables in the operation of the injection molding machine and hence included as optimization variables.

Table 3.2: List of design parameters

Serial No.	Term	Nomenclature
1.	A_{proj}	Total projected area of the cavity (along-with runner system), m^2
2.	A_{part}	Projected area of the part to be molded on the parting plane, m^2
3.	l_{part}	Length of the part, m
4.	d_p	Depth of the part, m
5.	v_p	Volume of the injection molded part, m^3
6.	Max_D	Maximum dimension corresponding to the largest cross-section, perpendicular to the direction of melt flow, m
7.	min_D	Minimum dimension corresponding to the smallest cross-section, perpendicular to the direction of melt flow, m
8.	φ	Ratio between width and thickness of the mold cavity
9.	$F_{clamp\ max}$	Maximum clamping force, N
10.	Q_{max}	Maximum volumetric flow rate of the melt, m^3/s
11.	$n_{downstream}$	Number of ramification streams
12.	n_c	Number of part cavities
13.	$d_{release}$	Mold opening distance, m
14.	$\bar{v}_F$	Velocity of the flow front, m/s
15.	T_{eject}	Recommended part ejection temperature, °C
16.	T_{mold}	Recommended mold temperature, °C
17.	P_{inj}	Required injection power, W

Table 3.3: List of design constants

Serial No.	Term	Nomenclature
1.	n	Power law index
2.	k	Viscosity evaluated at a shear rate of one reciprocal second, Pa·s^n
3.	α	Thermal diffusivity of the polymer material, m^2/s
4.	$\dot{\gamma}_{max}$	Maximum shear rate for the plastic, s^{-1}
5.	η_{aeff}	Apparent effective viscosity, Pa·s
6.	T_{melt}	Recommended polymer melt temperature, °C

The multidisciplinary design optimization (MDO) problem of the injection molding system for the design of a flexible multi-cavity insert is now ready to be formulated after the selection of the design variables, constants, and parameters. The next two chapters discuss the formulation of different optimization techniques that include deterministic optimization, robustness-based design optimization (RDO), reliability-based design optimization (RBDO), multi-objective optimization, and multidisciplinary design optimization (MDO).

CHAPTER 4

DESIGN OPTIMIZATION

Design optimization is a methodology that uses a mathematical description of a system, to find the best possible design on the basis of characteristic criteria of the system, subjected to recognized constraints (Papalambros and Wilde, 2000). Mathematical description of a system refers to an abstraction of a real system using mathematical expressions of relevant natural laws, physical properties, accumulated empirical evidence, and geometric features. A real system is difficult to analyze since a system existing in a real environment can undergo very complex situations. Thus, a mathematical description or model is essential to represent a system to increase the understanding of how a system works. Mathematical model representing a system generally includes the following elements—

System Variables: These are entities that can assume different values within acceptable ranges and thus affect the system condition. For example— the length and diameter of a shaft are the variables that can affect its volume.

System Parameters: These are entities that are given value set by the modeler to define a specific condition for the system. For example— the working temperature and material of a shaft can be set by a modeler.

System Constants: These are entities fixed by natural laws, physical properties, and geometric features. For example— the coefficient of linear thermal expansion of particular shaft material is constant.

Mathematical Relations: These are mathematical expressions that include equalities, and inequalities involving system variables, parameters, and constants. These relations are used to describe the objective function of the system, and the constraint functions representing the limitations imposed by its environment.

Design optimization requires a characteristic criterion of the system to be selected so that it can be used to compare the available alternatives for finding the best solution. The selected criterion is referred to as 'objective'. The mathematical relation representing the objective is known as 'objective function'. The system under design consideration can be subjected to limitations enforced by the natural laws, availability of material characteristics, and geometric compatibility. Thus, there exists a set of requirements that must be satisfied by any acceptable design. The conditional requirements are represented by the mathematical relation known as 'constraint function'. The term 'function' does not necessarily refer to a single mathematical relation rather it may be a system of equations. Therefore, the number of constraints and objective functions may be one or more.

The steps involved in the formulation of a typical design optimization problem can be summarized as follows (Papalambros and Wilde, 2000):

Step 1: Selecting a set of design variables from the system variables to describe the design alternatives.

Step 2: Selecting an objective function to be minimized or maximized. The objective function is expressed in terms of related design variables, parameters, and constants.

Step 3: Determining a set of constraint functions that must be satisfied by any acceptable design. The constraint functions are expressed in terms of related design variables, parameters, and constants.

Step 4: Determining a set of values for the design variables, which minimize or maximize the objective function and satisfy all the constraint functions simultaneously.

An optimization problem can be formulated using different methodologies according to the nature of the problem. The following categories of optimization are discussed in this thesis—

i. Deterministic optimization
ii. Robustness-based design optimization (RDO)
iii. Reliability-based design optimization (RBDO)
iv. Multi-objective optimization
v. Multidisciplinary design optimization (MDO)

The first four categories of optimization will be discussed in the following sections of this chapter. Chapter 5 is dedicated to a detailed discussion of multidisciplinary design optimization.

4.1 Deterministic optimization

Design variables and system parameters are considered deterministic in the formulation of this kind of optimization. The randomness in system parameters and uncertainty in obtaining precise design variables are not included in the formulation. The standard formulation of a deterministic optimization problem is as follows:

$$\underset{\boldsymbol{x}}{minimize} \quad f(\boldsymbol{x}) \tag{17}$$

$$subject\ to,$$

$$g_j(\boldsymbol{x}) \leq 0; \quad \text{for all } j$$

$$h_j(\boldsymbol{x}) = 0; \quad \text{for all } j$$

$$\boldsymbol{lb} \leq \boldsymbol{x} \leq \boldsymbol{ub}$$

Here, $f(\boldsymbol{x})$ is the objective function, $\boldsymbol{x}$ is the vector of design variables, $g_j(\boldsymbol{x})$ is the jth inequality constraint, $h_j(\boldsymbol{x})$ is the jth equality constraint, and $\boldsymbol{lb}$ and $\boldsymbol{ub}$ are the vectors of lower and upper bounds of design variables. In practice, the design variables and system parameters might be uncertain and solutions obtained from deterministic formulation can be sensitive due to the unaccounted uncertainty.

4.2 Robustness-based design optimization (RDO)

Robust design refers to a design that is able to withstand or overcome adverse conditions, i.e., the design remains less sensitive to the variation of input variables. RDO considers the uncertainty in the design variables and system parameters into its formulation and provides such a solution that the design outputs remain less sensitive to the variation of input variables (Zaman et al., 2011). Sources of uncertainty can be categorized into two types— aleatory and epistemic (Oberkampf et al., 2004). Aleatory uncertainty arises due to natural variation, e.g., lack of repeatability, geometric tolerance, operating conditions, physical properties, etc. Epistemic uncertainty arises due to lack of knowledge of the system under consideration, or approximation of the system behavior in the developed model, or unavailability of data, etc. Inclusion of epistemic uncertainty is out of the scope of this thesis. RDO used in this thesis is formulated to deal with aleatory uncertainty only.

The concept of robust design is explained with the help of Figure 4.1, where the x-axis denotes the value of the design variable, x, and the y-axis denotes the value of the objective function, f. The points $x^*_{det.}$ and $x^*_{rob.}$ on the x-axis, denote the optimal solution obtained in the deterministic and robust formulation, respectively. The corresponding optimum (minimum) functional values are denoted by Q and A, respectively. The uncertainty in the design variables can cause a shift in values of the objective function as shown in Figure 4.1, where the function value might be shifted from point Q to P (worst case for deterministic formulation) and from point A to B (worst case for robust formulation). This is evident from Figure 4.1 (where, $\Delta f_{rob.} \ll \Delta f_{det.}$) that the solution obtained in the robust formulation is less affected by the uncertainty of the design variables.

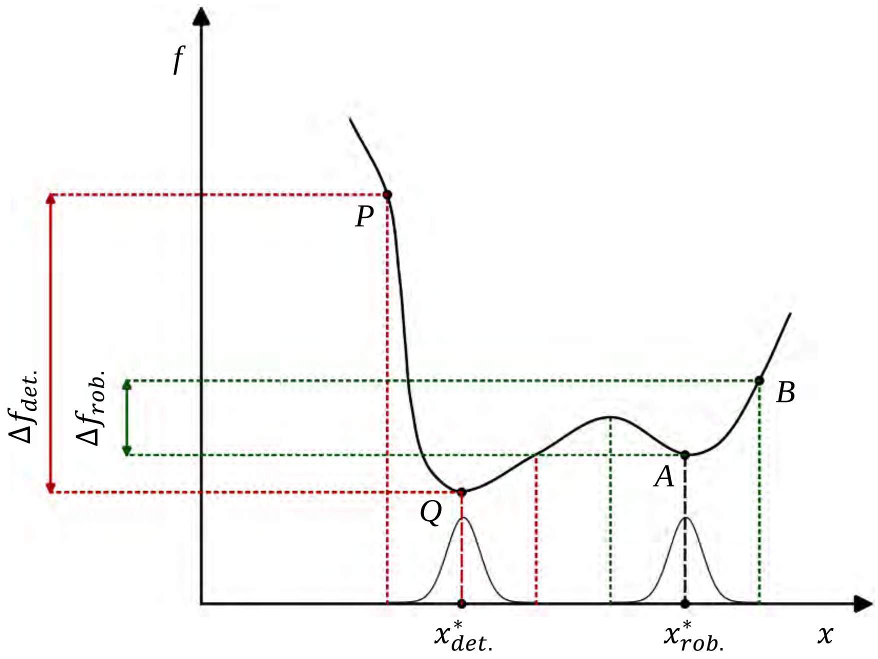

Figure 4.1: Illustration of the robust design concept

RDO includes the following elements—

(i) Objective robustness

(ii) Feasibility robustness

(iii) Estimating mean and measure of variation (variance) of the performance functions

(iv) Multi-objective optimization

The four elements are discussed briefly in the following subsections.

4.2.1 Objective robustness

Objective robustness can be achieved by optimizing the mean of the objective function and minimizing its variance simultaneously. Robustness can be measured by two means— variance (Du and Chen, 1999; Lee and Park, 2001) and percentile difference (Du et al., 2004).

4.2.2 Feasibility robustness

Feasibility robustness implies that the constraints of the design need to be satisfied under system uncertainty. Methods of maintaining feasibility robustness can be categorized into two groups— the first group includes a probabilistic feasibility formulation (Du and Chen, 1999; Lee et al., 2008), and a moment matching formulation (Parkinson et al., 1993) that use probabilistic and statistical analysis; the second group includes worst case analysis (Parkinson et al., 1993), corner space evaluation (Sundaresan et al., 1995), and manufacturing variation patterns (Yu and Ishii, 1998) that do not require probabilistic and statistical analysis.

The feasible region reduction method (Park et al., 2006), which is a variation of moment matching approach, is commonly used for feasibility robustness due to its generic nature. This method does not require normality assumption since it relies on the concept of tolerance design. Tolerance for the performance functions is defined by a reduction of feasible region in each direction by an amount of $k\sigma$, where k is a user-defined constant depending on the design purpose and σ is the standard deviation of the performance function.

4.2.3 Estimating mean and variance of the performance function

Taylor series expansion (Mahadevan and Haldar, 2000) method is a commonly used approach to estimate the mean and variance of the performance function. However, this method may not be appropriate for nonlinear performance function, if random variables have a large magnitude of variance. Other methods of estimating mean and variance of the performance function include sampling-based methods (Robert and Casella, 2004), point estimate methods (Huang and Du, 2007) and dimension reduction method (Lee et al., 2008).

4.2.4 Multi-objective optimization

In RDO, objective robustness results in two objectives— optimizing the mean of the objective function and minimizing its variance. Therefore, a multi-objective optimization method is to be incorporated within the RDO formulation. The weighed-sum method is the most common approach used in RDO (Lee and Park, 2001; Zou and Mahadevan, 2006). A detailed study of other methods of multi-objective optimization is available in Arora (2004).

The four elements of RDO combinedly results in a design formulation to deal with system uncertainty. In this thesis, the RDO formulation uses— 'variance' as a measure of the variation of the performance function to achieve objective robustness, the 'feasible region reduction method' to achieve feasibility robustness, 'first-order Taylor series expansion' to estimate the mean and variance of the performance function, and 'weighted sum method' for the multi-objective optimization. This combination of methods is used for the sake of illustration.

The robustness-based design optimization problem, with the above-stated combination, can be formulated as follows:

$$\underset{\boldsymbol{d}}{minimize} \quad f(\mu,\sigma) = (w \times \mu_f \ + v \times \sigma_f) \tag{18}$$

$$subject\ to,$$

$$LB_j + k \times \sigma_{g_j} \leq E(g_j) \leq UB_j - k \times \sigma_{g_j}; \qquad \text{for all } j$$

$$h_j(\boldsymbol{d}, \boldsymbol{\mu}_p) = 0; \qquad \text{for all } j$$

$$lb_i + k \times \sigma(x_{r_i}) \leq d_i \leq ub_i - k \times \sigma(x_{r_i}); \quad \text{for all } i = 1, 2, \dots, nrdv$$

$$lb_i \leq d_i \leq ub_i; \qquad \text{for all } i = 1, 2, \dots, nddv$$

Here, μ_f and σ_f are the mean value and standard deviation of the objective function, respectively; w and v are the weighting coefficients under associated conditions— $w \geq 0$; $v \geq 0$; and $w + v = 1$. The weighting coefficients denote the relative importance of μ_f and σ_f. The vector $\boldsymbol{d}$ includes deterministic design variables ($\boldsymbol{x}_d$) as well as the mean values of the random design variables ($\boldsymbol{x}_r$), i.e., $\boldsymbol{d} = [\boldsymbol{x}_d \ \boldsymbol{\mu}_{x_r}]$; $\boldsymbol{\mu}_p$ is the vector of mean values of random design parameters ($\boldsymbol{p}$); g_j is the jth inequality constraint; $E(g_j)$ is the mean and σ_{g_j} is the standard deviation of the jth inequality constraint; $h_j(\boldsymbol{d}, \boldsymbol{\mu}_p)$ is the jth equality constraint; $\boldsymbol{LB}$ and $\boldsymbol{UB}$ are the vectors of lower and upper bounds of all inequality constraints. The vectors $\boldsymbol{lb}$ and $\boldsymbol{ub}$ represent lower and upper bounds of all the design variables, respectively; $nrdv$ and $nddv$ are the numbers of the random design variables and deterministic design variables, respectively; $\sigma(\boldsymbol{x}_r)$ is the vector of standard deviations of the random design variables and k is a user-defined constant. The value of k sets the level of the conservativeness of the solution by reducing preset bounds by a value of k-standard deviation. In this thesis, k is chosen to be 1, which indicates that, with 84.13% probability, the constraint will be satisfied under the assumption that constraint functions are normally distributed. For $k = 2$ and $k = 3$, the corresponding probabilities are 97.72% and 99.87%, respectively.

The mean μ_f and the variance σ_f of the objective function are approximated using first-order Taylor series expansions (Park et al., 2006), as follows:

$$\mu_f \cong f(\boldsymbol{d}, \boldsymbol{\mu}_p) \tag{18}$$

$$\sigma_f^2 \cong \sum_{i=1}^{nrdv} \left(\frac{\partial f}{\partial d_i}\right)^2 \sigma_{d_i}^2 + \sum_{i=1}^{nrp} \left(\frac{\partial f}{\partial p_i}\right)^2 \sigma_{p_i}^2 \tag{19}$$

In Eq. (19), $\frac{\partial f}{\partial d_i}$ is the partial derivative of the objective function with respect to ith random design variable; $\sigma_{d_i}^2$ is the variance of ith random design variable; $\frac{\partial f}{\partial p_i}$ is the partial derivative of the objective function with respect to ith random design parameter; $\sigma_{p_i}^2$ is the variance of ith random design parameter.

In the same way, the mean $E(g_j)$ and the standard deviation σ_{g_j} of the jth constraint can be approximated using first-order Taylor series expansion, as follows:

$$E(g_j) \cong g_j(\boldsymbol{d}, \boldsymbol{\mu}_p) \tag{20}$$

$$\sigma_{g_j}^2 \cong \sum_{i=1}^{nrdv} \left(\frac{\partial g_j}{\partial d_i}\right)^2 \sigma_{d_i}^2 + \sum_{i=1}^{nrp} \left(\frac{\partial g_j}{\partial p_i}\right)^2 \sigma_{p_i}^2 \tag{21}$$

In Eq. (20), $\frac{\partial g_j}{\partial d_i}$ and $\frac{\partial g_j}{\partial p_i}$ are the partial derivatives of jth inequality constraint function with respect to ith random design variable and ith random design parameter, respectively.

The RDO formulation used in this thesis assumes— random design variables and random design parameters are normally distributed; all random variables are mutually independent; the values of their mean and variance are known. Note that the partial derivative expressions in Eqs. (19) and (21) are evaluated in terms of $\boldsymbol{d}$ and $\boldsymbol{\mu}_p$ during the optimization process.

In addition to RDO, there exists another optimization approach to deal with uncertainty in input variables, known as reliability-based design optimization (RBDO), which is discussed in the following section.

4.3 Reliability-based design optimization (RBDO)

In the field of optimization, RBDO is a tool that optimizes objective function(s) ensuring that the reliabilities of the inequality constraints or limit state functions are above an acceptable threshold limit, considering the uncertainty in design variables and system parameters. A reliability of 0.99 for an inequality constraint implies that the constraint will not be violated in 99% cases under uncertainty of the input variables. In case of equality constraints, the equality relation must hold under uncertainty of the input variables. Reliability estimation requires an analysis of uncertainty to calculate failure probability that is used in the constraint. A typical RBDO problem can be formulated as:

$$\underset{\boldsymbol{d}}{minimize} \quad f(\boldsymbol{d}, \boldsymbol{\mu}_p) \tag{22}$$

$$subject\ to,$$

$$P_{f_j} = P(g_j(\boldsymbol{x}_r, \boldsymbol{p}) \leq 0) \leq P_{f_j}^{allowable}; \qquad \text{for all } j$$

$$h_j(\boldsymbol{d}, \boldsymbol{\mu}_p) = 0; \qquad \text{for all } j$$

$$\boldsymbol{lb} \leq \boldsymbol{d} \leq \boldsymbol{ub};$$

Here, $f(\boldsymbol{d}, \boldsymbol{\mu}_p)$ is the objective function; $\boldsymbol{d}$ is the vector of deterministic design variables ($\boldsymbol{x}_d$) as well as the mean values of the random design variables ($\boldsymbol{x}_r$), i.e., $\boldsymbol{d} = [\boldsymbol{x}_d\ \boldsymbol{\mu}_{x_r}]$; $\boldsymbol{\mu}_p$ is the vector of mean values of random design parameters ($\boldsymbol{p}$); $g_j(\boldsymbol{x}_r, \boldsymbol{p})$ is the jth inequality constraint, which is also referred to as 'limit state function' in RBDO literature; P_{f_j} and $P_{f_j}^{allowable}$ represent the failure probability and allowable (maximum) failure probability for jth inequality constraint, respectively; $h_j(\boldsymbol{d}, \boldsymbol{\mu}_p)$ is the jth equality constraint. The vectors $\boldsymbol{lb}$ and $\boldsymbol{ub}$ represent lower and upper bounds of all the design variables, respectively. Note that the objective function value is estimated at $\boldsymbol{d}$ and $\boldsymbol{\mu}_p$ in RBDO. The first constraint is referred to as a probabilistic formulation of the inequality constraints or limit state functions. In RBDO literature, the functional relation $g_j(\boldsymbol{x}_r, \boldsymbol{p})$ is expressed in such a manner that failure or violation of inequality constraint is denoted by $g_j(\boldsymbol{x}_r, \boldsymbol{p}) \leq 0$.

The failure probability P_{f_j} for the jth inequality constraint may be obtained by evaluating the integral in Eq. (23), which is the fundamental expression of the structural reliability problem:

$$P_{f_j} = \int_{g_j(\boldsymbol{x}_r, \boldsymbol{p}) \leq 0} f_r(\boldsymbol{r}) d\boldsymbol{r} \tag{23}$$

Here, $\boldsymbol{r}$ is the vector of all the random variables (i.e., $\boldsymbol{r} = [\boldsymbol{x}_r\ \boldsymbol{p}]$); $f_r(\boldsymbol{r})$ is the joint probability density function (PDF) of random vector $\boldsymbol{r}$. Note that $g_j(\boldsymbol{x}_r, \boldsymbol{p})$ can also be rewritten as $g_j(\boldsymbol{r})$. Elements of $\boldsymbol{r}$ are assumed to be statistically independent and normally distributed.

The integral of Eq. (23) cannot be evaluated directly due to the unavailability of joint PDF for a large number of the random variables. Hence, several methods have been developed to approximate the integral for estimating the failure probability. These methods can be categorized into 3 major classes (Lopez et al., 2011), as follows:

(i) *Simulation methods*: Monte Carlo simulation (MCS) (Rubinstein and Kroese, 2016) is the most commonly used simulation method used for estimating the failure probability. It is computationally expensive and usually, it is used as the reference response to validate other approximation methods (Lopez and Beck, 2012). Other simulation methods include quasi-MCS (Niederreiter and Spanier, 2000), directional simulation (Nie and Ellingwood, 2000) and importance sampling (Engelund and Rackwitz, 1993).

(ii) *Numerical integration*: Multidimensional numerical integration methods can be employed for estimating failure probability (Seo and Kwak, 2002; Lee and Kwak, 2006). However, these methods are limited to dimension 5 or 6 (Lopez and Beck, 2012).

(iii) *Analytical methods*: First Order Reliability Method (FORM) is the most common analytical approach for estimating the failure probability. Second Order Reliability Method (SORM) is another analytical approach which is more accurate but computationally expensive compared to FORM. Detailed literature on FORM and SORM can be found in Mahadevan and Haldar (2000).

This thesis uses the FORM-based RBDO. In the FORM approach, failure probability for any limit state function can be estimated using 3 steps (McDonald and Mahadevan, 2008). These are as follows—

<u>Step 1:</u> Transformation of the random variables $\boldsymbol{r}$ to the standard normal space $\boldsymbol{u}$, such that

$$u_i = \frac{r_i - \mu_{r_i}}{\sigma_{r_i}}; \quad \text{for all } i \tag{24}$$

<u>Step 2:</u> Calculation of the most probable point (MPP) of failure, $\boldsymbol{u}^*$. This point is the solution to the constrained optimization problem—

$$\boldsymbol{u}^* = \arg\ min\,(\|\boldsymbol{u}\| |\ g(\boldsymbol{u}) = 0) \tag{25}$$

Here, $\|\boldsymbol{u}\|$ is the Euclidean norm of vector $\boldsymbol{u}$; $g(\boldsymbol{u})$ represents a limit state function. This optimization problem can be solved using the algorithms proposed in Rackwitz and Flessler, (1978), and Zhang and Der Kiureghian (1995).

<u>Step 3:</u> Calculation of the reliability index β. For most practical problems, β is greater than zero, in which case β is also equal to $\|\boldsymbol{u}^*\|$. The probability of failure is approximated as:

$P_f = \Phi(-\beta)$, where Φ is the standard Gaussian cumulative distribution function (CDF).

The main challenge in RBDO lies in handling the reliability constraints stated in Eq. (22), (Zaman and Mahadevan, 2017). RBDO methods can be classified into 3 groups based on how reliability analysis is handled in the optimization process (Sopory et al., 2004). These are— (i) nested double loop methods, (ii) single loop methods, and (iii) decoupled methods. RBDO based on FORM is a nested double loop approach that requires an optimization loop as well as a reliability loop, i.e., two optimizations are coupled. Such coupling of the two optimization loops is computationally expensive. Several single loop methods (Madsen and Hansen, 1992; Liang et al., 2004) and decoupled methods (Royset et al., 2001; Du and Chen, 2004; Zou et al., 2004) have been developed to reduce the computational burden of the nested approach.

RBDO based on FORM can be classified into two approaches— Reliability Index Approach (RIA) (Madsen et al., 1986; Melchers, 1999; Haldar and Mahadevan, 2000) and Performance Measure Approach (PMA) (Tu et al., 1999). The difference between RIA and PMA lies in the approach by which MPP is calculated. RIA calculates the MPP using the formulation as stated in Eq. (25): $\boldsymbol{u}^* = \arg\, min\,(\|\boldsymbol{u}\| \mid g(\boldsymbol{u}) = 0)$. On the other hand, PMA uses the formulation: $\boldsymbol{u}^* = \arg\, min\,(g(\boldsymbol{u}) \mid \|\boldsymbol{u}\| = \beta^T)$, where, β^T is the target reliability index for the limit state function (Lopez and Beck, 2012).

In this thesis, RBDO based on FORM is used that follows RIA. Therefore, the RBDO formulation stated by Eq. (22) can be reformulated as follows:

$$
\begin{aligned}
&\underset{\boldsymbol{d}}{minimize} \quad f(\boldsymbol{d}, \boldsymbol{\mu}_p) \\
&subject\ to, \\
&\qquad P_{f_j} = \Phi(-\beta_j) \le P_{f_j}^{allowable}; \\
&\qquad \text{where, } \beta_j = \|\boldsymbol{u}_j^*\|; \text{ and} \qquad\qquad \text{for all } j \\
&\qquad\qquad \boldsymbol{u}_j^* = \arg\, min\,(\|\boldsymbol{u}\| \mid g_j(\boldsymbol{u}) = 0) \\
&\qquad h_j(\boldsymbol{d}, \boldsymbol{\mu}_p) = 0; \qquad\qquad \text{for all } j \\
&\qquad \boldsymbol{lb} \le \boldsymbol{d} \le \boldsymbol{ub};
\end{aligned}
\tag{26}
$$

Note that the probabilistic formulation of reliability constraints stated in Eq. (22) is substituted by the reliability constraints of Eq. (26).

The RBDO formulation stated in Eq. (26) , is used to solve the design problem of the flexible multi-cavity insert. Note that RBDO used in this thesis is formulated to deal with aleatory uncertainty only; epistemic uncertainty is out of the scope of this thesis.

4.4 Multi-objective optimization

In many practical applications, a designer may want to optimize two or more objective functions simultaneously. These are called multi-objective, multi-criteria or vector optimization problems. An extensive survey on multi-objective optimization methods can be found in Arora (2004). Common approaches to multi-objective optimization include the weighted-sum method, ε-constraint method, global criterion method, lexicographic method, etc. These approaches are discussed briefly in the following subsections. Note that, in the following subsections, multi-objective optimization approaches use formulations that are developed in the essence of deterministic optimization. Necessary modifications will be required in the formulations if these approaches are to be employed in RDO or RBDO, as discussed in Section 4.2 and 4.3 respectively.

4.4.1 Weighted-sum method

This is a method that aggregates all the objective functions by multiplying each of them with a weighting coefficient w_i to form a single function, which is then minimized. The value of the weighting coefficients generally reflects the relative importance of the objectives. The optimization problem is formulated as follows:

$$\begin{aligned} &\underset{\boldsymbol{x}}{minimize} \quad \sum_{i=1}^{I} w_i f_i(\boldsymbol{x}) \qquad (27) \\ &subject\ to, \\ &\qquad g_j(\boldsymbol{x}) \leq 0; \quad \text{for all } j \\ &\qquad h_j(\boldsymbol{x}) = 0; \quad \text{for all } j \\ &\qquad \boldsymbol{lb} \leq \boldsymbol{x} \leq \boldsymbol{ub} \\ &\qquad \textstyle\sum_{i=1}^{I} w_i = 1; \quad w_i > 0 \end{aligned}$$

Here, $f_i(\boldsymbol{x})$ is the ith objective function; w_i is the weighting coefficient of ith objective function.

The weighting coefficients w can be used in two ways— the user may either set w_i to reflect preferences or systematically alter w_i to yield different Pareto optimal points.

In the weighted-sum method, it is recommended to scale the objective functions if their respective unit differs by a large magnitude, e.g., one objective function is in 'µm' and another objective function is in 'MPa'. The objective function in Eq. (27) can be modified following a common scaling approach as follows:

$$\sum_{i=1}^{I} w_i \frac{f_i(\boldsymbol{x}) - f_i^{min}(\boldsymbol{x}^*)}{f_i^{max}(\boldsymbol{x}^*) - f_i^{min}(\boldsymbol{x}^*)} \tag{28}$$

Here, $f_i^{min}(\boldsymbol{x}^*)$ and $f_i^{max}(\boldsymbol{x}^*)$ are the minimum and maximum functional values of ith objective function. Each of $f_i^{min}(\boldsymbol{x}^*)$ and $f_i^{max}(\boldsymbol{x}^*)$ is obtained by optimizing ith objective function, subject to existing constraints while disregarding the rest of the objective functions during the optimization process.

4.4.2 ε-constraint method

The ε-constraint approach minimizes the single most important objective function $f_s(\boldsymbol{x})$ with other objective functions treated as constraints. The optimization problem is formulated as follows:

$$\begin{aligned} &\underset{\boldsymbol{x}}{minimize} \quad f_s(\boldsymbol{x}) \\ &subject\ to, \\ &\qquad g_j(\boldsymbol{x}) \le 0; \quad \text{for all } j \\ &\qquad h_j(\boldsymbol{x}) = 0; \quad \text{for all } j \\ &\qquad f_i(\boldsymbol{x}) \le \varepsilon_i; \quad i = 1 \text{ to } I; \quad i \ne s \\ &\qquad \boldsymbol{lb} \le \boldsymbol{x} \le \boldsymbol{ub} \end{aligned} \tag{29}$$

Here, $f_s(\boldsymbol{x})$ is the single most important objective function, and other objective functions ($f_i(\boldsymbol{x});\ i \ne s$) are incorporated as constraints; ε_i is the expected value used as corresponding upper bound for $f_i(\boldsymbol{x})$. Variation of ε_i can yield a set of Pareto optimal solutions.

4.4.3 Global criterion method

Global criterion method involves no subjective information on the preference of decision-maker regarding the objective functions $f_i(\boldsymbol{x})$. This is a scalarization method that aggregates all objective functions to form a single function which is then minimized. The aggregation approach in this method differs from that of the weighted-sum method. At first, optimal solution, $f_i(\boldsymbol{x}^*)$ for the ith objective function is to be determined, subject to existing constraints while disregarding the rest of the objective functions during the optimization process. Next, all the objective functions are aggregated to form a single objective function that minimizes the difference between the individual objective function and its optimal solution, with respect to the optimal solution, as expressed in Eq. (30). The optimization problem is formulated as follows:

$$\underset{\boldsymbol{x}}{minimize} \quad \left\{ \sum_{i=1}^{I} \left\{ \frac{f_i(\boldsymbol{x}^*) - f_i(\boldsymbol{x})}{f_i(\boldsymbol{x}^*)} \right\}^p \right\}^{\frac{1}{p}} \tag{30}$$

$$subject\ to,$$

$$g_j(\boldsymbol{x}) \leq 0; \quad \text{for all } j$$

$$h_j(\boldsymbol{x}) = 0; \quad \text{for all } j$$

$$\boldsymbol{lb} \leq \boldsymbol{x} \leq \boldsymbol{ub}$$

Here, $f_i(\boldsymbol{x}^*)$ is the optimal solution for the ith objective function. Note that the objective function in Eq. (30) includes a parameter p that is proportional to the amount of emphasis placed on minimizing the function with the largest difference between $f_i(\boldsymbol{x})$ and $f_i(\boldsymbol{x}^*)$ with respect to $f_i(\boldsymbol{x}^*)$. The parameter p is assigned a fixed value during the optimization process, commonly the value '2'.

4.4.4 Lexicographic method

In the lexicographic method, preferences are imposed by ordering the objective functions according to their attractiveness and importance to the decision-maker. Objective functions $f_i(\boldsymbol{x})$ are ranked such that $f_1(\boldsymbol{x})$ is the most important; followed by $f_2(\boldsymbol{x})$, $f_3(\boldsymbol{x})$ and so on. The optimization problem is formulated as follows:

$$\underset{\boldsymbol{x}}{minimize} \quad f_i(\boldsymbol{x}) \tag{31}$$

$$subject\ to,$$

$$g_j(\boldsymbol{x}) \leq 0; \quad \text{for all } j$$

$$h_j(\boldsymbol{x}) = 0; \quad \text{for all } j$$

$$f_l(\boldsymbol{x}) \leq f_l(\boldsymbol{x}_l^*); \quad l = 1\ to\ (i-1); \quad i > 1$$

$$\boldsymbol{lb} \leq \boldsymbol{x} \leq \boldsymbol{ub}$$

Here, $f_l(\boldsymbol{x}_l^*)$ represents the optimum value for the lth objective function, found in the lth optimization problem.

This method involves a series of steps. First, the most important objective function $f_1(\boldsymbol{x})$ is optimized to obtain $f_1(\boldsymbol{x}_1^*)$, disregarding all other objective functions, subject to existing constraints. Next, $f_2(\boldsymbol{x})$ is optimized to obtain $f_2(\boldsymbol{x}_2^*)$, subject to one additional constraint

$f_1(\boldsymbol{x}) \leq f_1(\boldsymbol{x}_1^*)$. After that, $f_3(\boldsymbol{x})$ is optimized to obtain $f_3(\boldsymbol{x}_3^*)$, now subject to two additional constraints $f_1(\boldsymbol{x}) \leq f_1(\boldsymbol{x}_1^*)$ and $f_2(\boldsymbol{x}) \leq f_2(\boldsymbol{x}_2^*)$ and the process goes on in this manner. The algorithm terminates once a unique optimum is determined that is indicated when two consecutive optimization problems yield the same solution point, i.e., $\boldsymbol{x}_i^* = \boldsymbol{x}_{i-1}^*$.

This thesis uses the weighted-sum method in RDO and RBDO, for the sake of illustration. The following chapter discusses the different methodologies of multidisciplinary design optimization (MDO).

CHAPTER 5

MULTIDISCIPLINARY DESIGN OPTIMIZATION (MDO)

Engineering design optimization often encounters complex systems that comprise of multiple sub-systems or disciplines. Conventional optimization methodologies can be employed to optimize such systems if the disciplines are mutually independent. Complexity arises when there exist interactions between the disciplines. Multidisciplinary design optimization (MDO) emerged as a tool for the optimization of a complex system containing two or more disciplines that are coupled (Chiralaksanakul and Mahadevan, 2007). Two disciplines are said to be coupled if the analysis of one discipline depends on the output from the other one and vice versa. The output of MDO gives such values of design variables that optimize the overall system-level output ensuring compatibility among the coupled disciplines. The benefits of this system are vast yet limited to only a few fields, like aerospace, automobile, etc.

MDO highly depends on the multidisciplinary analysis (MDA) that involves integrating individual discipline-specific analyses, which are coupled with one another through shared input and output data. This coupling is mathematically represented by 'coupling variables' derived as output from one discipline but required as input to other disciplines. The feasibility of a multidisciplinary system depends on a set of compatible coupling variables that satisfy all disciplinary analyses simultaneously (Cramer et al., 1994). Figure 5.1 shows coupling in a two-discipline system (Mahadevan and Smith, 2006), for the sake of illustration:

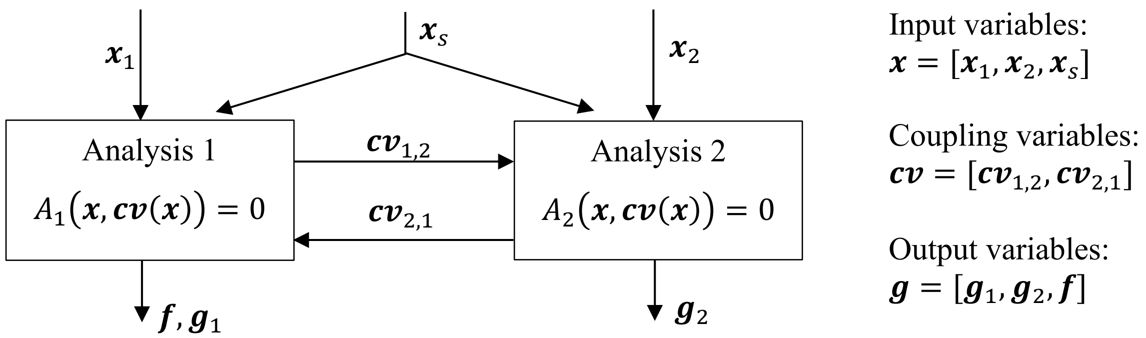

Figure 5.1: Feedback coupling of a two-discipline system

Here, $\boldsymbol{x}_1$ and $\boldsymbol{x}_2$ represent the vectors of local input variables to Analyses 1 and 2, respectively; $\boldsymbol{x}_s$ indicates the vector of input variables common to both analyses; $\boldsymbol{cv}_{1,2}$ and $\boldsymbol{cv}_{2,1}$ are the vectors of disciplinary coupling variables (defined such that $\boldsymbol{cv}_{i,j}$ $(i \neq j)$ is an output of disciplinary analysis i and an input to disciplinary analysis j); $\boldsymbol{cv}$ is the vector of all disciplinary coupling variables. The system output variables are $\boldsymbol{f}$, $\boldsymbol{g}_1$ and $\boldsymbol{g}_2$ in the context of optimization, $\boldsymbol{f}$ may represent a system objective function and $\boldsymbol{g}_1$, $\boldsymbol{g}_2$ may represent system constraints or limit-state functions for reliability analysis. $A_1\big(\boldsymbol{x}, \boldsymbol{cv}(\boldsymbol{x})\big)$ and $A_2\big(\boldsymbol{x}, \boldsymbol{cv}(\boldsymbol{x})\big)$ represent analyses of discipline 1 and discipline 2, respectively, that must be satisfied simultaneously to ensure the system compatibility. The system compatibility equations can be represented by Eq. (32), as follows:

$$A_j\big(\boldsymbol{x}, \boldsymbol{cv}(\boldsymbol{x})\big) = 0; \quad \text{for all } j \tag{32}$$

The two disciplinary analyses in Figure 5.1 are coupled by $\boldsymbol{cv}_{1,2}$ and $\boldsymbol{cv}_{2,1}$; hence, individual disciplinary analyses cannot be performed independently. In such cases, an iterative loop is required between these disciplines to solve the system compatibility equations that must be converged before getting realizations of the objective function and the constraints or limit-state functions. This convergence criterion between the disciplines is represented by the system compatibility or feasibility equations, e.g., Eq. (32). Several methodologies are found in MDO literature to deal with the system compatibility equations using different approaches. Common MDO methods include the multidisciplinary feasible (MDF) method, the all-at-once (AAO) method, and the individual disciplinary feasible (IDF) method. A detailed survey on the MDF, AAO, and IDF methods can be found in Cramer et al. (1994), and Chiralaksanakul and Mahadevan (2007).

The MDF, AAO, and IDF approaches are discussed briefly in the following sections.

5.1 Multidisciplinary feasible (MDF) method

MDF method is designed to solve the system compatibility equations outside the optimization algorithm as depicted in Figure 5.2.

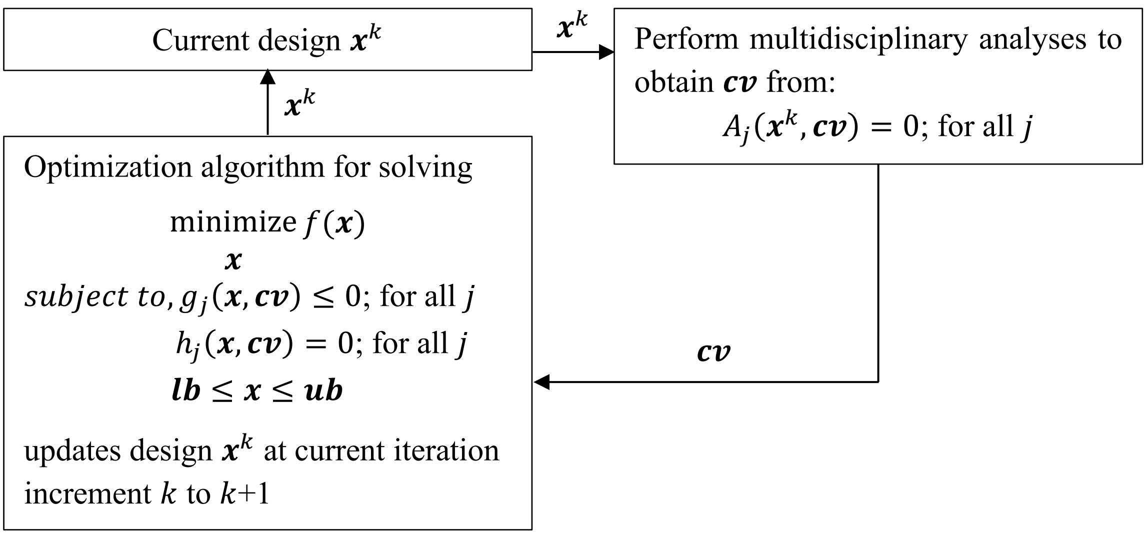

Figure 5.2: Diagram of the multidisciplinary feasible (MDF) method

Here, $f(\boldsymbol{x})$ is the objective function; $\boldsymbol{x}$ is the vector of design variables, $\boldsymbol{cv}$ is the vector of all disciplinary coupling variables, $g_j(\boldsymbol{x}, \boldsymbol{cv})$ is the jth inequality constraint or limit-state function for reliability analysis, $h_j(\boldsymbol{x}, \boldsymbol{cv})$ is the jth equality constraint, and $\boldsymbol{lb}$ and $\boldsymbol{ub}$ are the vectors of lower and upper bounds of design variables. $A_j(\boldsymbol{x}^k, \boldsymbol{cv})$ represents the system compatibility requirements involved in jth discipline that must be satisfied by the coupling variables ($\boldsymbol{cv}$) for a set of input design variables ($\boldsymbol{x}^k$) at each iteration.

Note that the objective function is to be minimized with respect to the design variables $\boldsymbol{x}$. All the system compatibility equations ($A_j(\boldsymbol{x}^k, \boldsymbol{cv}) = 0$; for all j) are solved outside the optimization process to obtain $\boldsymbol{cv}$, and then passed to the optimization algorithm. The obtained $\boldsymbol{cv}$ values are used to get realizations of the performance functions during the optimization process. In MDO literature, solving all the system compatibility equations simultaneously for compatible $\boldsymbol{cv}$ is referred to as 'multidisciplinary analysis'. The MDF method uses iterative loop that starts with an initial guess of design variables, which are used to carry out multidisciplinary analysis to obtain compatible coupling variables; the coupling variables are then passed to the optimization algorithm that produces a new set of design variables; the new set of design variables is used for multidisciplinary analysis in the next iteration, and the process continues until convergence.

5.2 All-at-once (AAO) method

AAO method is designed to solve the system compatibility equations inside the optimization algorithm by treating them as equality constraints, i.e., no multidisciplinary analyses or individual disciplinary analyses are performed outside the optimization algorithm. The AAO method is also known as the simultaneous analysis and design method in Haftka (1985), and the sequential compatibility constraint method in Braun et al. (1995).

In the AAO approach, the coupling variables are treated as optimization variables along with the design variables during the optimization process. Initial guesses for the coupling variables are required at the beginning of the optimization process since they are included as optimization variables. The feasibility of the system compatibility equations depends on the choice of initial guesses for the coupling variables. The evaluation of system compatibility equations for incompatible coupling variables may be difficult or impossible since the computer codes involved are typically designed for only compatible coupling variables (Chiralaksanakul and Mahadevan, 2007). The AAO method is depicted in Figure 5.3, as follows:

Current design $\boldsymbol{x}^k$ and $\boldsymbol{cv}^k$

Optimization algorithm for solving

$$\underset{\boldsymbol{x},\boldsymbol{cv}}{\text{minimize}}\ f(\boldsymbol{x})$$

$$\begin{aligned} \textit{subject to},\quad & g_j(\boldsymbol{x},\boldsymbol{cv}) \le 0;\ \text{for all } j \\ & h_j(\boldsymbol{x},\boldsymbol{cv}) = 0;\ \text{for all } j \\ & A_j(\boldsymbol{x},\boldsymbol{cv}) = 0;\ \text{for all } j \\ & \boldsymbol{lb} \le \boldsymbol{x} \le \boldsymbol{ub} \end{aligned}$$

updates design $\boldsymbol{x}^k$ and $\boldsymbol{cv}^k$ at current iteration

increment k to k+1

Figure 5.3: Diagram of the all-at-once (AAO) method

Here, $A_j(\boldsymbol{x},\boldsymbol{cv})$ are the system compatibility equations that treated as equality constraints. Note that the objective function is to be minimized with respect to the design variables $\boldsymbol{x}$ as well as the coupling variables $\boldsymbol{cv}$.

In AAO, the feasibility of the system compatibility equations is not attempted when far from optimum; multidisciplinary feasibility is automatically satisfied only at the optimization convergence (Zaman and Mahadevan, 2017).

5.3 Individual discipline feasible (IDF) method

The IDF method decouples the system analysis (by disciplines) and performs each disciplinary analysis separately, outside the optimization algorithm (Chiralaksanakul and Mahadevan, 2007). In MDO literature, 'disciplinary analysis' refers to solving system compatibility equations involved in only one discipline at a time. Thus, disciplinary analysis is different from the multidisciplinary analysis that solves all the system compatibility equations simultaneously for compatible coupling variables for all the disciplines, as discussed in section 5.1.

Similar to the AAO approach, IDF also treats the coupling variables as optimization variables along with the design variables during the optimization process. IDF uses 'surrogate coupling variables' $\boldsymbol{cv}_{js}$ corresponding to each coupling variables $\boldsymbol{cv}_j$ in order to carry out the jth disciplinary analysis. In IDF, interdisciplinary compatibility needs to be satisfied since individual disciplinary analyses are performed separately. The additional equality constraints: $\boldsymbol{cv} - \boldsymbol{cv}_s = 0$ needs to be included in IDF to ensure interdisciplinary compatibility.

The IDF method uses iterative loop that starts with an initial guess of design variables as well as the coupling variables (since the coupling variables are treated as optimization variables); individual disciplinary analyses are carried out to obtain compatible surrogate coupling variables corresponding to that discipline, using initial guesses of design variables and coupling variables corresponding to other disciplines as input during the analyses; the surrogate coupling variables from each disciplinary analyses are then passed to the optimization algorithm that produces a new set of design variables and coupling variables; the new set of design variables and coupling variables is used for individual disciplinary analyses in the next iteration, and the process continues until convergence. The IDF method is depicted in Figure 5.3, as follows:

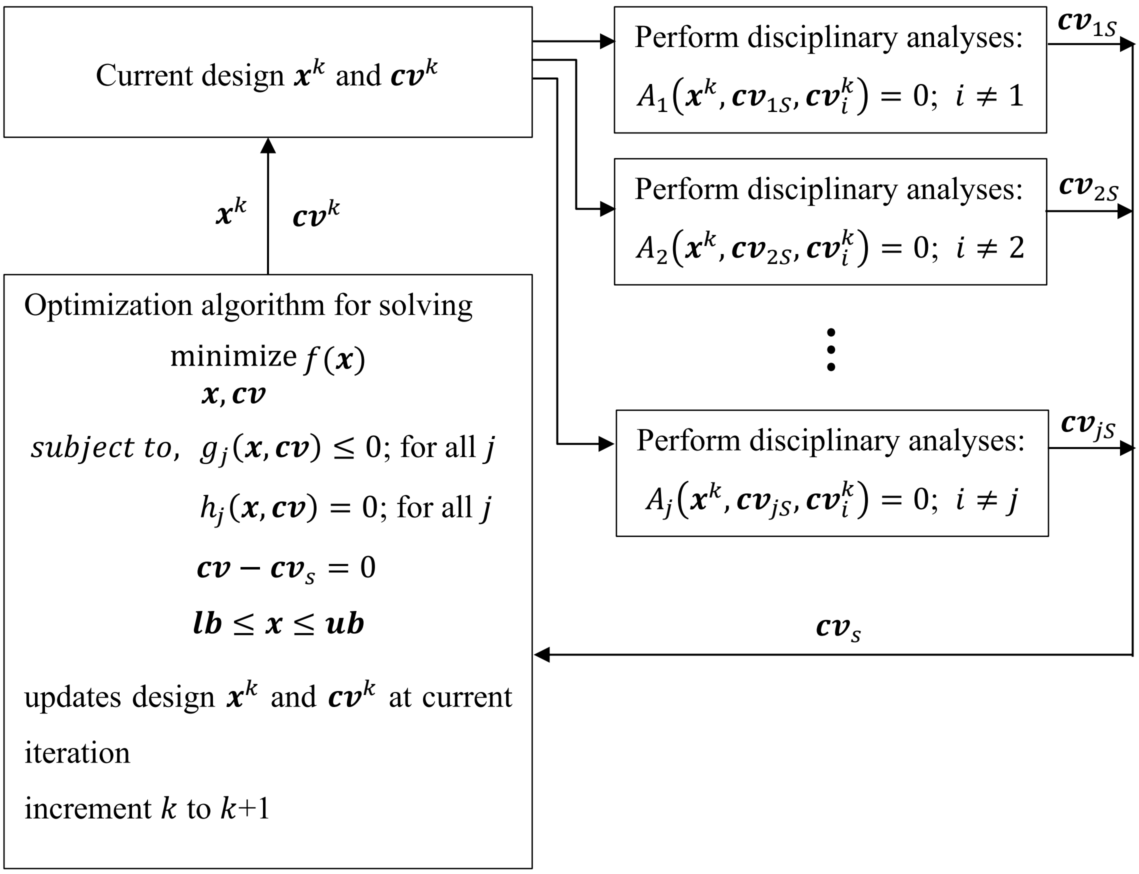

Figure 5.4: Diagram of the individual discipline feasible (IDF) method

Here, $A_j(\boldsymbol{x}^k, \boldsymbol{cv}_{jS}, \boldsymbol{cv}_i^k)$ represents the system compatibility equations involved in jth discipline that must be satisfied by jth disciplinary surrogate coupling variables ($\boldsymbol{cv}_{jS}$) for a set of input design variables ($\boldsymbol{x}^k$) and coupling variables of all other disciplines ($\boldsymbol{cv}_i^k;\ i \neq j$), at each iteration. Note that the objective function is to be minimized with respect to the design variables $\boldsymbol{x}$ as well as the coupling variables $\boldsymbol{cv}$. Unlike the MDF approach, all the system compatibility equations are not solved simultaneously, rather individual disciplinary analyses are performed separately at each iteration. For example, in analyses of discipline-1, system compatibility equations involved in discipline-1 are solved, to obtain corresponding disciplinary surrogate coupling variables $\boldsymbol{cv}_{1S}$ for a set of input design variables ($\boldsymbol{x}^k$) and coupling variables of the rest of the disciplines ($\boldsymbol{cv}_i^k$; $i \neq 1$). Thus, disciplinary surrogate coupling variables are obtained from individual disciplinary analyses that combinedly form the vector $\boldsymbol{cv}_s$, which is then passed to the optimization process (Figure 5.4). The value of surrogate coupling variables $\boldsymbol{cv}_s$ is incorporated in the optimization process with the help of the equality constraint: $\boldsymbol{cv} - \boldsymbol{cv}_s = 0$, that ensures interdisciplinary compatibility.

Note that the three methods – MDF, AAO and IDF as discussed in Sections 5.1-5.3 use deterministic formulation, i.e., uncertainty in input variables are not considered. The deterministic formulations need to be modified to incorporate uncertainty using robustness-based design optimization (RDO) formulation or reliability-based design optimization (RBDO) formulation. This thesis, for the sake of illustration, uses MDF and AAO methods for both RDO, and RBDO to find the optimum design for the flexible multi-cavity insert. The following sections discuss RDO/MDF, RDO/AAO, RBDO/MDF, and RBDO/AAO formulations, respectively.

5.4 RDO/MDF

The RDO/MDF formulation integrates the concept of robustness-based design optimization (RDO) within the deterministic formulation of the multidisciplinary feasible (MDF) method. The four elements of RDO – (i) objective robustness; (ii) feasibility robustness; (iii) estimating mean and measure of variation (variance) of the performance function and (iv) multi-objective optimization, as discussed in Section 4.2, are incorporated with deterministic MDF (Figure 5.5). The RDO/MDF formulation used in this thesis considers aleatory uncertainty in some design variables ($\boldsymbol{x}_r$) and design parameters ($\boldsymbol{p}$). The uncertain variables are assumed to be normally distributed, and their mean and standard deviation are known. The RDO/MDF formulation considers the coupling variables as deterministic. The RDO/MDF method is depicted in Figure 5.5, as follows:

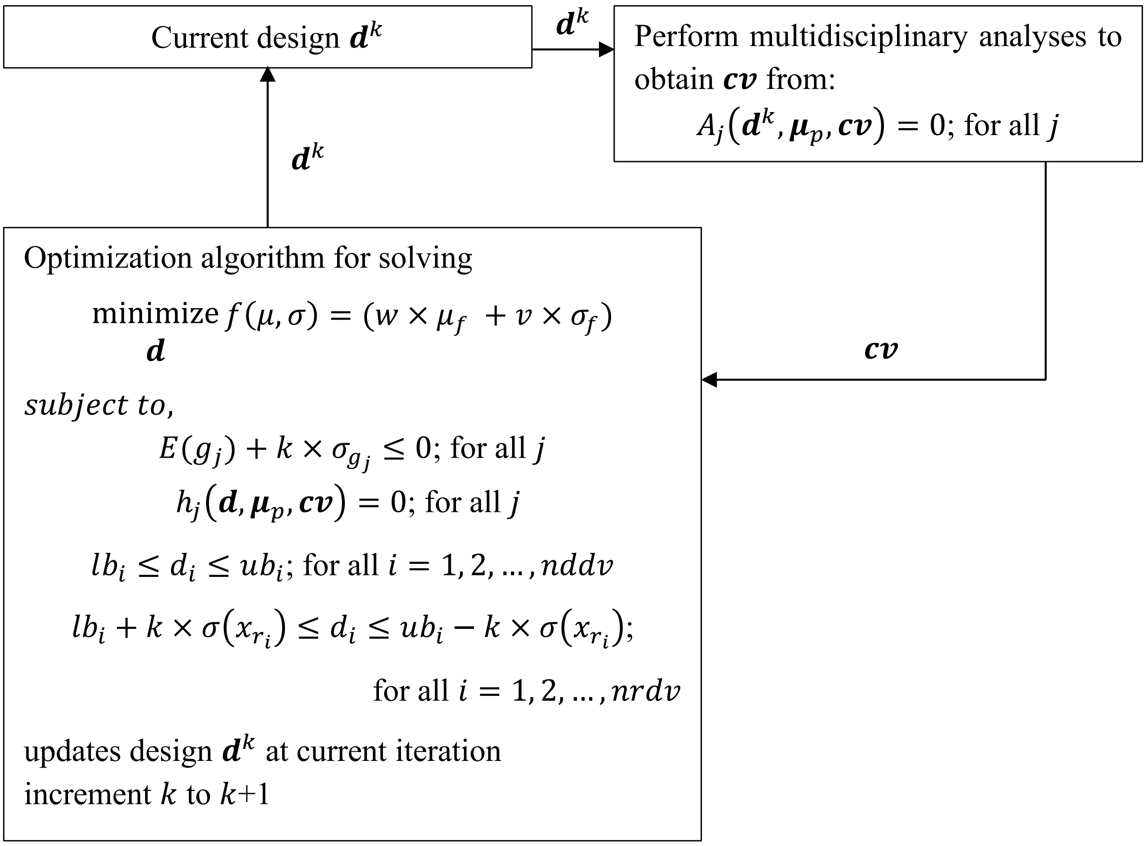

Figure 5.5: Diagram of the RDO/MDF method

Here, μ_f and σ_f are the mean value and standard deviation of the objective function, respectively; w and v are the weighting coefficients under associated conditions: $w \geq 0$; $v \geq 0$; and $w + v = 1$. The weighting coefficients denote the relative importance of μ_f and σ_f. The vector $\boldsymbol{d}$ includes deterministic design variables ($\boldsymbol{x}_d$) as well as the mean values of the random design variables ($\boldsymbol{x}_r$) i.e. $\boldsymbol{d} = [\boldsymbol{x}_d\ \boldsymbol{\mu}_{x_r}]$; $\boldsymbol{\mu}_p$ is the vector of mean values of random design parameters ($\boldsymbol{p}$); $\boldsymbol{cv}$ is the vector of all disciplinary coupling variables; g_j is the jth inequality constraint; $E(g_j)$ is the mean and σ_{g_j} is the standard deviation of the jth inequality constraint; $h_j(\boldsymbol{d}, \boldsymbol{\mu}_p, \boldsymbol{cv})$ is the jth equality constraint. The vectors $\boldsymbol{lb}$ and $\boldsymbol{ub}$ represent lower and upper bounds of all the design variables, respectively; $nrdv$ and $nddv$ are the numbers of the random design variables and deterministic design variables, respectively; $\sigma(\boldsymbol{x}_r)$ is the vector of standard deviations of the random design variables and k is a user-defined constant. In this thesis, k is chosen to be 1. $A_j(\boldsymbol{x}^k, \boldsymbol{\mu}_p, \boldsymbol{cv})$ represents the system compatibility requirements involved in jth discipline that must be satisfied by the coupling variables ($\boldsymbol{cv}$) for a set of input design variables ($\boldsymbol{d}^k$), and $\boldsymbol{\mu}_p$ at each iteration.

The mean μ_f and the variance σ_f of the objective function are approximated using Eq. (33) and Eq. (34) respectively.

$$\mu_f \cong f(\boldsymbol{d}, \boldsymbol{\mu}_p, \boldsymbol{cv}) \tag{33}$$

$$\sigma_f^2 \cong \sum_{i=1}^{nrdv} \left(\frac{\partial f}{\partial d_i}\right)^2 \sigma_{d_i}^2 + \sum_{i=1}^{nrp} \left(\frac{\partial f}{\partial p_i}\right)^2 \sigma_{p_i}^2 \tag{34}$$

In Eq. (34), $\frac{\partial f}{\partial d_i}$ is the partial derivative of the objective function with respect to ith random design variable; $\sigma_{d_i}^2$ is the variance of ith random design variable; $\frac{\partial f}{\partial p_i}$ is the partial derivative of the objective function with respect to ith random design parameter; $\sigma_{p_i}^2$ is the variance of ith random design parameter; $nrdv$ and nrp are the numbers of the random design variables and random design parameters, respectively. Note that the coupling variables are considered deterministic.

The mean $E(g_j)$ and the standard deviation $\sigma_{g_j}$of the jth constraint can be approximated using Eq. (35) and Eq. (36) respectively.

$$E(g_j) \cong g_j(\boldsymbol{d}, \boldsymbol{\mu}_p, \boldsymbol{cv}) \tag{35}$$

$$\sigma_{g_j}^2 \cong \sum_{i=1}^{nrdv} \left(\frac{\partial g_j}{\partial d_i}\right)^2 \sigma_{d_i}^2 + \sum_{i=1}^{nrp} \left(\frac{\partial g_j}{\partial p_i}\right)^2 \sigma_{p_i}^2 \tag{36}$$

In Eq. (36), $\frac{\partial g_j}{\partial d_i}$ and $\frac{\partial g_j}{\partial p_i}$ are the partial derivatives of jth inequality constraint function with respect to ith random design variable and ith random design parameter, respectively.

Note that the objective function is to be minimized with respect to the design variables $\boldsymbol{d}$. All the system compatibility equations ($A_j\left(\boldsymbol{d}^k, \boldsymbol{\mu}_p, \boldsymbol{cv}\right) = 0$; for all j) are solved outside the optimization process to obtain $\boldsymbol{cv}$, and then passed to the optimization algorithm. The obtained $\boldsymbol{cv}$ values are used to get realizations of the performance functions during the optimization process. The RDO/MDF method uses iterative loop that starts with an initial guess for deterministic design variables as well as the mean values of the random design variables that are used to carry out multidisciplinary analysis to obtain compatible coupling variables; the coupling variables are then passed to the optimization algorithm that produces a new set of design variables; the new set of design variables is used for multidisciplinary analysis in the next iteration, and the process continues until convergence.

5.5 RDO/AAO

The RDO/AAO formulation integrates the concept of robustness-based design optimization (RDO) within the deterministic formulation of the all-at-once (AAO) method. From the system compatibility equations represented by Eq. (32), the coupling variable of individual discipline can be expressed as a response variable that is functionally related to the design variables, design parameters and the coupling variables corresponding to other disciplines, as follows:

$$cv_j = F_{\boldsymbol{cv}_j}(\boldsymbol{d}, \boldsymbol{\mu}_p, \boldsymbol{cv}_i); \quad j \neq i \tag{37}$$

Uncertainty in some of the design variables and design parameters propagates uncertainty to the coupling variables; since the response variable of a random variable is also random (Mahadevan and Haldar, 2000). The RDO/AAO formulation treats the mean value of the coupling variables ($\boldsymbol{cv}$) as optimization variables. The standard deviations of the coupling variables are estimated by first-order Taylor series approximation at the mean values of all the input and the coupling variables (Zaman and Mahadevan, 2013), and then solving the following system of equations:

$$\sigma_{cv_j}^2 = \sum_{\substack{i=1 \\ i \neq j}}^{ncv} \left(\frac{\partial F_{\boldsymbol{cv}_j}}{\partial cv_i}\right)^2 \sigma_{cv_i}^2 + \sum_{i=1}^{nrdv} \left(\frac{\partial F_{\boldsymbol{cv}_j}}{\partial d_i}\right)^2 \sigma_{d_i}^2 + \sum_{i=1}^{nrp} \left(\frac{\partial F_{\boldsymbol{cv}_j}}{\partial p_i}\right)^2 \sigma_{p_i}^2; \quad \text{for all } j \tag{38}$$

Here, $\sigma_{cv_j}^2$ is the variance of jth coupling variable; $\sigma_{cv_i}^2$, $\sigma_{d_i}^2$, and $\sigma_{p_i}^2$ are the variances of ith coupling variable, random design variables, and random design parameters, respectively; $F_{\boldsymbol{cv}_j}$ is the functional relationship representing jth coupling variable, as stated in Eq. (37); ncv, $nrdv$, and nrp are the numbers of the coupling variables, random design variables, and random design parameters, respectively.

This thesis uses the single-loop formulation for robustness-based design optimization proposed in Zaman and Mahadevan (2013). The single-loop formulation includes the standard deviation of coupling variables ($\boldsymbol{\sigma}_{cv}$) as optimization variables along with $\boldsymbol{d}$ and $\boldsymbol{cv}$. The inclusion of the standard deviation of coupling variables as optimization variables overcome the difficulty in estimating the standard deviations of the objective function (σ_f) and the constraints (σ_g), respectively. These additional design variables $\boldsymbol{\sigma}_{cv}$will be constrained by Eq. (38). The single-loop formulation of the RDO/AAO method is depicted in Figure 5.6, as follows:

Current design $\boldsymbol{d}^k$, $\boldsymbol{cv}^k$ and $\boldsymbol{\sigma}_{cv}^k$

Optimization algorithm for solving

$$\underset{\boldsymbol{d},\boldsymbol{cv},\boldsymbol{\sigma}_{cv}}{\text{minimize}} \quad f(\mu,\sigma) = (w \times \mu_f + v \times \sigma_f)$$

$subject\ to,$

$$E(g_j) + k \times \sigma_{g_j} \leq 0;\ \text{for all } j$$

$$h_j(\boldsymbol{d}, \boldsymbol{\mu}_p, \boldsymbol{cv}) = 0;\ \text{for all } j$$

$$lb_i \leq d_i \leq ub_i;\ \text{for all } i = 1, 2, \ldots, nddv$$

$$lb_i + k \times \sigma(x_{r_i}) \leq d_i \leq ub_i - k \times \sigma(x_{r_i});\ \text{for all } i = 1, 2, \ldots, nrdv$$

$$A_j(\boldsymbol{d}, \boldsymbol{\mu}_p, \boldsymbol{cv}) = 0;\ \text{for all } j$$

$$\sigma_{cv_j}^2 = \sum_{\substack{i=1 \\ i \neq j}}^{ncv} \left(\frac{\partial F_{\boldsymbol{cv}_j}}{\partial cv_i}\right)^2 \sigma_{cv_i}^2 + \sum_{i=1}^{nrdv} \left(\frac{\partial F_{\boldsymbol{cv}_j}}{\partial d_i}\right)^2 \sigma_{d_i}^2 + \sum_{i=1}^{nrp} \left(\frac{\partial F_{\boldsymbol{cv}_j}}{\partial p_i}\right)^2 \sigma_{p_i}^2; \quad \text{for all } j$$

updates design $\boldsymbol{d}^k$, $\boldsymbol{cv}^k$ and $\boldsymbol{\sigma}_{cv}^k$ at current iteration

increment k to k+1

Figure 5.6: Diagram of the RDO/AAO method

The mean μ_f and the variance σ_f^2 of the objective function are approximated at the mean values of all the input and the coupling variables using Eq. (39) and Eq. (40), respectively.

$$\mu_f \cong f(\boldsymbol{d}, \boldsymbol{\mu}_p, \boldsymbol{cv}) \tag{39}$$

$$\sigma_f^2 \cong \sum_{i=1}^{nrdv} \left(\frac{\partial f}{\partial d_i}\right)^2 \sigma_{d_i}^2 + \sum_{i=1}^{nrp} \left(\frac{\partial f}{\partial p_i}\right)^2 \sigma_{p_i}^2 + \sum_{i=1}^{ncv} \left(\frac{\partial f}{\partial cv_i}\right)^2 \sigma_{cv_i}^2 \tag{40}$$

The mean $E(g_j)$ and the standard deviation σ_{g_j} of the jth constraint can be approximated at the mean values of all the input and the coupling variables using Eq. (41) and Eq. (42), respectively.

$$E(g_j) \cong g_j(\boldsymbol{d}, \boldsymbol{\mu}_p, \boldsymbol{cv}) \tag{41}$$

$$\sigma_{g_j}^2 \cong \sum_{i=1}^{nrdv} \left(\frac{\partial g_j}{\partial d_i}\right)^2 \sigma_{d_i}^2 + \sum_{i=1}^{nrp} \left(\frac{\partial g_j}{\partial p_i}\right)^2 \sigma_{p_i}^2 + \sum_{i=1}^{ncv} \left(\frac{\partial g_j}{\partial cv_i}\right)^2 \sigma_{cv_i}^2 \tag{42}$$

Note that the objective function is to be minimized with respect to $\boldsymbol{d}$, $\boldsymbol{cv}$ and $\boldsymbol{\sigma}_{cv}$ (Figure 5.6); therefore, their initial guesses need to be provided at the beginning of the optimization algorithm. The initial guesses for $\boldsymbol{cv}$ and $\boldsymbol{\sigma}_{cv}$ should be chosen carefully to ensure convergence of the system compatibility equations.

5.6 RBDO/MDF

The RBDO/MDF formulation integrates the concept of reliability-based design optimization (RBDO) within the deterministic formulation of the multidisciplinary feasible (MDF) method. The probabilistic formulation of the inequality constraints or limit state functions, as stated in Eq. (26), is incorporated in deterministic MDF (Figure 5.7). The coupling variables are considered as deterministic. The RBDO/MDF method is depicted in Figure 5.7, as follows:

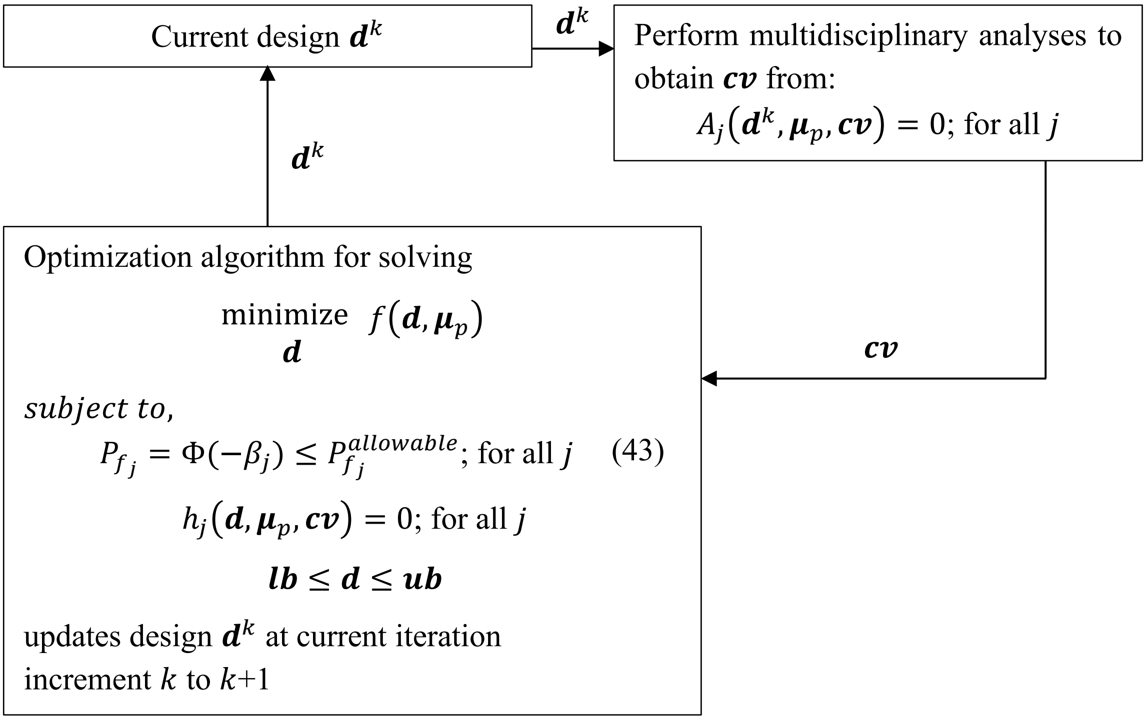

Figure 5.7: Diagram of the RBDO/MDF method

The reliability constraints in Eq. (43) are evaluated using the reliability index β for each of j limit state functions, solving the following optimization problem, as follows:

$$\underset{\boldsymbol{u}}{minimize} \quad \beta_j = \|\boldsymbol{u}\| \tag{44}$$

$$subject\ to,$$

$$g_j(\boldsymbol{u}, \boldsymbol{cv}) = 0 \tag{45}$$

$$A_i(\boldsymbol{u}, \boldsymbol{cv}) = 0; \text{ for all } i \tag{46}$$

Here, $\boldsymbol{u}$ is transformed standard normal space vector corresponding to the vector of all the random variables $\boldsymbol{r} = [\boldsymbol{x}_r\ \boldsymbol{p}]$; $\|\boldsymbol{u}\|$ is the Euclidean norm of vector $\boldsymbol{u}$; $g_j(\boldsymbol{u}, \boldsymbol{cv})$ is the transformed function corresponding to jth limit state function $g_j(\boldsymbol{x}_r, \boldsymbol{p}, \boldsymbol{cv})$, expressed in transformed standard normal space; β_j is the reliability index corresponding to jth transformed limit state function $g_j(\boldsymbol{u}, \boldsymbol{cv})$; $A_i(\boldsymbol{u}, \boldsymbol{cv})$ is the transformed function corresponding to ith system compatibility equation, expressed in transformed standard normal space.

Note that in the evaluation of the reliability index β_j, only jth limit state function is involved (Eq. (45)); however, all the system compatibility equations are included (Eq. (46)). The deterministic design variables and coupling variables are not transformed into standard normal space. The random design variables and random design parameters are transformed as follows:

$$u_{x_{r_i}} = \frac{x_{r_i} - d_i}{\sigma_{x_{r_i}}}; \quad \text{for all } i = 1, 2, \dots, nrdv$$

$$u_{p_i} = \frac{p_i - \mu_{p_i}}{\sigma_{p_i}}; \quad \text{for all } i = 1, 2, \dots, nrp$$

The random variables x_{r_i} and p_i included in the limit state functions and system compatibility equations are substituted by the expressions $(u_{x_{r_i}} \times \sigma_{x_{r_i}} + d_i)$ and $(u_{p_i} \times \sigma_{p_i} + \mu_{p_i})$, respectively, in the evaluation of the reliability index.

5.7 RBDO/AAO

The RBDO/AAO formulation integrates the concept of reliability-based design optimization (RBDO) within the deterministic formulation of the all-at-once (AAO) method. The RBDO/AAO method is depicted in Figure 5.8, as follows:

Current design $\boldsymbol{d}^k$ and $\boldsymbol{cv}^k$

Optimization algorithm for solving

$$\underset{\boldsymbol{d}, \boldsymbol{cv}}{\text{minimize}} \quad f(\boldsymbol{d}, \boldsymbol{\mu}_p, \boldsymbol{cv})$$

subject to,

$$P_{f_j} = \Phi(-\beta_j) \leq P_{f_j}^{allowable}; \text{ for all } j \tag{47}$$

$$h_j(\boldsymbol{d}, \boldsymbol{\mu}_p, \boldsymbol{cv}) = 0; \text{ for all } j$$

$$A_j(\boldsymbol{d}, \boldsymbol{\mu}_p, \boldsymbol{cv}) = 0; \text{ for all } j$$

$$\boldsymbol{lb} \leq \boldsymbol{d} \leq \boldsymbol{ub}$$

updates design $\boldsymbol{d}^k$ and $\boldsymbol{cv}^k$ at current iteration

increment k to k+1

Figure 5.8: Diagram of the RBDO/AAO method

RBDO/AAO differs from RBDO/MDF in two aspects: (1) the system compatibility equations are solved inside the optimization algorithm by treating them as equality constraints, i.e., no multidisciplinary analyses are performed outside the optimization algorithm; (2) the coupling variables are treated as optimization variables along with the design variables during the optimization process.

A detailed survey on multidisciplinary RDO and multidisciplinary RBDO is reported Zaman and Mahadevan (2013), and Zaman and Mahadevan (2017), respectively.

CHAPTER 6

FORMULATIONS OF ROBUST AND RELIABILITY-BASED MULTIDISCIPLINARY OPTIMIZATION OF INJECTION MOLDING SYSTEM

Design of a flexible multi-cavity injection mold that can handle the production of specified plastic part family members with minimized cycle time and pressure drop, subject to the constraints – is the focus of this thesis. Variation of geometric features of the parts to be molded requires the use of design optimization techniques (e.g. robustness-based design optimization (RDO), reliability-based design optimization (RBDO)) that can deal with the uncertainty in the input variables. Furthermore, the multidisciplinary nature of the injection molding system requires multidisciplinary design optimization (MDO) formulation that can satisfy the system compatibility requirements. Formulations of deterministic MDO, multidisciplinary RDO, and multidisciplinary RBDO have been discussed earlier in Chapter 5. This chapter uses the formulations presented in Chapter 5 to formulate the design problem of the flexible multi-cavity injection mold, which has been defined earlier in Chapter 3.

The objective functions, constraints and system compatibility equations involved in the MDO of the design problem are stated collectively followed by the deterministic design optimization formulation, as follows:

<u>Objective functions:</u>

$$
\begin{aligned}
f_1 = {} & \frac{2 \times v_s}{P_{inj} \times p_{inj}} + \frac{d_{gate}^2}{23.1\,\alpha} \times ln\left(0.692 \times \frac{T_{melt} - T_{mold}}{T_{eject} - T_{mold}}\right) \\
& + \frac{\left(d_{sprue} + \tan\left(\frac{\pi\,\alpha_{sprue}}{180}\right) \times l_{sprue}\right)^2}{23.1\,\alpha} \\
& \times ln\left(0.692 \times \frac{T_{melt} - T_{mold}}{T_{eject} - T_{mold}}\right) \\
& + 2 \times \frac{1000\, d_{release}}{184 + 13\log\left(\frac{p_{inj} \times A_{proj}}{9.8 \times 10^3 F_{ref}}\right)}
\end{aligned}
\tag{48}
$$

$$f_2 = \frac{4\,k\,l_{sprue}}{d_{sprue} + \tan\left(\frac{\pi\,\alpha_{sprue}}{180}\right) \times l_{sprue}} \times \left(\frac{\left(3 + \frac{1}{n}\right) Q}{\pi\,\left(\frac{d_{sprue} + \tan\left(\frac{\pi\,\alpha_{sprue}}{180}\right) \times l_{sprue}}{2}\right)^3} \right)^n + \frac{4\,k\,l_{runner}}{d_{runner}} \times \left(\frac{\left(3 + \frac{1}{n}\right) Q}{\pi\,\left(\frac{d_{runner}}{2}\right)^3} \right)^n + \frac{4\,k\,l_{gate}}{d_{gate}} \times \left(\frac{\left(3 + \frac{1}{n}\right) Q}{\pi\,\left(\frac{d_{gate}}{2}\right)^3} \right)^n \tag{49}$$

<u>Constraints:</u>

$$g_1 = -p_{inj} + \frac{32\,\left(l_{sprue} + l_{runner} + l_{gate} + l_{part}\right)\,\varphi\,\bar{v}_F \eta_{aeff}}{\left(\frac{2\,Max_D\,min_D}{Max_D + min_D}\right)} \leq 0 \tag{50}$$

$$g_2 = -F_{clamp\,max} + p_{inj} \times A_{proj} \leq 0 \tag{51}$$

$$g_3 = -d_{gate} + 2 \times \left(\frac{\left(3 + \frac{1}{n}\right) Q}{\pi\,\dot{\gamma}_{max}} \right)^{\frac{1}{3}} \leq 0 \tag{52}$$

$$g_4 = -d_{sprue} + d_{runner}\sqrt{n_{downstream}} \leq 0 \tag{53}$$

$$g_5 = -v_s + v_p(1 + \varepsilon)n_c + \frac{\pi d_{sprue}^2 l_{sprue}}{4} + 2 \times \left(\frac{\pi d_{gate}^2 l_{gate}}{4} + \frac{\pi d_{runner}^2 l_{runner}}{4} \right) \leq 0 \tag{54}$$

$$g_6 = -\left(\frac{\left(d_{sprue} + \tan\left(\frac{\pi\,\alpha_{sprue}}{180}\right) \times l_{sprue}\right)^2}{23.1\,\alpha} \times ln\left(0.692 \times \frac{T_{melt} - T_{mold}}{T_{eject} - T_{mold}}\right) \right) + 3 \leq 0 \tag{55}$$

System compatibility equations:

$$A_1 = p_{inj} - \frac{P_{inj} \times t_{inj}}{2 \times v_s} = 0 \tag{56}$$

$$A_2 = v_s - \frac{F_{clamp} \times v_p}{p_{inj} \times (A_{part} \times n_c)} = 0 \tag{57}$$

The optimization problem denoted by Eqs. (48) to (57) includes – two objective functions (f_1, f_2); six inequality constraints (g_1 to g_6); and two system compatibility equations (A_1, A_2). Now, for the sake of illustration, deterministic MDF and deterministic AAO formulations of the design problem are presented in Figures 6.1 and 6.2, respectively.

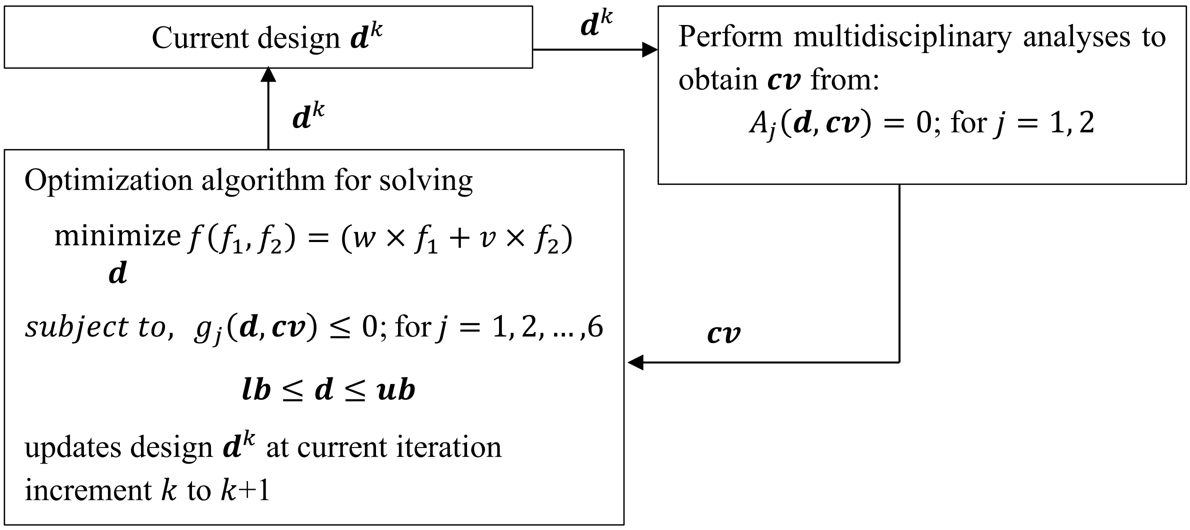

Figure 6.1: Diagram of deterministic MDF formulation for the injection molding system

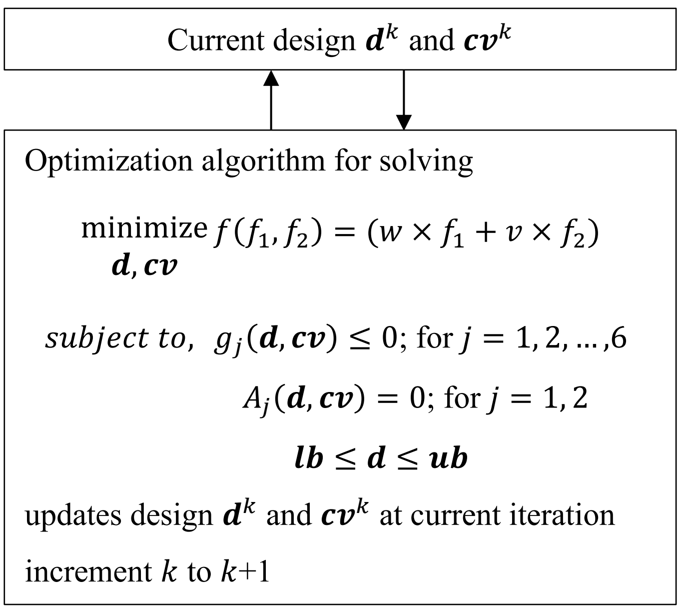

Figure 6.2: Diagram of deterministic AAO formulation for the injection molding system

Here, f_1 and f_2 represent cycle time (Eq. (48)) and pressure drop (Eq. (49)), respectively; g_j is the jth inequality constraint (Eqs. (50) to (55)) $A_j(\boldsymbol{d}, \boldsymbol{cv})$ represents the system compatibility equations of jth discipline (Eqs. (56) and (57)).

The integration of the deterministic MDO formulations with RDO and RBDO results in multidisciplinary RDO and multidisciplinary RBDO formulations, respectively. In the design consideration of the flexible multi-cavity insert, dimensions of the part family members are allowed to vary within a specified range. This thesis considers this variation in some of the design parameters as aleatory uncertainty. Moreover, aleatory uncertainty is also considered in the design variables considering the manufacturing tolerance and operating conditions. The uncertain design variables and parameters are assumed to follow the normal distribution. All the design variables in Table 3.1, excluding injection time (t_{inj}), are considered uncertain. The first five parameters in Table 3.3 are considered uncertain due to allowed variations in the dimensions of part family members.

Thus, the design problem includes one deterministic design variable ($\boldsymbol{x}_d$); eight random design variables ($\boldsymbol{x}_r$); five random design parameters ($\boldsymbol{p}$); two coupling variables ($\boldsymbol{cv}$); several single-valued design parameters and constants. Therefore, for the particular optimization problem of this thesis, the vectors $\boldsymbol{x}_d$, $\boldsymbol{x}_r$, $\boldsymbol{cv}$, $\boldsymbol{d}$, $\boldsymbol{p}$, and $\boldsymbol{r}$ can be defined as follows:

$\boldsymbol{x}_d = [t_{inj}]$; $\boldsymbol{x}_r = [Q, \alpha_{sprue}, d_{sprue}, d_{runner}, d_{gate}, l_{sprue}, l_{gate}, l_{runner}]$; $\boldsymbol{cv} = [p_{inj}, v_s]$;

$\boldsymbol{d} = [\boldsymbol{x}_d, \boldsymbol{\mu}_{x_r}] = [t_{inj}, \mu_Q, \mu_{\alpha_{sprue}}, \mu_{d_{sprue}}, \mu_{d_{runner}}, \mu_{d_{gate}}, \mu_{l_{sprue}}, \mu_{l_{gate}}, \mu_{l_{runner}}]$;

$\boldsymbol{p} = [A_{proj}, A_{part}, l_{part}, d, v_p]$;

$\boldsymbol{r} = [\boldsymbol{x}_r, \boldsymbol{p}] = [Q, \alpha_{sprue}, d_{sprue}, d_{runner}, d_{gate}, l_{sprue}, l_{gate}, l_{runner}, A_{proj}, A_{part}, l_{part}, d, v_p]$;

The following sections present the RDO/MDF, RDO/AAO, RBDO/MDF, and RBDO/AAO formulations for the injection molding system, respectively.

6.1 RDO/MDF formulation for the injection molding system

In standard RDO/MDF formulation, objective robustness is maintained by optimizing the mean value of an objective function and minimizing its standard deviation simultaneously using the weighted-sum method of multi-objective optimization. However, the scenario is different in the current MDO problem since it includes two objective functions – the cycle time (f_1) and the pressure drop (f_2). If the ε-constraint method is employed, setting the cycle time as the preferred objective function and the pressure drop as an inequality constraint, it is found that the mean cycle time (μ_{f_1}) and its standard deviation (σ_{f_1}) is minimized at a single point, i.e., no Pareto front is obtained. The outcome remains the same even if the pressure drop is set as the preferred objective function and the cycle time as inequality constraint. The Pareto front can be obtained if either the means (μ_{f_1} and μ_{f_2}) or the standard deviations (σ_{f_1} and σ_{f_2}) are incorporated in the objective function using the weighted-sum method.

In this thesis, standard deviations (σ_{f_1} and σ_{f_2}) are selected to be used in the objective function since the concept of robust design suggests to reduce the variation first (Park et al., 2006). Eq. (34) is used to calculate $\sigma_{f_1}^2$ and $\sigma_{f_2}^2$, as follows:

$$\begin{aligned}\sigma_{f_1}^2 &\cong \sum_{i=1}^{nrdv}\left(\frac{\partial f_1}{\partial d_i}\right)^2\sigma_{d_i}^2+\sum_{i=1}^{nrp}\left(\frac{\partial f_1}{\partial p_i}\right)^2\sigma_{p_i}^2\\ &\cong \left(\frac{\partial f_1}{\partial d_{gate}}\right)^2\sigma_{d_{gate}}^2+\left(\frac{\partial f_1}{\partial d_{sprue}}\right)^2\sigma_{d_{sprue}}^2+\left(\frac{\partial f_1}{\partial \alpha_{sprue}}\right)^2\sigma_{\alpha_{sprue}}^2\\ &\quad+\left(\frac{\partial f_1}{\partial l_{sprue}}\right)^2\sigma_{l_{sprue}}^2+\left(\frac{\partial f_1}{\partial A_{proj}}\right)^2\sigma_{A_{proj}}^2\end{aligned} \tag{58}$$

$$\begin{aligned}\sigma_{f_2}^2 &\cong \sum_{i=1}^{nrdv}\left(\frac{\partial f_2}{\partial d_i}\right)^2\sigma_{d_i}^2+\sum_{i=1}^{nrp}\left(\frac{\partial f_2}{\partial p_i}\right)^2\sigma_{p_i}^2\\ &\cong \left(\frac{\partial f_2}{\partial l_{sprue}}\right)^2\sigma_{l_{sprue}}^2+\left(\frac{\partial f_2}{\partial d_{sprue}}\right)^2\sigma_{d_{sprue}}^2+\left(\frac{\partial f_2}{\partial \alpha_{sprue}}\right)^2\sigma_{\alpha_{sprue}}^2\\ &\quad+\left(\frac{\partial f_2}{\partial l_{runner}}\right)^2\sigma_{l_{runner}}^2+\left(\frac{\partial f_2}{\partial d_{runner}}\right)^2\sigma_{d_{runner}}^2\\ &\quad+\left(\frac{\partial f_2}{\partial l_{gate}}\right)^2\sigma_{l_{gate}}^2+\left(\frac{\partial f_2}{\partial d_{gate}}\right)^2\sigma_{d_{gate}}^2+\left(\frac{\partial f_2}{\partial Q}\right)^2\sigma_{Q}^2\end{aligned} \tag{59}$$

The mean of the inequality constraints $E(g_j)$ are calculated using Eq. (35) during the optimization process. The standard deviations of the inequality constraints (σ_{g_j}) can be calculated using Eq. (36), as follows:

$$\begin{aligned}\sigma_{g_1}^2 &\cong \left(\frac{\partial g_1}{\partial l_{sprue}}\right)^2\sigma_{l_{sprue}}^2+\left(\frac{\partial g_1}{\partial l_{runner}}\right)^2\sigma_{l_{runner}}^2+\left(\frac{\partial g_1}{\partial l_{gate}}\right)^2\sigma_{l_{gate}}^2\\ &\quad+\left(\frac{\partial g_1}{\partial l_{part}}\right)^2\sigma_{l_{part}}^2\end{aligned} \tag{60}$$

$$\sigma_{g_2}^2 \cong \left(\frac{\partial g_2}{\partial A_{proj}}\right)^2\sigma_{A_{proj}}^2 \tag{61}$$

$$\sigma_{g_3}^2 \cong \left(\frac{\partial g_3}{\partial d_{gate}}\right)^2 \sigma_{d_{gate}}^2 + \left(\frac{\partial g_3}{\partial Q}\right)^2 \sigma_Q^2 \tag{62}$$

$$\sigma_{g_4}^2 \cong \left(\frac{\partial g_4}{\partial d_{sprue}}\right)^2 \sigma_{d_{sprue}}^2 + \left(\frac{\partial g_4}{\partial d_{runner}}\right)^2 \sigma_{d_{runner}}^2 \tag{63}$$

$$\begin{aligned}\sigma_{g_5}^2 \cong & \left(\frac{\partial g_5}{\partial l_{sprue}}\right)^2 \sigma_{l_{sprue}}^2 + \left(\frac{\partial g_5}{\partial d_{sprue}}\right)^2 \sigma_{d_{sprue}}^2 \\ & + \left(\frac{\partial g_5}{\partial l_{runner}}\right)^2 \sigma_{l_{runner}}^2 + \left(\frac{\partial g_5}{\partial d_{runner}}\right)^2 \sigma_{d_{runner}}^2 \\ & + \left(\frac{\partial g_5}{\partial l_{gate}}\right)^2 \sigma_{l_{gate}}^2 + \left(\frac{\partial g_5}{\partial d_{gate}}\right)^2 \sigma_{d_{gate}}^2 + \left(\frac{\partial g_5}{\partial v_p}\right)^2 \sigma_{v_p}^2\end{aligned} \tag{64}$$

$$\sigma_{g_6}^2 \cong \left(\frac{\partial g_6}{\partial d_{sprue}}\right)^2 \sigma_{d_{sprue}}^2 + \left(\frac{\partial g_6}{\partial l_{sprue}}\right)^2 \sigma_{l_{sprue}}^2 + \left(\frac{\partial g_6}{\partial \alpha_{sprue}}\right)^2 \sigma_{\alpha_{sprue}}^2 \tag{65}$$

Note that the system compatibility equations, the mean and standard deviation of both the objective functions and inequality constraints are approximated at the mean values of all the random design variables and random design parameters.

The tailored RDO/MDF formulation for the injection molding system is depicted in Figure 6.3, as follows:

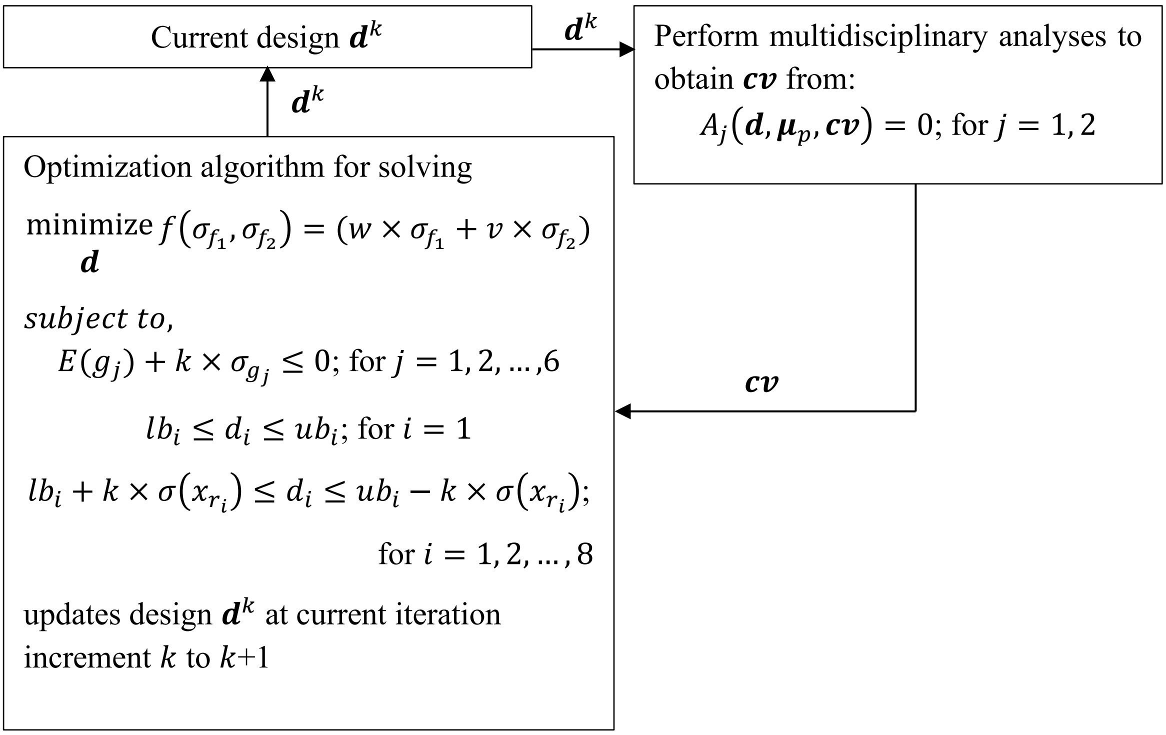

Figure 6.3: Diagram of the RDO/MDF formulation for the injection molding system

Here, σ_{f_1} and σ_{f_2} are the standard deviations of cycle time and pressure drop, respectively; w and v are the weighting coefficients under associated conditions— $w \geq 0$; $v \geq 0$; and $w + v = 1$. The weighting coefficients denote the relative importance of σ_{f_1} and σ_{f_2}. The vector $\boldsymbol{d}$ includes one deterministic design variable ($\boldsymbol{x}_d$) as well as the mean values of the eight random design variables ($\boldsymbol{x}_r$), i.e., $\boldsymbol{d} = [\boldsymbol{x}_d\ \boldsymbol{\mu}_{x_r}]$; $\boldsymbol{\mu}_p$ is the vector of mean values of the five random design parameters ($\boldsymbol{p}$); $\boldsymbol{cv}$ is the vector of the two coupling variables; g_j is the jth inequality constraint; $E(g_j)$ is the mean and σ_{g_j} is the standard deviation of the jth inequality constraint. The vectors $\boldsymbol{lb}$ and $\boldsymbol{ub}$ represent the lower and upper bounds of all the design variables, respectively; $\sigma(\boldsymbol{x}_r)$ is the vector of standard deviations of the eight random design variables and k is a user-defined constant that is chosen to be 1. $A_j(\boldsymbol{x}^k, \boldsymbol{\mu}_p, \boldsymbol{cv})$ represents the system compatibility requirements involved in jth discipline that must be satisfied by the coupling variables ($\boldsymbol{cv}$) for a set of input design variables ($\boldsymbol{d}^k$), and $\boldsymbol{\mu}_p$ at each iteration.

Note that the objective function is to be minimized with respect to the design variables $\boldsymbol{d}$, and the coupling variables are considered deterministic in this formulation.

6.2 RDO/AAO formulation for the injection molding system

The RDO/AAO formulation for the injection molding system differs from the RDO/MDF formulation in the following aspects: (i) the coupling variables and their standard deviations are treated as optimization variables; (ii) the system compatibility equations are not solved outside the optimization algorithm; rather the equations are treated as equality constraints within the optimization algorithm; (iii) the equations for estimating the standard deviations of the coupling variables by first-order Taylor series approximation are included as equality constraints within the optimization algorithm.

In the MDO of the injection molding system, the standard deviation of the coupling variables $\sigma_{p_{inj}}$ and σ_{v_s} can be calculated using Eq. (38), as follows:

$$\sigma_{p_{inj}}^2 \cong \left(\frac{\partial F_{p_{inj}}}{\partial v_s}\right)^2 \sigma_{v_s}^2 + \left(\frac{\partial F_{p_{inj}}}{\partial t_{inj}}\right)^2 \sigma_{t_{inj}}^2 \tag{66}$$

$$\sigma_{v_s}^2 \cong \left(\frac{\partial F_{v_s}}{\partial p_{inj}}\right)^2 \sigma_{p_{inj}}^2 + \left(\frac{\partial F_{v_s}}{\partial v_p}\right)^2 \sigma_{v_p}^2 + \left(\frac{\partial F_{v_s}}{\partial A_{part}}\right)^2 \sigma_{A_{part}}^2 \tag{67}$$

Here, $F_{p_{inj}}$ and F_{v_s} are the functional relationship of p_{inj} and v_s, presented in Eqs. (1) and (2), respectively. Eqs. (66) and (67) are used as equality constraints in the RDO/AAO formulation.

Inclusion of the coupling variables as optimization variables requires the use of Eqs. (40) and (42) for the estimation of the standard deviations of the objective functions and inequality constraints, respectively. Note that expressions in Eqs. (58)-(65) are not applicable to the RDO/AAO formulation.

Standard deviations of the two objective functions σ_{f_1} and σ_{f_2} are calculated using Eq. (40), as follows:

$$\sigma_{f_1}^2 \cong \sum_{i=1}^{nrdv} \left(\frac{\partial f_1}{\partial d_i}\right)^2 \sigma_{d_i}^2 + \sum_{i=1}^{nrp} \left(\frac{\partial f_1}{\partial p_i}\right)^2 \sigma_{p_i}^2 + \sum_{i=1}^{ncv} \left(\frac{\partial f_1}{\partial cv_i}\right)^2 \sigma_{cv_i}^2$$

$$\begin{aligned} &\cong \left(\frac{\partial f_1}{\partial d_{gate}}\right)^2 \sigma_{d_{gate}}^2 + \left(\frac{\partial f_1}{\partial d_{sprue}}\right)^2 \sigma_{d_{sprue}}^2 + \left(\frac{\partial f_1}{\partial \alpha_{sprue}}\right)^2 \sigma_{\alpha_{sprue}}^2 \\ &\quad + \left(\frac{\partial f_1}{\partial l_{sprue}}\right)^2 \sigma_{l_{sprue}}^2 + \left(\frac{\partial f_1}{\partial A_{proj}}\right)^2 \sigma_{A_{proj}}^2 \\ &\quad + \left(\frac{\partial f_1}{\partial p_{inj}}\right)^2 \sigma_{p_{inj}}^2 + \left(\frac{\partial f_1}{\partial v_s}\right)^2 \sigma_{v_s}^2 \end{aligned} \tag{68}$$

$$\sigma_{f_2}^2 \cong \sum_{i=1}^{nrdv} \left(\frac{\partial f_2}{\partial d_i}\right)^2 \sigma_{d_i}^2 + \sum_{i=1}^{nrp} \left(\frac{\partial f_2}{\partial p_i}\right)^2 \sigma_{p_i}^2 + \sum_{i=1}^{ncv} \left(\frac{\partial f_2}{\partial cv_i}\right)^2 \sigma_{cv_i}^2$$

$$\begin{aligned} &\cong \left(\frac{\partial f_2}{\partial l_{sprue}}\right)^2 \sigma_{l_{sprue}}^2 + \left(\frac{\partial f_2}{\partial d_{sprue}}\right)^2 \sigma_{d_{sprue}}^2 + \left(\frac{\partial f_2}{\partial \alpha_{sprue}}\right)^2 \sigma_{\alpha_{sprue}}^2 \\ &\quad + \left(\frac{\partial f_2}{\partial l_{runner}}\right)^2 \sigma_{l_{runner}}^2 + \left(\frac{\partial f_2}{\partial d_{runner}}\right)^2 \sigma_{d_{runner}}^2 \\ &\quad + \left(\frac{\partial f_2}{\partial l_{gate}}\right)^2 \sigma_{l_{gate}}^2 + \left(\frac{\partial f_2}{\partial d_{gate}}\right)^2 \sigma_{d_{gate}}^2 + \left(\frac{\partial f_2}{\partial Q}\right)^2 \sigma_Q^2 \end{aligned} \tag{69}$$

The mean of the inequality constraints $E(g_j)$ are calculated using Eq. (41) during the optimization process. The standard deviations of the inequality constraints (σ_{g_j}) can be calculated using Eq. (42), as follows:

$$\sigma_{g_1}^2 \cong \left(\frac{\partial g_1}{\partial l_{sprue}}\right)^2 \sigma_{l_{sprue}}^2 + \left(\frac{\partial g_1}{\partial l_{runner}}\right)^2 \sigma_{l_{runner}}^2 + \left(\frac{\partial g_1}{\partial l_{gate}}\right)^2 \sigma_{l_{gate}}^2 + \left(\frac{\partial g_1}{\partial l_{part}}\right)^2 \sigma_{l_{part}}^2 + \left(\frac{\partial g_1}{\partial p_{inj}}\right)^2 \sigma_{p_{inj}}^2 \tag{70}$$

$$\sigma_{g_2}^2 \cong \left(\frac{\partial g_2}{\partial A_{proj}}\right)^2 \sigma_{A_{proj}}^2 + \left(\frac{\partial g_2}{\partial p_{inj}}\right)^2 \sigma_{p_{inj}}^2 \tag{71}$$

$$\sigma_{g_3}^2 \cong \left(\frac{\partial g_3}{\partial d_{gate}}\right)^2 \sigma_{d_{gate}}^2 + \left(\frac{\partial g_3}{\partial Q}\right)^2 \sigma_Q^2 \tag{72}$$

$$\sigma_{g_4}^2 \cong \left(\frac{\partial g_4}{\partial d_{sprue}}\right)^2 \sigma_{d_{sprue}}^2 + \left(\frac{\partial g_4}{\partial d_{runner}}\right)^2 \sigma_{d_{runner}}^2 \tag{73}$$

$$\sigma_{g_5}^2 \cong \left(\frac{\partial g_5}{\partial l_{sprue}}\right)^2 \sigma_{l_{sprue}}^2 + \left(\frac{\partial g_5}{\partial d_{sprue}}\right)^2 \sigma_{d_{sprue}}^2 + \left(\frac{\partial g_5}{\partial l_{runner}}\right)^2 \sigma_{l_{runner}}^2 + \left(\frac{\partial g_5}{\partial d_{runner}}\right)^2 \sigma_{d_{runner}}^2 + \left(\frac{\partial g_5}{\partial l_{gate}}\right)^2 \sigma_{l_{gate}}^2 + \left(\frac{\partial g_5}{\partial d_{gate}}\right)^2 \sigma_{d_{gate}}^2 + \left(\frac{\partial g_5}{\partial v_p}\right)^2 \sigma_{v_p}^2 + \left(\frac{\partial g_5}{\partial v_s}\right)^2 \sigma_{v_s}^2 \tag{74}$$

$$\sigma_{g_6}^2 \cong \left(\frac{\partial g_6}{\partial d_{sprue}}\right)^2 \sigma_{d_{sprue}}^2 + \left(\frac{\partial g_6}{\partial l_{sprue}}\right)^2 \sigma_{l_{sprue}}^2 + \left(\frac{\partial g_6}{\partial \alpha_{sprue}}\right)^2 \sigma_{\alpha_{sprue}}^2 \tag{75}$$

Note that in the estimation of the standard deviations of the objective functions and inequality constraints using first-order Taylor series expansions, partial derivatives of the functions with respect to coupling variables are also included, if applicable.

The tailored RDO/AAO formulation for the injection molding system is depicted in Figure 6.4, as follow:

Current design $\boldsymbol{d}^k$, $\boldsymbol{cv}^k$ and $\boldsymbol{\sigma}_{cv}^k$

Optimization algorithm for solving

$$\underset{\boldsymbol{d},\boldsymbol{cv},\boldsymbol{\sigma}_{cv}}{\text{minimize}}\; f\left(\sigma_{f_1},\sigma_{f_2}\right) = \left(w \times \sigma_{f_1} + v \times \sigma_{f_2}\right)$$

$$subject\ to,$$

$$E(g_j) + k \times \sigma_{g_j} \leq 0; \text{ for } j = 1, 2, \ldots, 6$$

$$lb_i \leq d_i \leq ub_i; \text{ for } i = 1$$

$$lb_i + k \times \sigma\left(x_{r_i}\right) \leq d_i \leq ub_i - k \times \sigma\left(x_{r_i}\right); \text{ for } i = 1, 2, \ldots, 8$$

$$A_j\left(\boldsymbol{d}, \boldsymbol{\mu}_p, \boldsymbol{cv}\right) = 0; \text{ for } j = 1, 2$$

$$\sigma_{cv_j}^2 = \sum_{\substack{i=1\\ i\neq j}}^{ncv} \left(\frac{\partial F_{\boldsymbol{cv}_j}}{\partial cv_i}\right)^2 \sigma_{cv_i}^2 + \sum_{i=1}^{nrdv} \left(\frac{\partial F_{\boldsymbol{cv}_j}}{\partial d_i}\right)^2 \sigma_{d_i}^2 + \sum_{i=1}^{nrp} \left(\frac{\partial F_{\boldsymbol{cv}_j}}{\partial p_i}\right)^2 \sigma_{p_i}^2; \quad \text{for} j = 1, 2$$

updates design $\boldsymbol{d}^k$, $\boldsymbol{cv}^k$ and $\boldsymbol{\sigma}_{cv}^k$ at current iteration
increment k to k+1

Figure 6.4: Diagram of the RDO/AAO formulation for the injection molding system

6.3 RBDO/MDF formulation for the injection molding system

The RBDO/MDF formulation for the injection molding system handles the multi-objective optimization using the weighted-sum method for the sake of illustration. In this formulation, the objective function is optimized with respect to the design variables ($\boldsymbol{d}$). However, the coupling variables are considered deterministic. The system compatibility equations are solved outside the optimization algorithm. The reliability constraints in Eq. (76) (Figure 6.5) corresponding to each of the inequality constraints or limit state functions are evaluated using the reliability index β through solving the optimization problem presented in Eqs. (44)-(46). As discussed earlier, in the evaluation of the reliability index β_j, only the jth limit state function is involved; however, all the system compatibility equations are included. In the evaluation of the reliability index, the random variables x_{r_i} and p_i included in the limit state functions and system compatibility equations are transformed into standard normal space and substituted by the expressions ($u_{x_{r_i}} \times \sigma_{x_{r_i}} + d_i$) and ($u_{p_i} \times \sigma_{p_i} + \mu_{p_i}$), respectively. Note that this thesis uses $P_{f_j}^{allowable} = 0.0062$ that corresponds to $\beta_j = 2.5$, for the sake of illustration. The tailored RBDO/MDF formulation for the injection molding system is depicted in Figure 6.5, as follow:

Current design $\boldsymbol{d}^k$

$\boldsymbol{d}^k$

Perform multidisciplinary analyses to obtain $\boldsymbol{cv}$ from:

$$A_j\left(\boldsymbol{d}^k, \boldsymbol{\mu}_p, \boldsymbol{cv}\right) = 0; \text{ for } j = 1, 2$$

$\boldsymbol{cv}$

Optimization algorithm for solving

$$\underset{\boldsymbol{d}}{\text{minimize}} \quad f\left(\mu_{f_1}, \mu_{f_2}\right) = \left(w \times \mu_{f_1} + v \times \mu_{f_2}\right)$$

$subject\ to,$

$$P_{f_j} = \Phi(-\beta_j) \leq P_{f_j}^{allowable}; \text{ for } j = 1, 2, \dots, 6 \quad (76)$$

$$\boldsymbol{lb} \leq \boldsymbol{d} \leq \boldsymbol{ub}$$

updates design $\boldsymbol{d}^k$ at current iteration

increment k to k+1

$\boldsymbol{d}^k$

Figure 6.5: Diagram of the RBDO/MDF formulation for the injection molding system

6.4 RBDO/AAO formulation for the injection molding system

The RBDO/AAO formulation for the injection molding system also handles the multi-objective optimization using the weighted-sum method. In this formulation, the objective function is optimized with respect to the design variables ($\boldsymbol{d}$) as well as the coupling variables ($\boldsymbol{cv}$). The system compatibility equations are treated as equality constraints within the optimization algorithm. The tailored RBDO/AAO formulation for the injection molding system is depicted in Figure 6.6, as follow:

Current design $\boldsymbol{d}^k$ and $\boldsymbol{cv}^k$

Optimization algorithm for solving

$$\underset{\boldsymbol{d}, \boldsymbol{cv}}{\text{minimize}} \quad f\left(\mu_{f_1}, \mu_{f_2}\right) = \left(w \times \mu_{f_1} + v \times \mu_{f_2}\right)$$

$subject\ to,$

$$P_{f_j} = \Phi(-\beta_j) \leq P_{f_j}^{allowable}; \text{ for } j = 1, 2, \dots, 6$$

$$A_j\left(\boldsymbol{d}, \boldsymbol{\mu}_p, \boldsymbol{cv}\right) = 0; \text{ for } j = 1, 2$$

$$\boldsymbol{lb} \leq \boldsymbol{d} \leq \boldsymbol{ub}$$

updates design $\boldsymbol{d}^k$ and $\boldsymbol{cv}^k$ at current iteration

increment k to k+1

Figure 6.6: Diagram of the RBDO/AAO formulation for the injection molding system

6.5 Numerical illustration

This section presents a numerical illustration of the design problem of a flexible multi-cavity insert for the production of a specific plastic part family. A particular model of injection molding machine and a particular raw material are to be selected for assigning values to the design parameters and design constants, for the sake of illustration. This thesis considers the 'SUN-110' model of standard plastic injection molding machine manufactured by Steady Stream Business Co., Ltd. Polypropylene, a thermoplastic polymer, is considered as the raw material to be used in the injection molding machine. Now, specific values can be assigned to some of the design parameters and design constants according to machine specifications and selected polymer properties. The values of some other parameters are obtained from existing literature (e.g., Bolur, 2000; Menges et al., 2013) and design considerations of the flexible multi-cavity insert. Single valued design constants and design parameters are listed in Tables 6.1 and 6.2, respectively.

Table 6.1: List of specified design constants

Serial No.	Term	Nomenclature	Value	Source
1.	n	Power law index	0.38	Polymer property
2.	k	Viscosity evaluated at a shear rate of one reciprocal second, Pa·s^n	7500	Polymer property
3.	α	Thermal diffusivity of the polymer material, m^2/s	0.96×10^{-7}	Polymer property
4.	ε	Percentage shrinkage rate of the polymer from injection temperature to room temperature	1.5%	Polymer property
5.	$\dot{\gamma}_{max}$	Maximum shear rate for the plastic, s^{-1}	10^5	Polymer property
6.	η_{aeff}	Apparent effective viscosity, Pa·s	170	Polymer property
7.	T_{melt}	Recommended polymer melt temperature, °C	250	Polymer property

Table 6.2: List of specified design parameters

Serial No.	Term	Nomenclature	Value	Source
1.	$F_{clamp\ max}$	Maximum clamping force, N	1096042	Machine specification
2.	Q_{max}	Maximum volumetric flow rate of the melt, m^3/s	86×10^{-6}	Machine specification
3.	φ	Ratio between width and thickness of the mold cavity	1.5	Menges et al. (2013)
4.	$n_{downstream}$	Number of ramification streams	2	Design consideration
5.	n_c	Number of part cavities	2	Design consideration
6.	$d_{release}$	Mold opening distance, m	0.25	Design consideration
7.	$\bar{v}_F$	Velocity of the flow front, m/s	0.3	Menges et al. (2013)
8.	T_{eject}	Recommended part ejection temperature, °C	100	Menges et al. (2013)
9.	T_{mold}	Recommended mold temperature, °C	50	Menges et al. (2013)
10.	Max_D	Maximum dimension corresponding to the largest cross-section, perpendicular to the direction of melt flow, m	0.1	Design consideration
11.	min_D	Minimum dimension corresponding to the smallest cross-section, perpendicular to the direction of melt flow, m	0.003	Design consideration
12.	P_{inj}	Required injection power, W	10500	Bolur (2000)

The dimensional configurations of the part family members can be determined using the specifications of the selected model of the injection molding machine. The selected machine (SUN-110) can accommodate a mold size of 355 (length) × 355 (width) mm. The range of dimensions for the part family members is specified in Table 6.3 for the sake of illustration, considering the mold size restriction in the selected machine. Plastic parts without any intricate structure that have dimensions within the specified ranges can be molded using the flexible multi-cavity insert. Bounds for the identified design variables are determined considering the dimensional ranges allotted for the part family members, as shown in Table 6.4. Careful choice of the bounds is essential for convergence of the optimization process.

The five design parameters in Table 6.3 and eight design variables in Table 6.4 are considered uncertain that are assumed to follow normal distributions. The mean values of the uncertain parameters are assumed to be at the midpoint of the specified ranges and their standard deviation is assumed as one-twelfth of the specified range, for the sake of illustration. The mean values of the uncertain design variables are treated as design variables during the optimization process, as discussed in RDO and RBDO methodologies. The standard deviation values of the uncertain design variables are shown in Table 6.4. The standard deviations of Q and α_{sprue} are set at 10% of the mid-point of corresponding bounds since precise data is unavailable. CNC machining tolerance (125μm) is used as the standard deviation of sprue, runner and gate dimensions (Krar et al., 2001).

Table 6.3: List of uncertain design parameters

Serial No.	Term	Nomenclature	Range of values	Mean	Standard deviation
1.	A_{proj}	Total projected area of the cavity (along-with runner system), m^2	40×10^{-4}~80×10^{-4}	60×10^{-4}	3.33×10^{-4}
2.	A_{part}	Projected area of the part to be molded on the parting plane, m^2	10×10^{-4}~ 40×10^{-4}	25×10^{-4}	2.5×10^{-4}
3.	l_{part}	Length of the part, m	0.01~ 0.09	0.05	6.67×10^{-3}
4.	d_p	Depth of the part, m	0.005~ 0.045	0.025	3.33×10^{-3}
5.	v_p	Volume of the injection molded part, m^3	10×10^{-6}~ 90×10^{-6}	50×10^{-6}	6.67×10^{-6}

Table 6.4: List of design variables with corresponding bounds and standard deviation

Serial No.	Term	Nomenclature	Lower bound	Upper bound	Standard deviation
1.	Q	Volumetric flow rate of the melt, m^3/s	50×10^{-6}	86×10^{-6}	6.8×10^{-6}
2.	α_{sprue}	Draft angle of sprue, degree	1	4	0.25
3.	d_{sprue}	Initial diameter of sprue, m	7×10^{-3}	10×10^{-3}	125×10^{-6}
4.	d_{runner}	Diameter of runner, m	4×10^{-3}	8×10^{-3}	125×10^{-6}
5.	d_{gate}	Diameter of gate, m	1.25×10^{-3}	4×10^{-3}	125×10^{-6}
6.	l_{sprue}	Length of sprue, m	50×10^{-3}	80×10^{-3}	125×10^{-6}
7.	l_{runner}	Length of runner, m	15×10^{-3}	50×10^{-3}	125×10^{-6}
8.	l_{gate}	Length of gate, m	5×10^{-3}	10×10^{-3}	125×10^{-6}
9.	t_{inj}	Injection time, s	1	12	N/A

Two coupling variables – injection pressure (p_{inj}) and shot volume (v_s), are also involved in the MDO of the injection molding system along with the design variables, parameters, and constants, as discussed in Chapter 3. In the AAO-based formulations, the coupling variables and their standard deviations are needed to be included as optimization variables. Note that the bounds for the design variables and coupling variables (when treated as optimization variables) are subject to modification for maintaining compatibility due to change in dimensional ranges (Table 6.3) of the specified part family members.

The solutions to the numerical illustration of the design problem of flexible multi-cavity injection mold insert are presented and discussed in the following chapter.

CHAPTER 7

RESULTS AND DISCUSSIONS

This chapter presents the solutions to the design problem of the flexible multi-cavity injection mold insert obtained from the RDO/MDF, RDO/AAO, RBDO/MDF, and RBDO/AAO formulations, as presented in Sections 6.1-6.4. The four formulations are solved using the 'fmincon' function of MATLAB according to numerical illustration of the design problem specified in Section 6.5.

7.1 Results: RDO/MDF formulation

The RDO/MDF formulation presented in Figure 6.3 of Chapter 6 is solved with multiple combinations of the weighting coefficients to obtain Pareto front for the multi-objective optimization problem. The weighting coefficient v is substituted with $(1 - w)$ in the objective function and then Pareto optimal solutions are obtained by varying w from 0 to 1 with an increment of 0.1, for the sake of illustration. Mean values and standard deviations of the two objective functions (cycle time and pressure drop) corresponding to the Pareto optimal solutions are shown in Table 7.1, as follows:

Table 7.1: Mean values and standard deviations of cycle time and pressure drop corresponding to the Pareto optimal solutions of RDO/MDF formulation

Values of weighting coefficient, w	**Mean cycle time, μ_{f_1}(s)**	**Mean pressure drop, μ_{f_2}(MPa)**	**Standard deviation of cycle time, σ_{f_1}(s)**	**Standard deviation of pressure drop, σ_{f_2} (MPa)**
w = 0.0	90.90	5.13	3.20	0.23
w = 0.1	72.72	5.54	2.81	0.25
w = 0.2	65.52	5.79	2.65	0.26
w = 0.3	56.90	6.62	2.44	0.30
w = 0.4	49.22	7.73	2.23	0.36
w = 0.5	43.37	8.96	2.06	0.43
w = 0.6	43.37	8.96	2.06	0.43
w = 0.7	43.37	8.96	2.06	0.43
w = 0.8	43.37	8.96	2.06	0.43
w = 0.9	41.36	9.42	2.05	0.46
w = 1.0	38.13	15.24	2.03	1.06

Note that as the weighting coefficient (w) increases the mean values and standard deviations of cycle time decrease and those of pressure drop increase. The Pareto optimal solutions corresponding to w = 0.5, 0.6, 0.7, and 0.8 are found to be identical in RDO/MDF formulation.

The Pareto fronts of the standard deviation of pressure drop (σ_{f_2}) vs standard deviation of cycle time (σ_{f_1}) and corresponding pressure drop (f_2) vs cycle time (f_1) obtained in the RDO/MDF formulation are depicted in Figures 7.1(a) and 7.1(b), respectively, as follows:

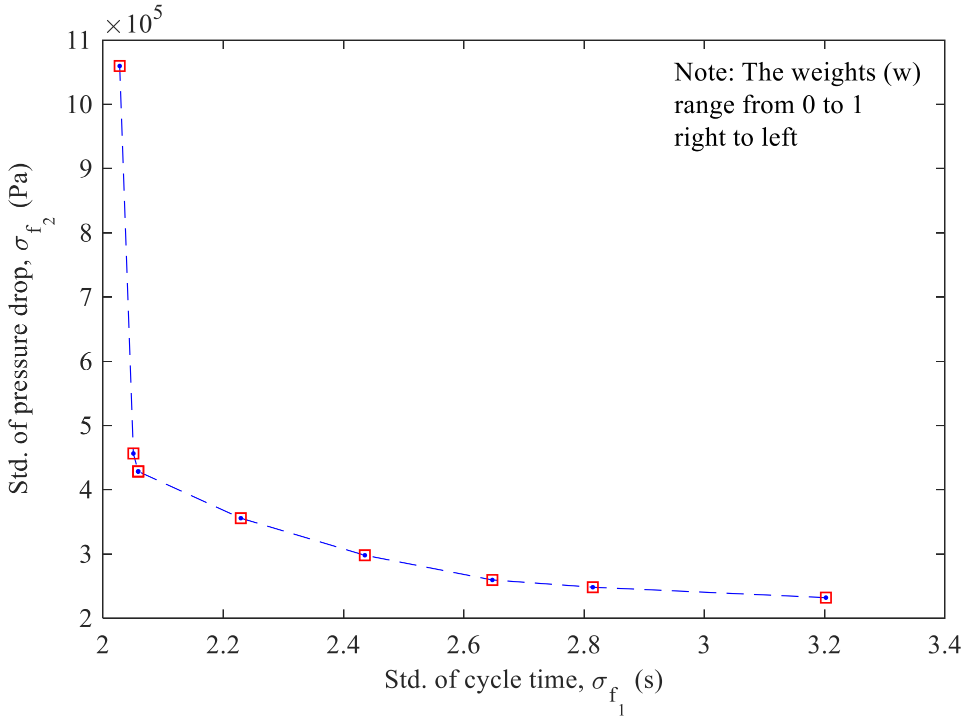

(a) Standard deviations of cycle time and pressure drop

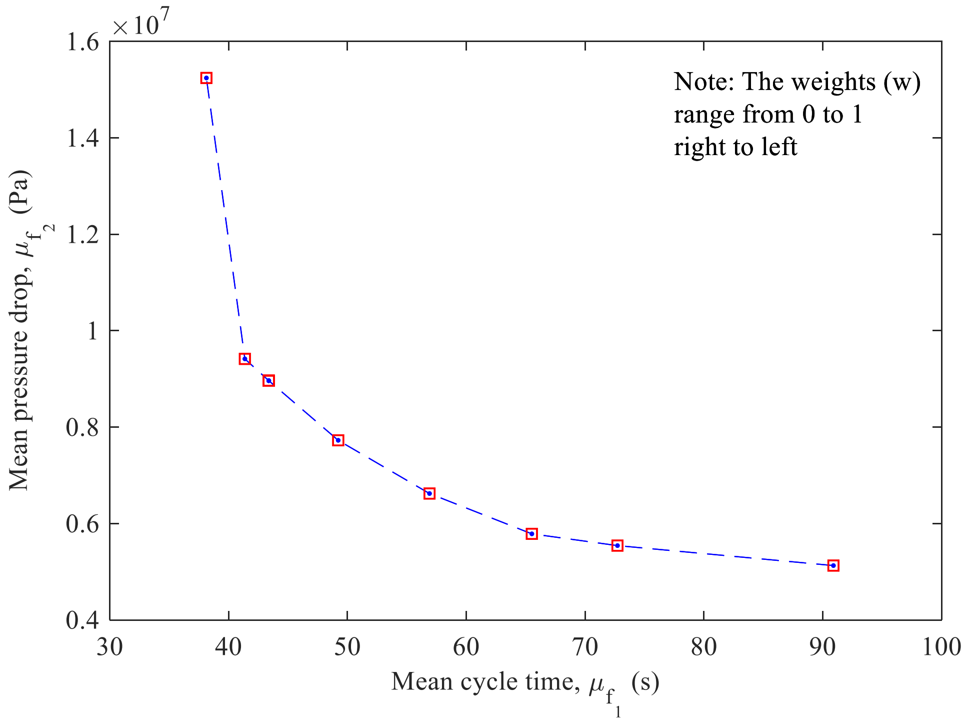

(b) Mean values of cycle time and pressure drop

Figure 7.1: Pareto fronts obtained in RDO/MDF formulation

Values of the design variables corresponding to the Pareto optimal solutions obtained in RDO/MDF formulation are shown in Table 7.2, as follows:

Table 7.2: Pareto optimal solutions obtained in RDO/MDF formulation

Design variables (d)	**Pareto optimal solutions corresponding to weighting coefficient, w**										
	w=0.0	**w=0.1**	**w=0.2**	**w=0.3**	**w=0.4**	**w=0.5**	**w=0.6**	**w=0.7**	**w=0.8**	**w=0.9**	**w= 1.0**
Volumetric flow rate of the melt (cm^3/sec)	83.00	83.00	83.00	83.00	83.00	83.00	83.00	83.00	83.00	83.00	56.55
Draft angle of sprue (degree)	3.75	2.01	1.25	1.25	1.25	1.25	1.25	1.25	1.25	1.25	1.25
Diameter of sprue (mm)	9.75	9.75	9.75	8.85	7.98	7.25	7.25	7.25	7.25	7.25	7.25
Diameter of runner (mm)	6.74	6.74	6.74	6.11	5.49	4.97	4.97	4.97	4.97	4.97	4.73
Diameter of gate (mm)	3.77	3.77	3.77	3.77	3.77	3.77	3.77	3.77	3.77	3.42	2.16
Length of sprue (mm)	52.50	52.50	52.50	52.50	52.50	52.50	52.50	52.50	52.50	52.50	52.50
Length of runner (mm)	17.92	17.92	17.92	17.92	17.92	17.92	17.92	17.92	17.92	17.92	21.39
Length of gate (mm)	5.42	5.42	5.42	5.42	5.42	5.42	5.42	5.42	5.42	5.42	5.91
Injection time (second)	4.72	4.72	4.72	4.72	4.72	4.72	4.72	4.72	4.72	3.01	3.01

7.2 Results: RDO/AAO formulation

The RDO/AAO formulation presented in Figure 6.4 is solved by substituting the weighting coefficient v with $(1-w)$ in the objective function and then Pareto optimal solutions are obtained by varying w from 0 to 1 with an increment of 0.1, for the sake of illustration. Note that coupling variables and their standard deviations are treated as optimization variables in the RDO/AAO formulation. Mean values and standard deviations of the two objective functions (cycle time and pressure drop) corresponding to the Pareto optimal solutions are shown in Table 7.3, as follow:

Table 7.3: Mean values and standard deviations of cycle time and pressure drop corresponding to the Pareto optimal solutions of RDO/AAO formulation

Values of weighting coefficient, w	**Mean cycle time, μ_{f_1} (s)**	**Mean pressure drop, μ_{f_2} (MPa)**	**Standard deviation of cycle time, σ_{f_1} (s)**	**Standard deviation of pressure drop, σ_{f_2} (MPa)**
w = 0.0	89.74	5.14	3.21	0.23
w = 0.1	58.44	6.33	2.52	0.28
w = 0.2	43.95	8.55	2.12	0.40
w = 0.3	42.22	8.96	2.07	0.43
w = 0.4	42.22	8.96	2.07	0.43
w = 0.5	42.22	8.96	2.07	0.43
w = 0.6	42.22	8.96	2.07	0.43
w = 0.7	41.23	9.34	2.07	0.45
w = 0.8	40.30	9.85	2.06	0.49
w = 0.9	39.49	10.77	2.05	0.56
w = 1.0	37.74	16.07	2.04	1.12

Note that as the weighting coefficient (w) increases the mean values and standard deviations of cycle time decrease and those of pressure drop increase. The Pareto optimal solutions corresponding to w = 0.3, 0.4, 05, and 0.6 are found to be identical in RDO/AAO formulation.

The Pareto fronts of the standard deviation of pressure drop (σ_{f_2}) vs standard deviation of cycle time (σ_{f_1}) and corresponding pressure drop (f_2) vs cycle time (f_1) obtained in the RDO/AAO formulation are depicted in Figure 7.2(a) and Figure 7.2(b), respectively, as follows:

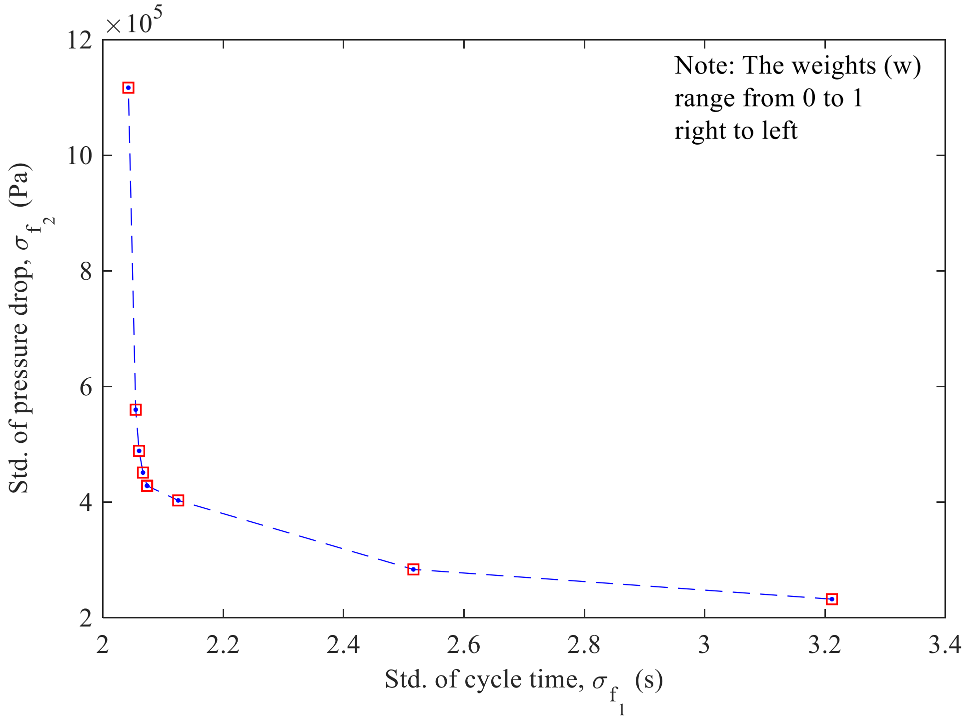

(a) Standard deviations of cycle time and pressure drop

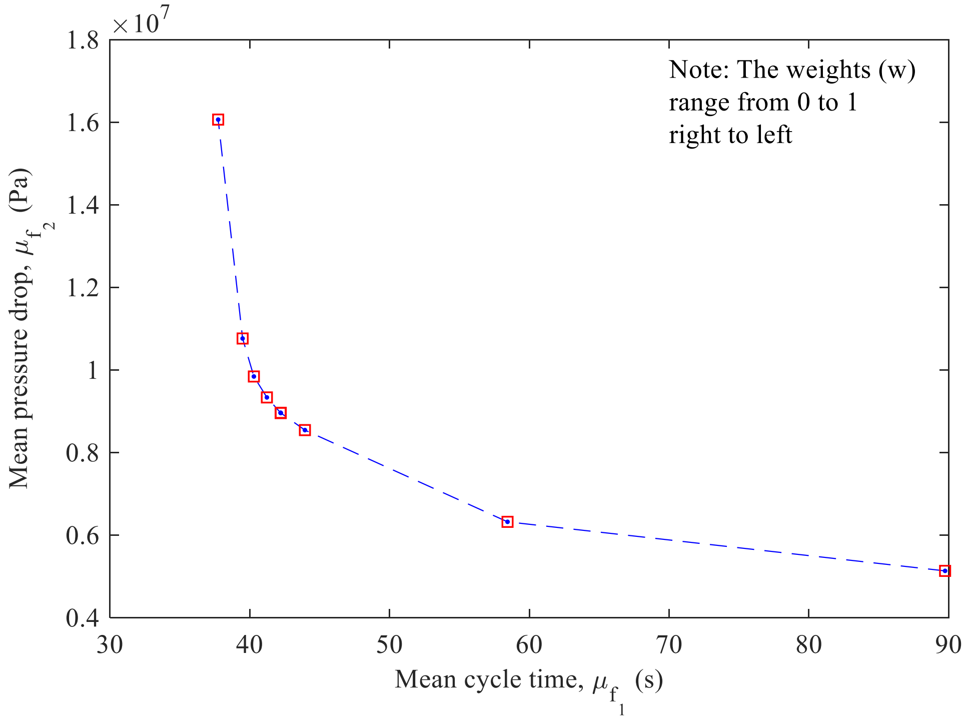

(b) Mean values of cycle time and pressure drop

Figure 7.2: Pareto fronts obtained in RDO/AAO formulation

Pareto optimal solutions of the optimization variables obtained in RDO/AAO formulation are shown in Table 7.4, as follows:

Table 7.4: Pareto optimal solutions obtained in RDO/AAO formulation

Optimization variables	**Pareto optimal solutions corresponding to weighting coefficient, *w***										
	***w*=0.0**	***w*=0.1**	***w*=0.2**	***w*=0.3**	***w*=0.4**	***w*=0.5**	***w*=0.6**	***w*=0.7**	***w*=0.8**	***w*=0.9**	***w*= 1.0**
Volumetric flow rate of the melt (cm^3/sec)	76.48	64.63	64.35	83.00	83.00	83.00	71.61	64.42	63.58	57.65	53.00
Draft angle of sprue (degree)	3.75	1.25	1.25	1.25	1.25	1.25	1.25	1.25	1.25	1.25	1.25
Diameter of sprue (mm)	9.75	9.14	7.33	7.25	7.25	7.25	7.25	7.25	7.25	7.25	7.25
Diameter of runner (mm)	6.74	6.31	5.03	4.97	4.97	4.97	4.97	4.97	4.97	4.87	4.33
Diameter of gate (mm)	3.77	3.77	3.77	3.77	3.77	3.77	3.77	3.47	3.17	2.88	2.12
Length of sprue (mm)	52.50	52.50	52.50	52.50	52.50	52.50	52.50	52.50	52.50	52.50	52.50
Length of runner (mm)	17.92	17.92	17.92	17.92	17.92	17.92	17.92	17.92	17.92	18.40	20.35
Length of gate (mm)	5.42	5.42	5.42	5.42	5.42	5.42	5.42	5.42	5.42	5.42	5.77
Injection time (second)	1.92	1.92	1.92	1.92	1.92	1.92	1.92	1.92	1.92	1.92	1.92
Injection pressure (MPa)	83.85	83.85	83.85	83.85	83.85	83.85	83.85	83.85	83.85	83.85	83.85
Shot volume (cm^3)	120	120	120	120	120	120	120	120	120	120	120
Standard deviation of injection pressure (MPa)	9.20	9.20	9.20	9.20	9.20	9.20	9.20	9.20	9.20	9.20	9.20
Standard deviation of shot volume (cm^3)	8.56	8.56	8.56	8.56	8.56	8.56	8.56	8.56	8.56	8.56	8.56

7.3 Results: RBDO/MDF formulation

The RBDO/MDF formulation presented in Figure 6.5 is solved by substituting the weighting coefficient v with $(1 - w)$ in the objective function and then Pareto optimal solutions are obtained by varying w from 0 to 1 with an increment of 0.25, for the sake of illustration. The design optimization loop includes reliability constraints that require prior evaluation of the reliability index (β) through additional optimization processes for each limit state function or inequality constraint. The optimization processes for the evaluation of β are executed in terms of standard normal vectors $\boldsymbol{u}$ corresponding to the random vector $\boldsymbol{r}$. No lower or upper bounds are imposed on $\boldsymbol{u}$. The system compatibility equations are also included as equality constraints in terms of standard normal vectors $\boldsymbol{u}$ for the minimization of β for each limit state function. The nested optimizations require higher computational effort compared to RDO approaches.

The Pareto front obtained in RBDO/MDF formulation is depicted in Figure 7.3, and the mean values of the two objective functions (cycle time and pressure drop) corresponding to the Pareto optimal solutions are shown in Table 7.5, as follows:

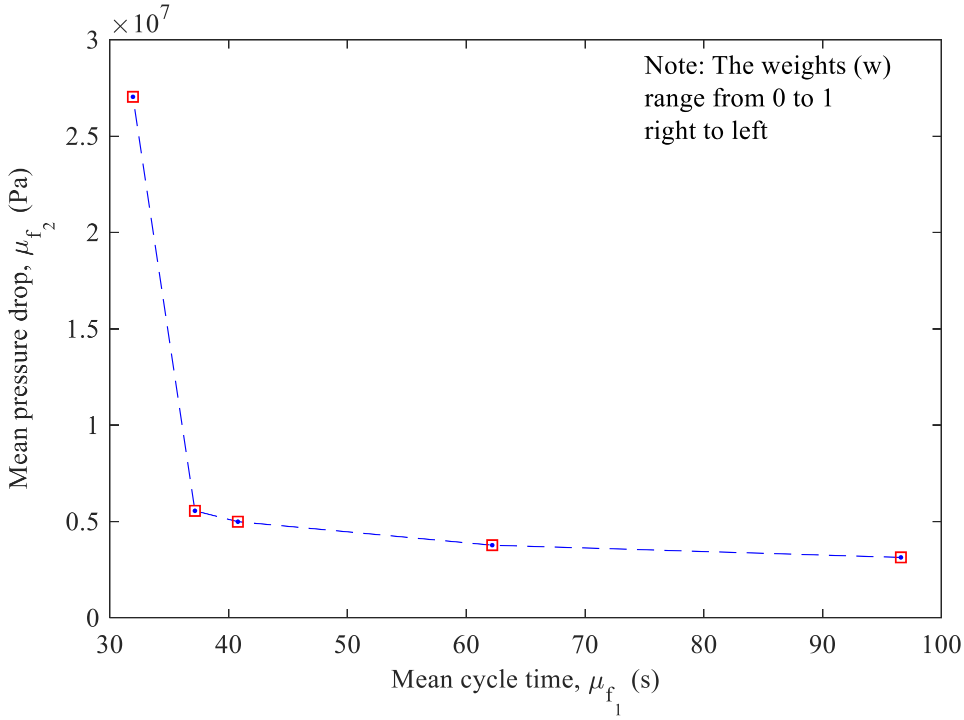

Figure 7.3: Pareto front obtained in RBDO/MDF formulation

Table 7.5: Mean values of cycle time and pressure drop corresponding to the Pareto optimal solutions of RBDO/MDF formulation

Values of weighting coefficient, w	**Mean cycle time, μ_{f_1} (s)**	**Mean pressure drop, μ_{f_2} (MPa)**
w = 0.00	96.59	3.14
w = 0.25	62.19	3.77
w = 0.50	40.78	4.99
w = 0.75	37.16	5.56
w = 1.00	31.94	27.04

Pareto optimal solutions of the optimization variables obtained in RBDO/MDF formulation are shown in Table 7.6, as follow:

Table 7.6: Pareto optimal solutions obtained in RBDO/MDF formulation

Optimization variables	**Pareto optimal solutions corresponding to weighting coefficient, w**				
	w=0.00	**w=0.25**	**w=0.50**	**w=0.75**	**w=1.00**
Volumetric flow rate of the melt (cm^3/sec)	50	50	50	50	52.11
Draft angle of sprue (degree)	4	4	1.12	1	1
Diameter of sprue (mm)	10	7.15	7.18	7	7
Diameter of runner (mm)	8	8	8	8	6.46
Diameter of gate (mm)	4	4	4	3.6	1.25
Length of sprue (mm)	50	50	50	50	50
Length of runner (mm)	15	15	15	15	15
Length of gate (mm)	5	5	5	5	7.1
Injection time (second)	6.98	1.32	1.35	1.32	1.29

7.4 Results: RBDO/AAO formulation

The RBDO/AAO formulation presented in Figure 6.6 is solved by substituting the weighting coefficient v with $(1 - w)$ in the objective function and then Pareto optimal solutions are obtained by varying w from 0 to 1 with an increment of 0.25, for the sake of illustration. Note that the RBDO/AAO formulation treats the coupling variables as optimization variables alongside the design variables. The system compatibility equations are treated as equality constraints. The Pareto front obtained in RBDO/AAO formulation is depicted in Figure 7.4, and the mean values of the two objective functions (cycle time and pressure drop) corresponding to the Pareto optimal solutions are shown in Table 7.7, as follows:

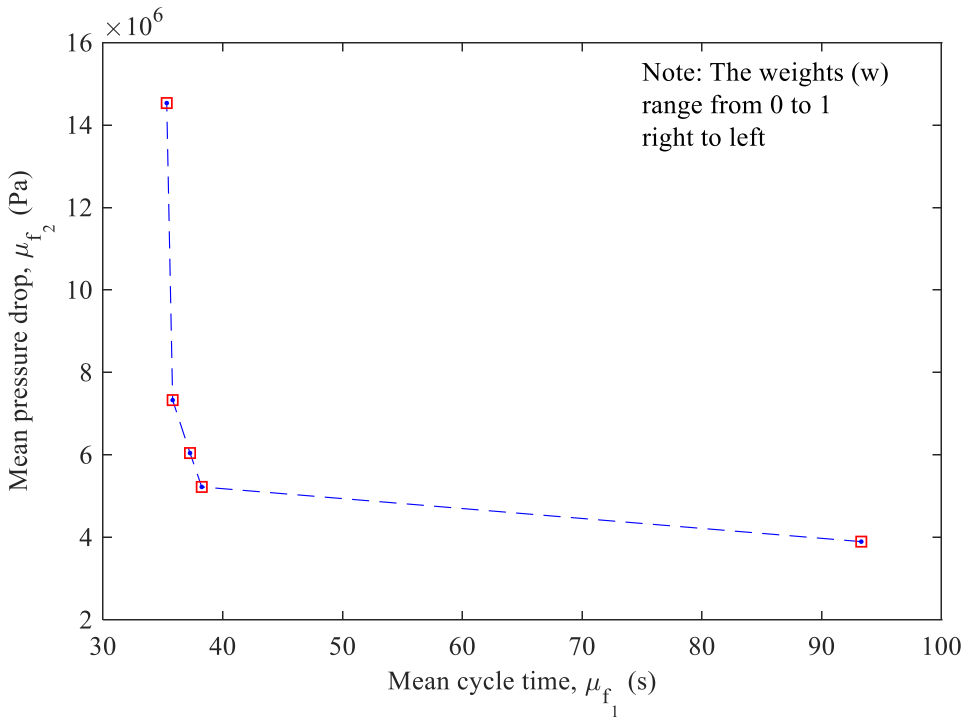

Figure 7.4: Pareto front obtained in RBDO/AAO formulation

Table 7.7: Mean values of cycle time and pressure drop corresponding to the Pareto optimal solutions of RBDO/AAO formulation

Values of weighting coefficient, w	**Mean cycle time, μ_{f_1} (s)**	**Mean pressure drop, μ_{f_2} (MPa)**
$w = 0.00$	93.31	3.90
$w = 0.25$	38.25	5.22
$w = 0.50$	37.27	6.04
$w = 0.75$	35.82	7.33
$w = 1.00$	35.32	14.53

Pareto optimal solutions of the optimization variables obtained in RBDO/AAO formulation are shown in Table 7.8, as follow:

Table 7.8: Pareto optimal solutions obtained in RBDO/AAO formulation

Optimization variables	Pareto optimal solutions corresponding to weighting coefficient, w				
	w=0.00	w=0.25	w=0.50	w=0.75	w=1.00
Volumetric flow rate of the melt (cm^3/sec)	65.36	50	50	68.24	66.42
Draft angle of sprue (degree)	4	1	1	1	1
Diameter of sprue (mm)	10	7	7	7	7
Diameter of runner (mm)	7.64	8	8	8	5.33
Diameter of gate (mm)	3.64	4	3.18	2.9	2.63
Length of sprue (mm)	50	50	50	50	50
Length of runner (mm)	15	15	15	15	35.75
Length of gate (mm)	5	5	5	5	7.86
Injection time (second)	2.19	1	2.78	2.1	2.28
Injection pressure (MPa)	95.68	43.75	121.41	91.90	99.95
Shot volume (cm^3)	120.00	120.00	120.00	120.00	120.00

7.5 Discussions of results

Pareto optimal solutions to the RDO/MDF, RDO/AAO, RDO/MDF, and RBDO/AAO formulations provide multiple alternative sets of optimal values for the design variables to manufacture a flexible multi-cavity injection mold insert. The computational efforts and time of the different methods used in this thesis are compared in Table 7.9, for a particular case with the weighting coefficient, w = 0.5.

Table 7.9: Computational effort and time for RDO/MDF, RDO/AAO, RDO/MDF, and RBDO/AAO formulations

Comparison Metric	RDO		RBDO	
	RDO/MDF	RDO/AAO	RBDO/MDF	RBDO/AAO
Disciplinary Analysis (DA)	4,300	4,660	5,162,637	1,327,628
System Analysis (SA)	2,580	0	2,598	0
Computational time, s	5.43	1.55	1,418.20	377.19

The Pareto fronts obtained in different methods are plotted on a single graph in Figure 7.5 to compare the values of the two objective functions corresponding to different Pareto optimal solutions.

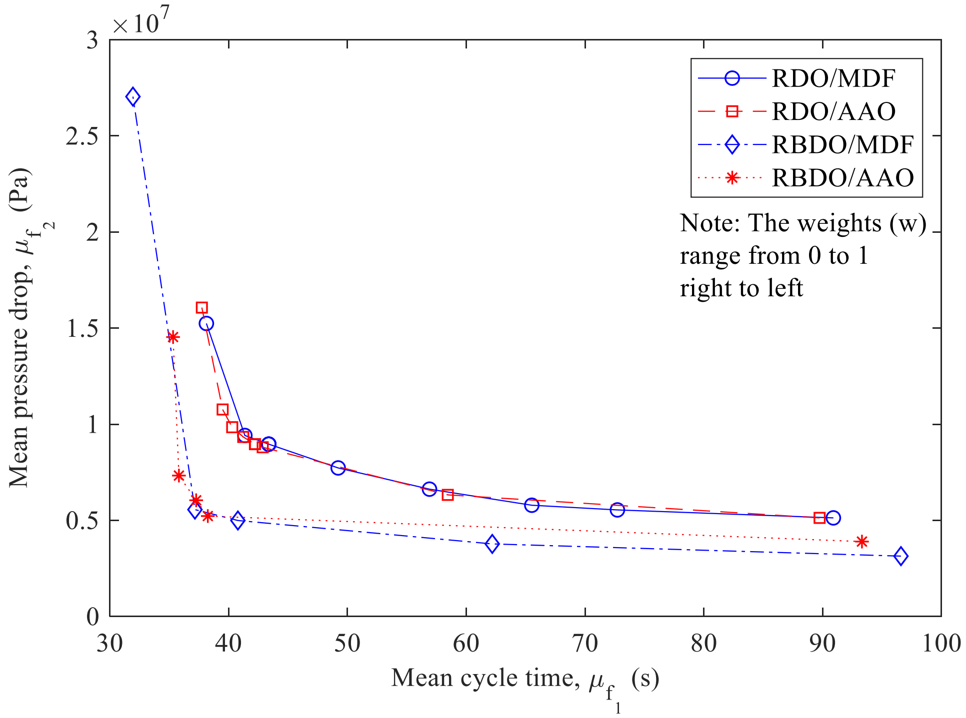

Figure 7.5: Contrast among the Pareto fronts obtained in RDO/MDF, RDO/AAO, RDO/MDF, and RBDO/AAO formulations

The Pareto optimal solutions offer a set of alternative combinations of mean cycle time and mean pressure drop to be chosen according to the requirements or preferences of the designer. The designer can choose one of the Pareto optimal solutions and then manufacture the flexible multi-cavity insert according to the values of the design variables corresponding to the chosen combination of mean cycle time and pressure drop. It can be observed from Figure 8.4 that the objective function values provided by the RBDO solutions are preferable compared to those of RDO. In contrast, the computational effort as well as the computational time involved in RBDO approaches is significantly higher compared to RDO approaches. From Table 7.9, it can be concluded that RDO/MDF and RBDO/MDF methods are not recommended. The selection of RBDO/MDF or RDO/AAO method will depend on the computational budget of the designer. However, RBDO/AAO can be recommended to the mold designers since the injection molding process usually involves the mass production of plastic parts. Therefore, the incurred computational expense in RBDO/AAO approach is justified since the obtained solutions can contribute to long term profitability by reducing cycle time and pressure drop. Additionally, ease of manufacturability is to be considered in the selection of the final design solution.

CHAPTER 8

CONCLUSIONS AND FUTURE WORK

8.1 Conclusions

This thesis uses multidisciplinary robustness-based design optimization (RDO/MDF, RDO/AAO) and multidisciplinary reliability-based design optimization (RBDO/MDF, RBDO/AAO) techniques to solve the design problem of a flexible multi-cavity injection mold insert that can handle the production of specified plastic part family members with minimized cycle time and pressure drop.

The proposed flexible design of the multi-cavity mold insert can help manufacture plastic parts with similar geometric features with reduced mold-making costs. The use of the sub-inserts provides the flexibility in molding parts such that if a new part is to be molded, only the sub-inserts need to be replaced, rather than the whole insert. An additional advantage offered by the flexible multi-cavity insert is that, besides two identical parts, two different part family members can be molded at a time by fitting appropriate sub-inserts. Thus, the conventional multi-cavity insert can be replaced with the flexible multi-cavity insert to reduce the overall production cost of plastic parts having similar dimensions. The design of the conventional multi-cavity insert is deterministic since it is machined for the molding of a single part model. However, the design of a flexible multi-cavity insert involves uncertainty in design parameters related to dimensions. Hence, RDO and RBDO optimization approaches are used to deal with the accounted uncertainty.

The proposed design formulation simultaneously minimizes cycle time and pressure drop using the weighted-sum method of multi-objective optimization. Minimization of cycle time contributes to higher productivity and minimization of pressure drop is essential to maintain good quality of the molded parts. The user can select a preferred combination of cycle time and pressure drop from the Pareto optimal solutions obtained in RDO/MDF, RDO/AAO, and RBDO/AAO formulations of the proposed design problem. The optimal values of the design variables provide specifications for the standard runner system of the flexible multi-cavity insert. The final design solution, i.e., the combination of cycle time and pressure drop should be selected from the multiple Pareto optimal solutions considering the ease of manufacturability of the runner system.

The flexible multi-cavity insert can be an economical solution for the production of small plastic parts of toys, cosmetic boxes, household containers, hair clips, electric switches, etc.

8.2 Future work

There exist a number of potential research scopes to be investigated. Epistemic uncertainty in the input variables can be considered within the formulations of the design problem. The proposed design can be extended to adopt a significant change in part features and dimensions. The design of the proposed multi-cavity insert can be extended for the cold runner system and hot runner system. The parabolic and trapezoidal cross-section for the runner system can be included in design considerations for the simpler machining of the mold insert. The design of the modular ejection system for the proposed multi-cavity insert can be investigated. A physical prototype can be manufactured to test design solutions. Packages of CAD software (e.g., Autodesk Moldflow, Solidworks Plastics) can be used to develop a 3D model of the design solutions and perform comparative study through simulation.

REFERENCES

Agarwal, H., Mozumder, C. K., Renaud, J. E. and Watson, L. T. (2007). "An inverse-measure-based unilevel architecture for reliability-based design optimization". Structural and Multidisciplinary Optimization 33(3): pp. 217-227.

Allen, J. K., Seepersad, C., Choi, H. and Mistree, F. (2006). "Robust design for multiscale and multidisciplinary applications". Journal of Mechanical Design 128(4): pp. 832-843.

Aoues, Y. and Chateauneuf, A. (2010). "Benchmark study of numerical methods for reliability-based design optimization". Structural and multidisciplinary optimization 41(2): pp. 277-294.

Arora, J. S. (2004). "Introduction to optimum design", Elsevier.

Baliman, R., Shusman, T. and Toor, H. (1959). "Injection Molding-Flow of a Molten Polymer into a Cold Cavity". Industrial & Engineering Chemistry 51(7): pp. 847-850.

Ben-Tal, A. and Nemirovski, A. (2002). "Robust optimization–methodology and applications". Mathematical Programming 92(3): pp. 453-480.

Bolur, P. C. (2000). "A guide of injection moulding of plastics". India, Allied Publishers Ltd.

Braun, R. D. and Kroo, I. M. (1997). "Development and application of the collaborative optimization architecture in a multidisciplinary design environment". Multidisciplinary design optimization: state of the art 80: pp. 98.

Broyer, E., Gutfinger, C. and Tadmor, Z. (1975). "A theoretical model for the cavity filling process in injection molding". Transactions of the Society of Rheology 19(3): pp. 423-444.

Chen, W. and Lewis, K. (1999). "Robust design approach for achieving flexibility in multidisciplinary design". Aiaa Journal 37(8): pp. 982-989.

Chen, X., Hasselman, T. and Neill, D. (1997). "Reliability based structural design optimization for practical applications". 38th Structures, structural dynamics, and materials conference, pp. 1403.

Chiralaksanakul, A. and Mahadevan, S. (2005). "First-order approximation methods in reliability-based design optimization". Journal of Mechanical Design 127(5): pp. 851-857.

Chiralaksanakul, A. and Mahadevan, S. (2007). "Decoupled approach to multidisciplinary design optimization under uncertainty". Optimization and Engineering 8(1): pp. 21-42.

Choi, J.-H., Choi, S.-H., Park, D., Park, C.-H., Rhee, B.-O. and Choi, D.-H. (2012). "Design optimization of an injection mold for minimizing temperature deviation". International Journal of Automotive Technology 13(2): pp. 273-277.

Cramer, E. J., Dennis, J., John E, Frank, P. D., Lewis, R. M. and Shubin, G. R. (1994). "Problem formulation for multidisciplinary optimization". SIAM Journal on Optimization 4(4): pp. 754-776.

Dang, X.-P. (2014). "General frameworks for optimization of plastic injection molding process parameters". Simulation Modelling Practice and Theory 41: pp. 15-27.

Dimla, D., Camilotto, M. and Miani, F. (2005). "Design and optimisation of conformal cooling channels in injection moulding tools". Journal of Materials Processing Technology 164: pp. 1294-1300.

Doltsinis, I. and Kang, Z. (2004). "Robust design of structures using optimization methods". Computer methods in applied mechanics and engineering 193(23-26): pp. 2221-2237.

Du, X. and Chen, W. (1999). "Towards a better understanding of modeling feasibility robustness in engineering design". J. Mech. Des. 122(4): pp. 385-394.

Du, X. and Chen, W. (2002). "Efficient uncertainty analysis methods for multidisciplinary robust design". Aiaa Journal 40(3): pp. 545-552.

Du, X. and Chen, W. (2004). "Sequential optimization and reliability assessment method for efficient probabilistic design". J. Mech. Des. 126(2): pp. 225-233.

Du, X. and Huang, B. (2007). "Reliability-based design optimization with equality constraints". International journal for numerical methods in engineering 72(11): pp. 1314-1331.

Du, X., Sudjianto, A. and Chen, W. (2004). "An integrated framework for optimization under uncertainty using inverse reliability strategy". J. Mech. Des. 126(4): pp. 562-570.

Engelund, S. and Rackwitz, R. (1993). "A benchmark study on importance sampling techniques in structural reliability". Structural Safety 12(4): pp. 255-276.

Evans, J. R. (2006). "Injection moulding". Materials Science and Technology.

Ferreira, I., Cabral, J., Saraiva, P. and Oliveira, M. (2014). "A multidisciplinary framework to support the design of injection mold tools". Structural and multidisciplinary optimization 49(3): pp. 501-521.

Ferreira, I., de Weck, O., Saraiva, P. and Cabral, J. (2010). "Multidisciplinary optimization of injection molding systems". Structural and multidisciplinary optimization 41(4): pp. 621-635.

Haldar, A. and Mahadevan, S. (2000). "Reliability assessment using stochastic finite element analysis", John Wiley & Sons.

Hao, L., Lijuan, W., Zongyu, C. and Li, D. (2013). "Application of the multidisciplinary design optimization to the improvement design of rear door". Mechanical Science and Technology for Aerospace Engineering 32(5): pp. 766-770.

Huang, B. and Du, X. (2007). "Analytical robustness assessment for robust design". Structural and multidisciplinary optimization 34(2): pp. 123-137.

Hulme, K. and Bloebaum, C. (2000). "A simulation-based comparison of multidisciplinary design optimization solution strategies using CASCADE". Structural and multidisciplinary optimization 19(1): pp. 17-35.

Kamal, M. and Kenig, S. (1972). "The injection molding of thermoplastics part I: Theoretical model". Polymer Engineering & Science 12(4): pp. 294-301.

Kamal, M. and Kenig, S. (1972). "The injection molding of thermoplastics part II: experimental test of the model". Polymer Engineering & Science 12(4): pp. 302-308.

Kang, M.-A. and Lyu, M.-Y. (2008). "Investigation of the filling unbalance and dimensional variations in multi-cavity injection molded parts". Polymer Korea 32(6): pp. 501-508.

Kazmer, D. and Barkan, P. (1997). "Multi-cavity pressure control in the filling and packing stages of the injection molding process". Polymer Engineering & Science 37(11): pp. 1865-1879.

Krar, S. F., Gill, A. and Smid, P. (2001). "Computer numerical control simplified", Industrial Press Inc.

Kumar, A., Ghoshdastidar, P. and Muju, M. (2002). "Computer simulation of transport processes during injection mold-filling and optimization of the molding conditions". Journal of Materials Processing Technology 120(1-3): pp. 438-449.

Lam, Y., Zhai, L., Tai, K. and Fok, S. (2004). "An evolutionary approach for cooling system optimization in plastic injection moulding". International journal of production research 42(10): pp. 2047-2061.

Lee, I., Choi, K., Du, L. and Gorsich, D. (2008). "Dimension reduction method for reliability-based robust design optimization". Computers & Structures 86(13-14): pp. 1550-1562.

Lee, K.-H. and Park, G.-J. (2001). "Robust optimization considering tolerances of design variables". Computers & Structures 79(1): pp. 77-86.

Lee, K. and Lin, J. (2006). "Design of the runner and gating system parameters for a multi-cavity injection mould using FEM and neural network". The International Journal of Advanced Manufacturing Technology 27(11-12): pp. 1089-1096.

Lee, S. H. and Kwak, B. M. (2006). "Response surface augmented moment method for efficient reliability analysis". Structural Safety 28(3): pp. 261-272.

Li, J.-q., Li, D.-q., Guo, Z.-y. and Lv, H.-y. (2007). "Single gate optimization for plastic injection mold". Journal of Zhejiang University-Science A 8(7): pp. 1077-1083.

Li, Z., Wang, X., Gu, J., Ruan, S., Shen, C., Lyu, Y. and Zhao, Y. (2018). "Topology optimization for the design of conformal cooling system in thin-wall injection molding based on BEM". The International Journal of Advanced Manufacturing Technology 94(1-4): pp. 1041-1059.

Liang, J., Mourelatos, Z. P. and Tu, J. (2004). "A single-loop method for reliability-based design optimization". ASME 2004 international design engineering technical conferences and computers and information in engineering conference, American Society of Mechanical Engineers Digital Collection, pp. 419-430.

Liu, G., Tan, G., Li, G. and Rong, Y. K. (2013). "Multidisciplinary design optimization of a milling cutter for high-speed milling of stainless steel". The International Journal of Advanced Manufacturing Technology 68(9-12): pp. 2431-2438.

LIU, W. and Cui, W. (2004). "Multidisciplinary Design Optimization (MDO): A promising tool for the design of HOV". Journal of ship mechanics 8(6): pp. 95-112.

Lopez, R. H. and Beck, A. T. (2012). "Reliability-based design optimization strategies based on FORM: a review". Journal of the Brazilian Society of Mechanical Sciences and Engineering 34(4): pp. 506-514.

Lopez, R. H., de Cursi, J. E. S. and Lemosse, D. (2011). "Approximating the probability density function of the optimal point of an optimization problem". Engineering Optimization 43(3): pp. 281-303.

Madan, J., Mani, M. and Lyons, K. W. (2013). "Characterizing energy consumption of the injection molding process". ASME 2013 International Manufacturing Science and Engineering Conference collocated with the 41st North American Manufacturing Research Conference, American Society of Mechanical Engineers, pp. V002T004A015-V002T004A015.

Madsen, H. and Hansen, P. F. (1992). "A comparison of some algorithms for reliability based structural optimization and sensitivity analysis". Reliability and Optimization of Structural Systems' 91, Springer: pp. 443-451.

Madsen, H., Krenk, S. and Lind, N. (1986). "Methods of structural safety. Englewood Cliff", NJ: Prentice-Hall.

Mahadevan, S. and Haldar, A. (2000). "Probability, reliability and statistical method in engineering design". John Wiley & Sons.

Mahadevan, S. and Smith, N. (2006). "Efficient first-order reliability analysis of multidisciplinary systems". International Journal of Reliability and Safety 1(1-2): pp. 137-154.

Marler, R. T. and Arora, J. S. (2004). "Survey of multi-objective optimization methods for engineering". Structural and multidisciplinary optimization 26(6): pp. 369-395.

McDonald, M. and Mahadevan, S. (2008). "Design optimization with system-level reliability constraints". Journal of Mechanical Design 130(2): pp. 021403.

Melchers, R. E. (1999). "Structural Reliability Analysis and Prediction–John Wiley & Sons". New York, NY.

Menges, G., Michaeli, W. and Mohren, P. (2013). "How to make injection molds", Carl Hanser Verlag GmbH Co KG.

Merrill, A. M. (1955). "Plastics Technology", Rubber/Automotive Division of Hartman Communications, Incorporated.

Moayyedian, M., Abhary, K. and Marian, R. (2018). "Optimization of injection molding process based on fuzzy quality evaluation and Taguchi experimental design". CIRP Journal of Manufacturing Science and Technology 21: pp. 150-160.

Nannapaneni, S. and Mahadevan, S. (2014). "Uncertainty quantification in performance evaluation of manufacturing processes". 2014 IEEE International Conference on Big Data (Big Data), IEEE, pp. 996-1005.

Nie, J. and Ellingwood, B. R. (2000). "Directional methods for structural reliability analysis". Structural Safety 22(3): pp. 233-249.

Niederreiter, H. and Spanier, J. (2000). "Monte Carlo and quasi-Monte Carlo methods, 1998: proceedings of a conference held at the Claremont Graduate University, Claremont, California, USA, June 22-26, 1998", Springer.

Oberkampf, W. L., Helton, J. C., Joslyn, C. A., Wojtkiewicz, S. F. and Ferson, S. (2004). "Challenge problems: uncertainty in system response given uncertain parameters". Reliability Engineering & System Safety 85(1-3): pp. 11-19.

Oktem, H., Erzurumlu, T. and Uzman, I. (2007). "Application of Taguchi optimization technique in determining plastic injection molding process parameters for a thin-shell part". Materials & Design 28(4): pp. 1271-1278.

Pandelidis, I. and Zou, Q. (1990). "Optimization of injection molding design. Part I: Gate location optimization". Polymer Engineering & Science 30(15): pp. 873-882.

Papalambros, P. Y. and Wilde, D. J. (2000). "Principles of optimal design: modeling and computation", Cambridge university press.

Park, G.-J., Lee, T.-H., Lee, K. H. and Hwang, K.-H. (2006). "Robust design: an overview". AIAA journal 44(1): pp. 181-191.

Park, H.-S. and Dang, X.-P. (2010). "Optimization of conformal cooling channels with array of baffles for plastic injection mold". International Journal of precision engineering and manufacturing 11(6): pp. 879-890.

Parkinson, A., Sorensen, C. and Pourhassan, N. (1993). "A general approach for robust optimal design". Journal of Mechanical Design 115(1): pp. 74-80.

Perez, R., Liu, H. and Behdinan, K. (2004). "Evaluation of multidisciplinary optimization approaches for aircraft conceptual design". 10th AIAA/ISSMO multidisciplinary analysis and optimization conference, pp. 4537.

Rackwitz, R. and Flessler, B. (1978). "Structural reliability under combined random load sequences". Computers & Structures 9(5): pp. 489-494.

Ramu, P., Qu, X., Youn, B. D., Haftka, R. T. and Choi, K. K. (2006). "Inverse reliability measures and reliability-based design optimisation". International Journal of Reliability and Safety 1(1-2): pp. 187-205.

Robert, C. and Casella, G. (2004). "Monte carlo statistical methods springer-verlag". New York.

Rosato, D. V. and Rosato, M. G. (2012). "Injection molding handbook", Springer Science & Business Media.

Royset, J. O., Der Kiureghian, A. and Polak, E. (2001). "Reliability-based optimal structural design by the decoupling approach". Reliability Engineering & System Safety 73(3): pp. 213-221.

Rubin, I. I. and Rubin, A. A. (1972). "Injection molding: theory and practice", Wiley New York.

Rubinstein, R. Y. and Kroese, D. P. (2016). "Simulation and the Monte Carlo method", John Wiley & Sons.

Seo, H. S. and Kwak, B. M. (2002). "Efficient statistical tolerance analysis for general distributions using three-point information". International journal of production research 40(4): pp. 931-944.

Shen, C.-Y., Yu, X.-R., Li, Q. and Li, H.-M. (2004). "Gate location optimization in injection molding by using modified hill-climbing algorithm". Polymer-Plastics Technology and Engineering 43(3): pp. 649-659.

Shen, C., Wang, L. and Li, Q. (2007). "Optimization of injection molding process parameters using combination of artificial neural network and genetic algorithm method". Journal of Materials Processing Technology 183(2-3): pp. 412-418.

Sim, M. (2004). "Robust optimization", Massachusetts Institute of Technology.

Sobieszczanski-Sobieski, J., Agte, J. S. and Sandusky, R. R. (2000). "Bilevel integrated system synthesis". Aiaa Journal 38(1): pp. 164-172.

Sobieszczanski-Sobieski, J. and Haftka, R. T. (1997). "Multidisciplinary aerospace design optimization: survey of recent developments". Structural optimization 14(1): pp. 1-23.

Sobieszczanski-Sobieski, J. and Kodiyalam, S. (2001). "BLISS/S: a new method for two-level structural optimization". Structural and multidisciplinary optimization 21(1): pp. 1-13.

Sopory, A., Mahadevan, S., Mourelatos, Z. P. and Tu, J. (2004). "Decoupled and single loop methods for reliability-based optimization and robust design". ASME 2004 International

Design Engineering Technical Conferences and Computers and Information in Engineering Conference, American Society of Mechanical Engineers Digital Collection, pp. 719-727.

Spencer, R. and Gilmore, G. (1951). "Some flow phenomena in the injection molding of polystyrene". Journal of Colloid Science 6(2): pp. 118-132.

Sundaresan, S., Ishii, K. and Houser, D. R. (1995). "A robust optimization procedure with variations on design variables and constraints". Engineering Optimization+ A35 24(2): pp. 101-117.

Tang, L. Q., Chassapis, C. and Manoochehri, S. (1997). "Optimal cooling system design for multi-cavity injection molding". Finite Elements in Analysis and Design 26(3): pp. 229-251.

Tu, J., Choi, K. K. and Park, Y. H. (1999). "A new study on reliability-based design optimization". Journal of Mechanical Design 121(4): pp. 557-564.

Van Dijk, R., d Ippolito, R., Tosi, G. and La Rocca, G. (2011). "Multidisciplinary design and optimization of a plastic injection mold using an integrated design and engineering environment". NAFEMS World Congress 2011, Boston, USA, 23-26 May, 2011, NAFEMS ltd.

Weissman, A., Ananthanarayanan, A., Gupta, S. K. and Sriram, R. D. (2010). "A systematic methodology for accurate design-stage estimation of energy consumption for injection molded parts". ASME 2010 International Design Engineering Technical Conferences and Computers and Information in Engineering Conference, American Society of Mechanical Engineers Digital Collection, pp. 525-536.

White, J. L. (1975). "Fluid mechanical analysis of injection mold filling". Polymer Engineering & Science 15(1): pp. 44-50.

Yao, W., Chen, X., Luo, W., van Tooren, M. and Guo, J. (2011). "Review of uncertainty-based multidisciplinary design optimization methods for aerospace vehicles". Progress in Aerospace Sciences 47(6): pp. 450-479.

Yin, F., Mao, H. and Hua, L. (2011). "A hybrid of back propagation neural network and genetic algorithm for optimization of injection molding process parameters". Materials & Design 32(6): pp. 3457-3464.

Youn, B. D., Choi, K., Yang, R.-J. and Gu, L. (2004). "Reliability-based design optimization for crashworthiness of vehicle side impact". Structural and multidisciplinary optimization 26(3-4): pp. 272-283.

Youn, B. D., Choi, K. K. and Park, Y. H. (2003). "Hybrid analysis method for reliability-based design optimization". J. Mech. Des. 125(2): pp. 221-232.

Yu, J.-C. and Ishii, K. (1998). "Design for robustness based on manufacturing variation patterns". Trans ASME 120: pp. 196–202.

Zaman, K. and Mahadevan, S. (2013). "Robustness-based design optimization of multidisciplinary system under epistemic uncertainty". Aiaa Journal 51(5): pp. 1021-1031.

Zaman, K. and Mahadevan, S. (2017). "Reliability-based design optimization of multidisciplinary system under aleatory and epistemic uncertainty". Structural and multidisciplinary optimization 55(2): pp. 681-699.

Zaman, K., McDonald, M., Mahadevan, S. and Green, L. (2011). "Robustness-based design optimization under data uncertainty". Structural and multidisciplinary optimization 44(2): pp. 183-197.

Zhai, M. and Xie, Y. (2010). "A study of gate location optimization of plastic injection molding using sequential linear programming". The International Journal of Advanced Manufacturing Technology 49(1-4): pp. 97-103.

Zhao, M., Huang, Z. and Chen, L. (2008). "Multidisciplinary design optimization of tool head for heavy duty CNC vertical turning mill". Engineering Computations 25(7): pp. 657-676.

Zou, T. and Mahadevan, S. (2006). "Versatile formulation for multiobjective reliability-based design optimization". Journal of Mechanical Design 128(6): pp. 1217-1226.

Zou, T., Mahadevan, S. and Sopory, A. (2004). "A reliability-based design method using simulation techniques and efficient optimization approach". ASME 2004 International Design Engineering Technical Conferences and Computers and Information in Engineering Conference, American Society of Mechanical Engineers Digital Collection, pp. 847-855.